



Universität für Bodenkultur Wien



HARVARD
MEDICAL SCHOOL



**BRIGHAM AND
WOMEN'S HOSPITAL**
A Teaching Affiliate of Harvard Medical School

University of Natural Resources and Life Sciences, Vienna
Institute of Biotechnology

**Murine Gammaherpesvirus 68 LANA mediates Episome
Persistence through a cross-species conserved Mechanism that
provides a Basis for an *in vivo* Model of KSHV LANA**

Thesis Advisor: Em.O.Univ.Prof. Dipl.-Ing. Dr.nat.techn. Hermann Katinger

Dissertation in partial fulfilment of the requirements for a doctorate degree

**Doctor rerum naturalium technicarum
- Dr.nat.techn. -**

in the field of

Virology

Submitted by

Dipl.-Biol. Aline Habison

Vienna, October 2017

Für meinen besten Freund Chris

Abstract

Murine gammaherpesvirus 68 (MHV68) ORF73 (mLANA) has sequence homology to Kaposi's sarcoma-associated herpesvirus (KSHV) latency-associated nuclear antigen (kLANA). kLANA is the KSHV episome maintenance protein, and it is necessary and sufficient to maintain KSHV episomes. kLANA acts on KSHV terminal repeat (kTR) DNA to mediate episome persistence. Disruption of mLANA in context of MHV68 virus results in severe deficiencies in the establishment and maintenance of MHV68 latency in infected mice, suggesting a major role of mLANA in the persistence of the episomal viral genome.

MHV68 TR (mTR)-associated DNA persisted as an episome in latently MHV68-infected tumor cells, demonstrating that the mTR elements can serve as a *cis*-acting element for MHV68 episome maintenance. We also assessed the roles of mTRs and mLANA in the absence of infection. DNA containing both mLANA and mTRs *in cis* persisted as an episome in murine cells. In contrast, mTR DNA never persisted as an episome in the absence of mLANA. mLANA also acted *in trans* on mTR DNA to mediate episome persistence. Analogous to kLANA, mLANA broadly associated with host mitotic chromosomes, but redistributed and concentrated to dots in the presence of episomes. These findings indicate that mLANA acts on mTR elements to maintain MHV68 episomes.

Additionally, we discovered that despite ~60 million years of evolutionary divergence, mLANA and kLANA act reciprocally on kTR DNA to mediate episome persistence. Vice versa, kLANA can also support maintenance of mTR DNA as episomes.

Further, we found that a chimeric MHV68 expressing kLANA instead of mLANA was capable of establishing latent infection in splenic B cells at moderate levels. Therefore kLANA can functionally substitute for mLANA, allowing kLANA investigations in a murine model of latent infection.

Key Words: MHV68, KSHV, LANA / ORF73, terminal repeats, episome maintenance

Kurzfassung

Das murine Gammaherpesvirus 68 LANA vermittelt episomale Persistenz durch einen artübergreifend konservierten Mechanismus, der als Basis für ein *in vivo* Modell von KSHV LANA dient.

Das murine Gammaherpesvirus 68 (MHV68) ORF73 Protein (mLANA) weist Sequenzhomologien zu dem Latenz-assoziierten nukleären Antigen (kLANA) des Kaposi Sarcom-assoziierten Herpesvirus (KSHV) auf. kLANA ist für die Etablierung und Erhaltung des KSHV Episoms notwendig und ausreichend. Dazu bindet kLANA an virale Wiederholungssequenzen (terminal repeats, kTR). Ein Defekt von mLANA beeinträchtigt MHV68 in der Bildung und Erhaltung der viralen Latenz in infizierten Mäusen, was auf eine wichtige Rolle von mLANA bei der Persistenz des episomalen viralen Genoms schließen lässt.

MHV68 TR (mTR)-assoziierte DNS persistiert als Episom in latent MHV68-infizierten Tumorzellen; dies zeigt, dass mTR-Elemente die *cis*-agierende Komponente für die Persistenz des episomalen Genoms sind. Wir untersuchen auch die Funktion der mTR-Elemente und mLANA in nicht infizierten Zellen. Wir zeigen, dass Vektor-DNS, die mLANA und mTR-Elemente *in cis* enthält, als Episom in Mauszellen persistiert. Im Gegensatz dazu persistiert mTR-DNS, in Abwesenheit von mLANA, nicht als Episom. mLANA interagiert auch *in trans* mit mTR-DNS und begünstigt die Persistenz des Episoms. Analog zu kLANA bindet mLANA an mitotische Chromosomen; in der Anwesenheit von Episomen findet eine Umverteilung an lokalisierten Stellen statt. Diese Ergebnisse zeigen, dass mLANA mit mTR-Elementen interagiert, um die Persistenz der MHV68 Episome zu gewährleisten.

Zusätzlich zeigen wir, dass trotz ~60 Millionen Jahre evolutionärer Divergenz, nicht nur kLANA sondern auch mLANA mit kTR-DNS interagiert, und zu einer Persistenz des viralen Episoms führt. Umgekehrt unterstützt auch kLANA die Erhaltung von mTR-DNS als Episom. Darüber hinaus zeigen wir, dass ein chimeres MHV68, welches kLANA anstelle von mLANA exprimiert, in der Lage ist, eine moderate, latente Infektion in B-Zellen der Milz von Mäusen zu etablieren. Daher kann kLANA funktionell mLANA ersetzen. Dies ermöglicht die Untersuchung von kLANA in einem Mausmodell für latente Infektion.

Schlagwörter: MHV68, KSHV, LANA / ORF73, terminale Wiederholungssequenzen, episomale Persistenz

Table of Contents

Abstract.....	ii
Kurzfassung.....	iii
1 Introduction	1
1.1 The family <i>Herpesviridae</i>	2
1.2 Kaposi's sarcoma associated herpesvirus (KSHV).....	5
1.2.1 Genome of KSHV.....	5
1.2.2 Clinical diseases associated with KSHV infection.....	6
1.2.3 Epidemiology of KSHV infection	8
1.2.4 Transmission of KSHV	10
1.2.5 Life cycle of KSHV	10
1.2.6 Latency associated nuclear antigen (LANA).....	13
1.2.7 KSHV-mediated oncogenesis	17
1.2.8 Animal models for KSHV.....	18
1.3 Murine gammaherpesvirus 68 (MHV68)	20
1.4 Dissertation objectives	25
2 References	26
3 Murine Gammaherpesvirus 68 LANA Acts on Terminal Repeat DNA To Mediate Episome Persistence.....	35
4 Cross-species conservation of episome maintenance provides a basis for in vivo investigation of Kaposi's sarcoma herpes virus LANA	50
Supporting Information.....	76
5 Acknowledgements	92
6 Curriculum Vitae	94

1 Introduction

1.1 The family *Herpesviridae*

Members of the *Herpesviridae* family are widely distributed in nature and more than 100 different virus species across the animal kingdom have been identified. They are highly adapted to their hosts and are thought to have co-existed and co-evolved with their hosts for millions of years.

The family name is derived from the Greek word *herpein*, which means “to creep”, referring to latent and reoccurring infections, a hallmark of herpesviruses.

All herpesviruses share several biological properties and a common but unique four-layered virion structure. A typical viral particle is composed of a linear double-stranded DNA genome (~124 to 250 kilobases, kb), contained in a central core, which is encased within an icosahedral capsid (100-110 nm in diameter), composed of 162 capsomeres. The capsid itself is surrounded by an amorphous protein coat called the tegument, containing viral proteins and viral mRNAs. It is surrounded by an envelope, a lipid bilayer membrane, in which viral glycoproteins are embedded (Roizmann B *et al.*, 1992, Roizman & Pellett, 2002).

Other biological characteristics comprise of the following properties:

- (1) The viral genome encodes a large array of proteins that can regulate host cell gene expression, DNA synthesis and processing of proteins.
- (2) Viral DNA synthesis and capsid assembly occurs in the nucleus of the infected cell.
- (3) Production of infectious progeny virus results in the death of the infected cell (lytic life cycle).
- (4) After primary infection, herpesviruses can establish a life-long latent infection in their natural hosts, due to their ability to evade host immune responses. In latently infected cells, the viral genome is present as a covalently closed circularized, extrachromosomal molecule, termed episome. Additionally, during latent infection only a limited subset of genes is expressed (latent life cycle).

Up to now, eight known human herpesviruses (HHV) have been identified, and most of the human population is infected with one or more of these viruses; they rarely cause severe disease, unless the host immune system is compromised.

Herpesviruses have been classified into three subfamilies, according to their host range, pathogenicity, cell tropism, length of replicative cycle, cell type in which latency is established, and nucleotide sequence (see Figure 1-1).

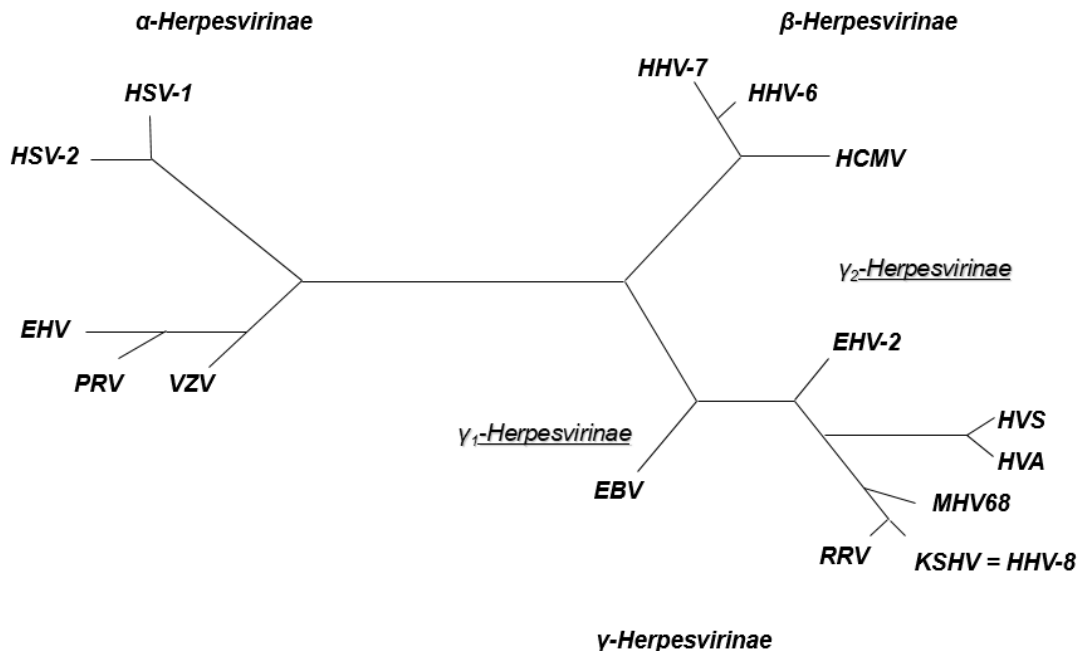


Figure 1-1. Phylogenetic tree of the family Herpesviridae (modified from Moore PS *et al.*, 1996). The family *Herpesviridae* is classified into three subfamilies: *Alpha*-, *Beta*- and *Gammaherpesvirinae*. Subfamilies can further be divided into γ_1 - (*Lymphocryptovirus*) and γ_2 - (*Rhadinovirus*) herpesviruses. There are human herpesviruses in all three subfamilies: The Herpes simplex viruses 1 and 2 (HSV-1, HSV-2) and the Varicella zoster virus (VZV) belong to the *Alphaherpesvirinae*, the Human Cytomegalovirus (HCMV) and the Human herpesviruses 6 and 7 (HHV 6, HHV 7) are members of the *Betaherpesvirinae*. The Epstein Barr virus (EBV) is the only member of the genus *Lymphocryptovirus* (γ_1), whereas the Human herpesvirus 8 (HHV-8)/ Kaposi's Sarcoma associated herpesvirus (KSHV) represents a *Rhadinovirus* (γ_2). Members of the *Rhadinoviruses* are also found in mice (Murine gammaherpesvirus 68 (MHV 68), primates (rhesus rhadinovirus (RRV), herpesvirus saimiri (HVS), herpesvirus ateles (HVA), and equine herpesvirus 2 (EHV-2)).

Alpha (α) – *herpesvirinae* have a broad host cell range, reproduce more quickly than other subfamilies, spread rapidly in cell culture, efficiently and productively destroy infected cells and are capable of establishing latency mostly in the sensory ganglia.

Human herpes simplex (HSV) type 1 and type 2 (HHV-1 and HHV-2) and Varicella-zoster virus (VZV or HHV-3) are members of viruses infecting humans.

Beta (β) – *herpesvirinae* can be distinguished by a more stringent host range, relatively slow replication cycles and their capability to establish latent persistence in secretory glands, lympho-reticular cells, such as lymphoid cells, monocytes and macrophages, and kidneys.

Human cytomegalovirus (CMV or HHV-5), Roseolovirus (HHV-6, variants A and B), and HHV-7 are examples of human viruses.

Gamma (γ) – *herpesvirinae*, members of which are noted for their ability to replicate in epithelial cells and establish latent infections within lymphocytes, either specific for B- or T-lymphocytes. Additionally, they have a very restricted host range, are known for their potential to induce lymphoproliferative disease and their close association with a variety of lymphoid and non-lymphoid cell tumors. Based on genomic organisation, gene content and sequence similarities, this subfamily can be further divided into two genera, Lymphocryptovirus (gamma-1 herpesvirus) and Rhadinovirus (gamma-2 herpesvirus).

Epstein-Barr virus (EBV or HHV-4) is a member of the gamma-1 herpesviruses, whereas Kaposi's sarcoma associated herpesvirus (KSHV or HHV-8) is the only human representative of gamma-2 herpesviruses. Murine gammaherpesvirus 68 (MHV68) is the most prominent representative infecting small rodents (Simas JP & Efstathiou S, 1998).

In the following sections, the gamma-2 herpesviruses KSHV and MHV68 will be discussed in further detail.

1.2 Kaposi's sarcoma associated herpesvirus (KSHV)

In 1872, the Hungarian physician and dermatologist Dr. Moritz Kaposi first described an “idiopathic multiple pigmented sarcoma of the skin”, which was initially thought to be an uncommon rare form of skin cancer in elderly men of Italian, Mediterranean or Jewish descent. Twenty years later, it was named after its discoverer Kaposi's Sarcoma (KS).

Approximately one century later, as the incidence rate ascended in correlation with the HIV pandemic, it was first suggested that a viral agent was responsible.

Kaposi's sarcoma associated herpesvirus (KSHV), now formally known as human herpesvirus 8 (HHV-8), was identified by Yuan Chang, Patrick Moore and colleagues in 1994, by detection of herpesvirus-like DNA sequences in KS tumors derived from AIDS patients (Chang Y *et al.*, 1994). It is now not only considered as the causative agent of KS, but is also closely associated with two rare lymphoproliferative diseases in the context of AIDS, primary effusion lymphoma (PEL) (Cesarman E *et al.*, 1995) and the plasma cell variant of multicentric Castleman disease (MCD) (Soulier J *et al.*, 1995).

1.2.1 Genome of KSHV

Shortly after the discovery and isolation, the KSHV genome, a linear double stranded DNA molecule ranging from 165kb to 170kb in size, was sequenced. It revealed a central, long unique region (LUR) of about 140kb, containing at least 90 open reading frames (ORFs), which is flanked by terminal repeat (TR) DNA elements at both ends of the linear viral genome. Each TR element consists of 0.8kb that is 85% GC-rich (Russo JJ *et al.*, 1996). The number of TR elements varies among different isolates, ranging from 16 to 75 copies, which accounts for the variation in genome size (Judde JG *et al.*, 2000 and Duprez RV *et al.*, 2007).

The KSHV genome shows a high degree of similarity to other gammaherpesviruses, such as murine gammaherpesvirus 68 (MHV68) (see Figure 1-3), retroperitoneal fibromatosis-associated herpesvirus (RFHV), rhesus monkey rhadinovirus (RRV), herpesvirus saimiri (HVS) and to some extent to Epstein Barr virus (EBV). Many of the ORFs encoded in KSHV are conserved in alpha- and beta-herpesviruses and frequently have multiple functions. Many of these genes are involved in several aspects of the viral life cycle, for example ORF21, a thymidine kinase for nucleotide synthesis, ORF9, a DNA polymerase

for DNA replication, and structural proteins, such as ORF25, the major capsid protein, and ORF64-67, coding for tegument proteins (Russo J *et al.*, 1996).

KSHV also contains genes that are only homologous to other gamma-2 herpesviruses, notably ORF73, the latency associated nuclear antigen (LANA), which is also present in MHV68 and HSV (Virgin HW *et al.*, 1997; Albrecht JC, 1992). Additionally, a significant number of genes have been identified that are unique to KSHV, termed K1 to K15, based on their relative location (from left to right) in the viral genome. Moreover, KSHV, as well as other herpesviruses, contain at least one, often several ORFs that are believed to be hijacked from the host cell genome in the course of evolution, presumably leading to growth advantages and improved immune evasion strategies, such as the inhibition of apoptosis (Cai Q *et al.*, 2010; Moore PS & Chang Y, 1998). Examples for such orthologous genes include viral interleukin-6 (vIL-6/K2), vCyclinD (ORF72), vBcl-2 (ORF72) and vFlip (K13). Recently twelve microRNAs, small non-coding RNAs involved in (post-) transcriptional regulation of gene expression, have been identified within the KSHV genome, all of which are expressed during latency, with only a small subset being upregulated during the lytic cycle (Pearce M *et al.*, 2005; Samols MA *et al.*, 2005).

1.2.2 Clinical diseases associated with KSHV infection

In addition to Kaposi's Sarcoma (KS), KSHV infection has been associated with two other B-lymphocyte malignancies: primary effusion lymphoma (PEL), and the plasmablastic variant of multicentric Castleman disease (MCD) (reviewed in Wen KW *et al.*, 2010; Dourmishev LA *et al.*, 2003).

Kaposi's Sarcoma

Kaposi's Sarcoma only develops in KSHV infected individuals. It is a vascular tumor of endothelial origin, characterized by skin lesions with different neoplastic manifestations. Typically, KSHV infected cells are poorly differentiated, highly proliferative and elongated, and are therefore known as "spindle" cells. These tumor lesions also contain multiple cell types due to extravasation of erythrocytes, infiltration of several inflammatory cells, such as macrophages, lymphocytes, and plasma cells and are characterized by extensive neoangiogenesis (Gessain A & Duprez R, 2005). Infected spindle cells express four latent viral genes: LANA (ORF73), kaposin (K12), vFLIP (K13), vCyclinD (ORF72). The major population of spindle cells harbours viral episomes, however, in some spindle cells KSHV

is not strictly latent but undergoes lytic replication (Staskus KA *et al.*, 1997; Parravicini C *et al.*, 2000; Katano H *et al.*, 2000).

KS initially presents as multifocal dermatologic lesions, which are red, brown or purple in pigmentation. As the disease progresses, spindle cells are the major cell population; they begin to compress the vascular slits, resulting in nodular lesions. More aggressive forms of the disease also involve lesions to the oral cavity, lymph nodes and visceral organs. There are four discrete subtypes of KS, based on epidemiological and clinical data, extent of immunosuppression and severity of infection: classic/sporadic, endemic/African, epidemic/AIDS-associated, and iatrogenic/post-transplant (Cai Q *et al.*, 2010).

The form of KS, originally described by Dr. Moritz Kaposi, is now referred to as classic KS, and is predominantly found in HIV negative elderly man of Mediterranean and Eastern European ancestry. It is an infrequent, relatively indolent disease that often affects the skin of extremities, rarely spreading to lymph nodes and internal organs (Friedman-Birnbaum R *et al.*, 1990; Iscovich J *et al.*, 1999).

The endemic form of KS is seen in Equatorial, Eastern and Southern Africa and is more aggressive, involving lymphatic and/or visceral organs. In contrast to classic KS, the endemic type is often found in children as a lymphadenopathy, with high fatality rates (Wabinga HR *et al.*, 1993; Ziegler JL & Katongole-Mbidde E, 1996).

The most prevalent and aggressive variant is the acquired immune deficiency syndrome (AIDS) -associated KS, affecting human immunodeficiency virus (HIV)-infected individuals, due to its associated immunosuppressive environment. It is the most common malignancy present in HIV infected individuals and commonly occurs throughout the body, including skin, mucus membranes of the oral cavity, gastrointestinal tract and visceral organs (Beral V & Newton, R, 1998). This form is found with increased frequency in young homosexual AIDS patients in developed nations as well as in developing countries. AIDS-KS can be indirectly treated with highly active antiretroviral therapies (HAART) to increase the immune response (Winceslaus J, 1998).

Iatrogenic/acquired or post-transplant KS develops in transplant patients undergoing long-term immunosuppressive therapy in order to prevent graft rejection. Renal transplant recipients are the most likely group to develop this form of KS (Penn I, 1988). KSHV-infected lymphocytes or epithelial cells present in these KS lesions often originate from donor tissues. Reduction of withdrawal of immunosuppressive therapy is an effective option to resolve iatrogenic KS, though risking allograft complications or rejection (Barozzi P *et al.*, 2003).

Primary effusion lymphoma

In addition to KS, primary effusion lymphoma (PEL), also referred to as body cavity-based lymphoma (BCBL), is a rare and unique form of rapidly progressing non-Hodgkin B cell lymphoma (NHL). It has been strongly associated with KSHV infection and is commonly found in HIV-infected individuals. Unlike KS, PEL is derived from clonally expanded malignant B cells; it often lacks a distinct tumor mass and presents as malignant effusions in the pericardial, pleural or peritoneal cavities (Jenner RG & Boshoff C, 2002), but there are also reports of PELs showing a solid mass in the lymph nodes, lungs and gastrointestinal tract (Arvanitakis L *et al.*, 1996). PEL cells express latent genes LANA, vFLIP, vCyclinD and kaposin. Lytic gene expression has only been detected in a very small subset of cells, such as the viral interleukin-6 homologue (vIL-6), kbZIP (K8), the viral membrane glycoprotein K8.1, the three viral interferon regulatory factors K9 - K11, a viral processivity factor PF-8 (ORF59) and the minor capsid protein ORF65 (Parravicini C *et al.*, 2000; Katano H *et al.*, 2000). PEL cells can be single-positive for KSHV, or double-positive through co-infection with EBV. KSHV genomes in PEL cells are maintained at high copy numbers, ranging from 50 to 150 copies per cell, in contrast to much lower numbers present in KS lesions.

Multicentric Castleman disease

Unlike the hyaline variant of Multicentric Castleman disease (MCD), the plasmablastic variant of MCD is also highly associated with KSHV. It is a lymphoproliferative disorder, characterized by expanded germinal centers with often polyclonal B cell and vascular proliferation in the lymph node, containing large plasmablastic cells (Cai Q *et al.*, 2010). Dysregulated interleukin 6 (IL-6) levels, partially contributed by the virally encoded homolog, the lytic gene vIL-6 (K2), are considered a likely contributor to pathophysiology of MCD (Parravicini C *et al.*, 1997). KSHV genomes can be detected in almost all HIV-positive MCD and approximately 50% of HIV-seronegative MCD cases (Soulier J *et al.*, 1995).

1.2.3 Epidemiology of KSHV infection

Seroepidemiologic studies revealed that KSHV is widespread throughout the world, though it appears that there is an astonishing variation in local seroprevalence, defining the number of persons in a population tested positive for the presence of KSHV based on

blood serum specimens. The association between KS prevalence and KSHV seroprevalence is high.

The gene K1, encoding a transmembrane glycoprotein, is highly variable in KSHV and can therefore be used as a marker in order to trace KSHV variants associated with specific populations. The K1 sequence is most heterogeneous and can differ up to 44%, whereas the sequence variation in most regions of the genome is less than three percent. Phylogenetic studies of the K1 gene identified five main variants of KSHV termed A through E and at least 24 subgroups. Subtypes A and C are mainly found in Northern European, American and Northern Asian populations, type B is almost exclusively found in Africa. Old Asian and Polynesian populations are affected by subtype D, Brazilian Amerindians by subtype E.

To further study the abundance and the uneven worldwide distribution of KSHV among different countries and risk groups, antibody based serological assays were established, since KSHV DNA cannot be detected continuously in all infected individuals. The first assays were based on the detection of antibodies to the latency associated nuclear antigen (LANA/ORF73) by immunofluorescence (Gao SJ *et al.*, 1996; Kedes DH *et al.*, 1996), or to recombinant structural proteins, e.g. the capsid protein encoded by ORF65, by ELISA or western blot (Simpson GR *et al.*, 1996; Lenette ET *et al.*, 1996). Two years later, the KSHV structural glycoprotein K8.1 was identified as a more reliable diagnostic antigen with high sensitivity and specificity (Raab MS *et al.*, 1998)

KSHV is widespread in sub-Saharan Africa, where KSHV is found in more than 50% of the adults, and relatively prevalent in countries from the Mediterranean region, ranging from three percent in Northern Italy up to 30% in Sicily. In northern Europe, Asia, and North America the rate is lower than five percent. Despite co-infection with HIV, increased seroprevalence rates are observed in populations with high risk factors, such as multiple sex partners and homosexual contacts.

For instance, in the United States, 40% of HIV positive homosexual man are also seropositive for KSHV, whereas less than 20% of homosexual men, negative for HIV, are affected (Ahmadpoor P, 2009).

1.2.4 Transmission of KSHV

Primary KSHV infection can either occur during childhood or as an adult. It can be transmitted either via sexual or non-sexual routes, allowing for both vertical and horizontal transmission. Possible sources of infection are peripheral blood mononuclear cells (PBMCs), saliva, oropharyngeal mucosa, semen, cervico-vaginal secretions and prostate glands, where KSHV can be found (Chen T *et al.*, 2006). Depending on the endemicity in different parts of the world, the mode of transmission varies. In endemic countries like Africa most KSHV transmission occurs during childhood, rising after the age of one. This implicates a non-sexual route of propagation by horizontal transmission, through exposure within family members while kissing, playing or sharing eating utensils. There is also evidence for sexual transmission of KSHV in endemic areas. Additionally, maternal-infant transmission during labor and delivery or transplacentally accounts for a portion of KSHV infections in areas where infections are highly endemic (Mayama S *et al.*, 1998). In non-endemic regions, the spread of KSHV among homosexual and bisexual men is clearly linked to an active sexual lifestyle, the prevalence rising with the number of sexual partners. Besides sexual transmission, other possible horizontal transmission routes include KSHV contaminated blood transfusion, organ transplantation or needle sharing (Kalt I *et al.*, 2009).

1.2.5 Life cycle of KSHV

In the virion particle, the double-stranded KSHV genome is linear. In the process of KSHV primary infection the virion is delivered into the host cells by a multistep process, starting with the attachment of the virion to the host cell through contact of several cellular co-receptors with viral surface glycoproteins. Through direct fusion of the viral envelope with the plasma membrane or internalization by endocytosis, the viral capsid penetrates into the cytoplasm. Subsequently, the capsid is moved to the perinuclear region, disassembled, and the viral DNA is released into the nucleus via nuclear pores (Cai Q *et al.*, 2010; Boshoff C *et al.*, 2012).

Once in the nucleus, KSHV can, similar to other gammaherpesviruses, persist in cells after primary infection, exhibiting a biphasic life cycle with predominant lifelong latent infection and typical short-lived lytic phase. The shift from latency to the lytic cycle is termed reactivation. Maintaining a balance between latent and lytic phase is important for long-term persistence of the virus in the host. Gene products from both expression programs serve crucial roles in the pathogenesis of KSHV-associated disease.

Gene expression profiles of KSHV from biopsies from KS tissues, PELs and MCD, as well as *in vitro* infection of cultured cells show that the majority of tumor cells contain KSHV viral DNA and express latent transcripts, and that only a small subpopulation, less than five percent undergo lytic reactivation (Staskus KA *et al.*, 1997).

The lytic cycle is important for the propagation of the virus to adjacent cells and hosts, but mainly occurs during primary infection and is characterized by the replication of linear viral genomes that culminates in the production of virions, ultimately resulting in the death of the infected cell. Productive herpesvirus infection requires a profound, time-controlled remodelling of the viral transcriptome and proteome. During the lytic cycle, more than 80 transcripts are expressed in a highly sequential, temporal order of immediate-early, early, and late categories (Jenner RG *et al.*, 2001; Paulose-Murphy M *et al.*, 2001). Immediate-early genes are the first group of genes expressed during the lytic cycle; their transcription generally does not require *de novo* protein synthesis. They are important for modulating the host cell environment for viral replication and the regulation of the subsequent transcriptional cascade of downstream genes, such as RTA (replication and transcription activator/ORF50). RTA is the best characterized immediate-early gene coding for an E3 ubiquitin ligase. It targets a number of transcriptional repressor proteins for degradation by the ubiquitin proteasome pathway, and is considered a latent - lytic master switch protein that is necessary and sufficient for the initiation and completion of the lytic phase. Additionally, RTA can upregulate LANA expression to suppress lytic reactivation and thus acts as a negative feedback regulator of RTA (Lan K. *et al.*, 2005). The immediate-early gene k-bZIP (basic leucine zipper/K8) appears to antagonize RTA transcription activity (Rossetto C *et al.*, 2007). The immediate-early genes also control the expression of early and late genes by either directly binding to RTA response elements or through binding to other cellular host factors (West JT & Wood C, 2003). The early gene transcripts mostly encode proteins that are involved in nucleic acid metabolism and modulation of cellular functions. They typically mediate viral DNA replication and require *de novo* protein synthesis for expression. Their expression is not suppressed by drugs that inhibit viral DNA replication. The expression of late genes is dependent on the replication of viral genomes and mainly include virion structural proteins, to facilitate viral assembly and egress.

Apart from spontaneous lytic reactivation, lytic replication can also be modelled *in vitro* by specific intracellular or extracellular stimuli, e.g. chemical induction using sodium-butyrate (NaB) or 12-O-tetradecanoylphorbol-13-acetate (TPA) (Renne R *et al.*, 1996). Such chemicals affect chromatin regulatory factors, by remodelling of viral chromatin from the heterochromatin to the euchromatin state. As a result, the viral episome gradually relaxes its compact chromatin structure, leading to the expression of all viral genes and the

production of infectious virion particles. Acyclovir, a nucleosid-analagon, inhibits lytic virus synthesis and virus secretion (Medveczky MM *et al.*, 1997).

Latency is the quiescent state of the viral life cycle, which is characterized by the expression of a limited subset of viral transcripts without production of functional or infectious viral particles, and persistence of the viral genome. During latency, infected cells downregulate cell surface markers to evade detection by the host immune surveillance. Within KS lesions, the vast majority of cells are latently infected, including spindle cells that arise from latently infected endothelial cells after the establishment of the inflammatory lesion.

Upon entry into the nucleus, the linear gammaherpesvirus genome circularizes through recombination at terminal repeats (TRs) through a not-yet-known mechanism and persists as a non-integrated extrachromosomal mini-chromosome, termed episome (plasmid) in the form of highly ordered chromatin structure. During latency, KSHV expresses only a small number of viral transcripts such as ORF73 (LANA), ORF 72 (viral Cyclin), ORF71 (K13/vFLIP), and ORFK12 (kaposins A, B, and C), along with 12 distinct microRNAs, which facilitate the establishment of life-long latency in its host and survival against the host innate and adaptive immune surveillance mechanisms (Wen KW & Damania B, 2010). The latency associated viral products have an essential role in the development of KSHV associated malignancies, since most tumor cells in KS, PEL, and MCD are latently infected with KSHV. In addition to the very limited number of genes expressed during latency to minimize the immune response, another mechanism is to downregulate the number of major histocompatibility complex class I (MHC-I) proteins (with different specificities concerning HLA allotypes) on the surface of infected cells. Therefore, antigens will not be presented efficiently and cytotoxic T lymphocytes recognize the infected cells less adequately. For example, KSHV encodes two homologous membrane-associated E3 ubiquitin ligases, modulator of immune recognition MIR1 (K3) and MIR2 (K5) to evade host immune recognition. Both MIR1 and MIR2 downregulate the surface expression of MHC-I molecules through ubiquitin-mediated endocytosis, which is followed by lysosomal degradation (Coscoy L & Ganem D, 2000). Additionally, MIR2 downregulates ICAM-1 (intracellular adhesion molecule) and B7-2 molecules that promote cell-to-cell contact efficient killing, resulting in the inhibition of natural killer (NK) cell mediated cytotoxicity (Coscoy L & Ganem D, 2001; Ishido S *et al.*, 2000).

KSHV infected PEL cells maintain similar copy numbers of the viral episome over multiple rounds of cell division, therefore suggesting a faithful mechanism of viral genome segregation after each cell division (Skalsky RL *et al.*, 2007). Besides replication, episomes must segregate and retain in the cell nucleus, since accumulation of the

genome in the cytoplasm leads to degradation, resulting in the loss of the episome. In eukaryotic cells, partitioning of the DNA is achieved by attaching microtubules to the centromere, more precisely, the kinetochore of mitotic chromosomes. During Metaphase, chromosomes are aligned along the equatorial plane, centrally located between the two centrosomes, and sister chromatids are pulled towards opposite ends of the dividing cell to ensure equitable distribution of chromosomes into newly forming nuclei. Obviously, the KSHV genome has none of these features, however there is strong evidence for LANA (ORF73) tethering KSHV episomes to host mitotic chromosomes thereby exploiting the segregation machinery of the infected cell (Ballestas M *et al.*, 1999; Barbera AJ *et al.*, 2004; Fejer G *et al.*, 2003; Kelley-Clarke B *et al.*, 2009).

1.2.6 Latency associated nuclear antigen (LANA)

Among the few proteins expressed during latency, the latency associated nuclear antigen (LANA), encoded by open reading frame 73 (ORF73), is the most consistently detected antigen in KSHV-infected cells of KS, PELs, and MCD origin and is therefore considered a hallmark of KSHV episome persistence (Ballestas M *et al.*, 1999; Cotter MA & Robertson ES, 1999; Dupin N *et al.*, 1999). LANA is a multifunctional nuclear protein, ranging in size from 1089 to 1162 amino acids (220 – 240kDA), depending on the specific viral isolate. It is transcribed from the same locus in as ORF71 (v-FLIP) and ORF72 (v-cyclin) as a tri-cistronic, differentially spiced mRNA. The transcription is regulated by a common promoter upstream of LANA (Dittmer D *et al.*, 1998), that functions bidirectionally and also drives expression of K14 and ORF74 (vGPCR) during the lytic cycle (Chiou CJ *et al.*, 2002). LANA is heavily posttranslationally modified.

Based on the primary sequence, LANA can be divided into three main domains: a conserved proline- and serine-rich N-terminal region, a central region which is variable in length and composed of several acidic repeats including a putative leucine zipper motif, and a conserved C-terminal domain containing a proline-rich region and a region rich in charged and hydrophobic amino acids. The variation in size is due to the different number of acidic internal repeat elements in the central region (Russo JJ *et al.*, 1996). Both the C-terminus and the N-terminus of LANA contain a nuclear localisation signal (NLS). Isolated LANA N- and C-terminal regions localise to the nucleus, but only the C-terminus accumulates as nuclear speckles characteristic of the intact protein. The C-terminus of LANA is responsible for the formation of stable LANA homodimers or possibly multimers in vitro (Schwam DR *et al.*, 2000; Piolot T *et al.*, 2001).

Other gamma-2 herpesviruses encode homologous proteins in their ORF73, though mainly the C-terminal region is conserved among the rhadinoviruses, whereas the rest of the protein varies by domain. For example, murine gammaherpesvirus 68 (MHV68) lacks the internal acidic repeat sequence but has an N-terminal proline region. In the case of herpesvirus saimiri (HVS), ORF73 has a central acidic repeat region but lacks the proline rich domain. Aside from these differences, the degree of sequence similarity is indicative of conserved biological functions (Fowler P *et al.*, 2003; Calderwood M *et al.*, 2004).

LANA's interaction with host mitotic chromosomes

For stable persistence in infected cells, the viral genome must be replicated each cell division and segregated to daughter nuclei. For segregation two components are necessary, a cis-acting DNA binding sequence within the viral genome as well as a trans-acting viral factor that links the binding sequence to the host cellular chromosomes. In KSHV, this is accomplished by the cis-acting terminal repeat (TR) units and the trans-acting LANA protein through attachment of the viral episome to host chromatin (see Figure 1-2).

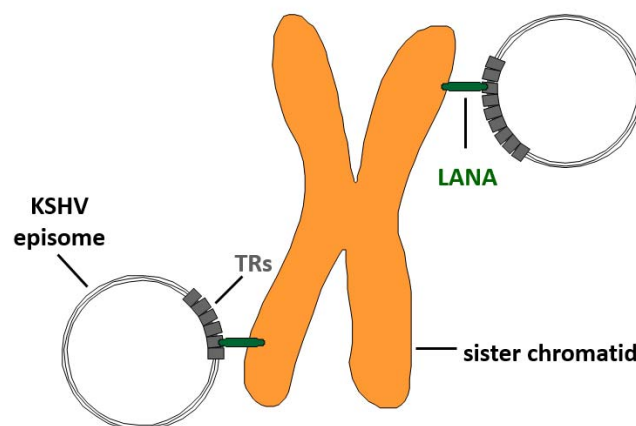


Figure 1-2. LANA tethers the KSHV genome host chromosomes by directly binding to the viral terminal repeat sequences (TRs) and to mitotic chromosomes. LANA has an N-terminal and C-terminal chromosome association region. Each TR element contains two LANA binding sites, which C-terminal LANA binds to as an oligomer. LANA mediated tethering of KSHV episomes to chromosomes ensures that during cell division episomes are efficiently replicated and segregated along with sister chromatids to the progeny nuclei.

LANA is the protein necessary and sufficient for the replication and persistence of TR-containing episomes in the absence of other viral genes (Ballesta ME *et al.*, 1999; Barbera AJ *et al.*, 2004). In KSHV infected cells, LANA can be detected as specific

punctate dots in immunofluorescence assays (Lennette ET *et al.*, 1996). These punctate dots co-localize with hybridisation signals for the KSHV genome by immuno-fluorescence in situ hybridization (FISH) assays along chromosomes of infected cells (Cotter MA *et al.*, 1999). Expression of LANA in uninfected cells diffusely paints chromosomes, showing some preferential localization near centromeres and telomeres. In contrast, transfection of TR-containing plasmids into cells stably expressing LANA leads to a relocation of LANA, concentrating to nuclear dots on chromosomes at sites of TR DNA, similar to the pattern seen in KSHV latently infected cells. LANA has an N-terminal as well as a C-terminal chromosome association region (Barbera AJ *et al.*, 2004; Barbera AJ *et al.*, 2006; Kelley-Clarke B *et al.*, 2007; Krithivas A *et al.*, 2002; Piolot T *et al.*, 2001). Chromosome association mediated by N-terminal LANA (aa 5-13) is critical for episome replication and persistence, since the abrogation or impairment of chromosome tethering greatly affects the ability of LANA to maintain TR-containing episomes (Barbera AJ *et al.*, 2004). N-terminal LANA chromosome association is mediated through interaction of histones H2A/H2B on the nucleosomal surface and has been corroborated by crystallography data (Barbera AJ *et al.*, 2006). Although the N-terminal LANA chromosome association region has a dominant role in episome persistence, the C-terminal chromosome binding region also contributes to TR-DNA maintenance, but it is only detected when the N-terminal chromosome binding region is impaired (Kelley-Clarke B *et al.*, 2009). The methyl CpG binding protein MeCP2 and the protein DEK play a role in chromosome association and have been identified as potential cellular proteins involved in chromatin binding. Furthermore, LANA has been shown to bind to histone H1 (Cotter MA & Robertson ES, 1999). Bromo domain proteins BRD2/RING3 and BRD4, members of the BET/fsh family of nuclear chromatin associated proteins, have also been identified to interact with LANA (Platt GM *et al.*, 1999).

Other DNA Viruses that establish latency also express proteins that tether their genome to mitotic chromosomes. In many cases these proteins do not exhibit amino acid similarity, but the key mechanistic features of these proteins seem to be conserved. Examples of tethering proteins include EBNA1 from Epstein Bar Virus (EBV), the E2 protein from papillomavirus (Bastien N & McBride AA, 2000; Hung SC *et al.*, 2001; Ilves I *et al.*, 1999; Lehman CW & Botchan MR, 1998). For EBNA1 two different mechanisms of interaction with mitotic chromosomes have been proposed. On the one hand, the major chromosomal protein partner for EBNA1 is a nucleolar protein termed EBNA1 binding protein 2 (EBP2/p40) (Wu H *et al.*, 2000). Additionally, it has been proposed that EBNA1 can directly interact with cellular DNA at places of AT hooks (Sears J *et al.*, 2004). For HVS ORF73, a homolog of KSHV ORF73, MeCP2 is the proposed chromosome binding partner (Calderwood MA *et al.*, 2004; Griffiths R & Whitehouse A, 2007.).

LANA's role in replication

Similar to segregation, LANA also mediates replication by direct interaction with the terminal repeats (TR). As mentioned above, each KSHV TR unit is composed of 801bp high in G+C content. The exact number of TR units varies among different isolates, but on average 40 copies are present in the KSHV genome (Russo JJ *et al.*, 1996). LANA's C-terminal domain oligomerizes and cooperatively binds to two adjacent sites within the TR, LANA binding site -1 and -2 (LBS-1 and LBS-2). These LBSs, approximately 20 bp in size, are separated by 22bp, measured from center to center. The minimal region required for replication, termed latent origin of replication, also comprises an adjacent 29- to 32-bp-long GC-rich element, referred to as replication element (RE), located upstream of the LBSs; its deletion completely abolishes replication (Hu J Renne R, 2005). Vermer *et al.* recently identified a latent replication origin in the long unique region (LUR) of the viral genome, which initiates replication independent of viral proteins *in trans*, suggesting an autonomously replicating element in the LUR. In contrast to the LANA dependent replication origin within the TR, this autonomously replicating element is high in AT content and can recruit the host cell replication machinery to initiate replication (Verma SC. *et al.*, 2007). C-terminal LANA, which has structural homology to that of EBNA-1 and papillomavirus E2, is required and sufficient to mediate low level transient replication *in vitro* (Grundhoff A & Ganem D, 2003). Inclusion of the N-terminal chromosome binding sequence enhances replication, suggesting that chromosome association also plays an important role in DNA replication (Komatsu T. *et al.*, 2004). Although LANA, like EBNA-1, does not seem to have enzymatic activity for replication function, it is essential for TR-mediated replication primarily because it recruits the required cellular replication machinery to the RE element of the TR. The primary replication protein termed origin recognition complex (ORC) serves as a starting basis for the further recruitment of other proteins to the RE site, such as minichromosome maintenance complexes (MCMs). It is a component of the pre-replicative complex (pre-RC), which triggers DNA replication (Tye BK, 1999). Recently, Sun Q *et al.*, 2002 found that LANA recruits replication factor C (RFC), the DNA polymerase clamp [proliferating cell nuclear antigen (PCNA)] loader, through this sequence to mediate viral DNA replication and episome persistence. EBNA-1 also associates with ORC2, which is necessary for the replication of plasmids containing the EBV oriP (Dhar SK *et al.*, 2001), suggesting that gammaherpesviruses share a similar mechanism of replication.

In addition to tethering the KSHV genome to host mitotic chromosomes, LANA not only plays a role in the maintenance of latency through repression of RTA, but also induces oncogenesis by disrupting p53 and Rb function of tumor suppression.

1.2.7 KSHV-mediated oncogenesis

Due to the association of KSHV with different human malignancies, as discussed in previous sections, KSHV is considered to be a human oncogenic virus (Brooks LA. *et al.*, 1997; Cathomas G, 2003). KSHV has the capacity to manipulate the control of cellular proliferation through interference with the cell cycle regulatory system and fend off the host immune response. Infection not only leads to cell morphology changes, as for example seen in spindle cells, growth rate, and extended life span, but also provokes deregulated angiogenesis, inflammation, and modulation of the host immune system in favor of tumor growth (Dagna L. *et al.*, 2005). Especially latent infection plays a key role in KSHV-induced malignancy and pathogenesis. KSHV targets multiple pathways to induce proliferation, inhibition of apoptosis, and survival for the promotion of tumor growth. Genetic instability is often observed in KSHV infected cells, and KSHV infection is sufficient to induce such chromosomal instability (Gaidano G. *et al.*, 1996; Pan H. *et al.*, 2004). Among other genes LANA, RTA and k-ZIP have been shown to interact with and suppress the function of tumor suppressor p53 and Rb, resulting in their suppression. The loss of p53 and Rb leads to the inhibition of DNA damage repair, control of cell-cycle checkpoints, and cell death, thereby contributing to oncogenesis.

Additionally, in order to accelerate cellular proliferation, the KSHV encoded vCyclinD promotes cell-cycle progression from G1 to S phase by interaction with phosphorylated Cdk6 (cyclin-dependent kinase 6) (Cai Q. *et al.*, 2011). KSHV also constitutively activates the NF- κ B pathway (nuclear factor kappa-light-chain-enhancer of activated B cells) by encoding the viral homolog of GPCR (G protein-coupled receptor; vGPCR) to produce several cytokines and chemokines. KSHV also promotes cell proliferation by autocrine and/or paracrine signaling through induction of various growth factors, such as IL-6 and the viral counterpart vIL-6, mediating STAT and mitogen-activated protein kinase (MAPK) signaling pathways (Xie J. *et al.*, 2005; Molden, J. *et al.*, 1997). It is believed that a variety of cellular growth factors and cytokines, which are regulated by KSHV, all play pivotal roles in the development and progression of KS. KSHV also directly induces angiogenesis in an autocrine and paracrine fashion through a complex interplay of various viral and cellular pro-angiogenic and inflammatory factors. Furthermore, immune evasion strategies exploited by KSHV lead to uncontrolled cell proliferation, thereby promoting tumorigenesis. KSHV encodes multiple proteins, which are directly involved in the inhibition of host innate and adaptive immunity. These include viral proteins that interfere with interferon signaling, dysregulate the complement system, induce cytokine secretion, and disruption of antigen processing and presentation (Choi J. *et al.*, 2001; Means RE. *et al.*, 2002)

1.2.8 Animal models for KSHV

Animal Models are essential for understanding the biology of human disease, including KS and KSHV-associated lymphomas. KSHV is difficult to grow in cell culture and does not efficiently infect any species other than humans. Most primates carry their own rhadinoviruses, such as the primate homolog of KSHV named rhesus radinovirus (RRV). Several PEL cell lines that are latently infected with KSHV have been established (Arvanitakis L *et al.*, 1996) and studies on KSHV latency in the context of the complete genome used to be limited to these cell lines.

In addition, KSHV does not infect mice, but humanized immuno-deficient mice are capable of being infected by KSHV and can to some extent serve as small animal model for drug efficacy studies and pathogenesis. Xenograft models of KSHV lymphoma, where KSHV infected cell lines were injected into Nod/SCID (non-obese diabetic/severe combined immunodeficiency disease) mice, have been able to mimic tumors seen in humans. These studies helped to understand the involvement of the tumor microenvironment, depending on the site and form of application (Staudt MR *et al.*, 2004), and host signaling molecules (Keller, SA *et al.*, 2006) in course of lymphoma development. Similarly, injection of KSHV in human skin engrafted on SCID mice induced lesions that were morphologically and phenotypically consistent with KS, including the presence of angiogenesis and spindle-shaped cells latently infected with KSHV (Foreman KE *et al.*, 2001). The group of Dittmer D *et al.* (1999), used SCID-hu Thy/Liv mice reconstituted with human fetus liver and thymus to study viral transcription as well as the susceptibility of the mice to infection with BCBL-1 derived KSHV, leading to lytic and latent infection, most abundant in CD19 positive B lymphocytes. Additionally, Parson CH *et al.* (2006) investigated the immune response to KSHV by implanting Nod/SCID mice with functional human hematopoietic tissue grafts, resulting in infected murine B cells, macrophages, NK cells and dendritic cells. Latent and lytic transcripts were detectable over a period of several months and a subset of KSHV infected animals produced human KSHV-specific antibodies. Furthermore, they have shown that Nod/SCID mice infected with purified KSHV provide a possible system for demonstrating latent and lytic replication. In 2014, Wang LX *et al.* reported, that a humanized BLT (bone marrow, liver, and thymus) mouse (hu-BLT) model generated from Nod/SCID/IL2ry mice permitted KSHV infection, resulting in various tissues tested positive for KSHV DNA, as well as both latent and lytic viral transcripts, via various routes of infection. Additionally, two types of cell lines carrying KSHV genome are able to generate KSHV-associated tumors. One is based on HUVECs (Human umbilical vein endothelial cells) that express telomerase (TIVE-LTC) (An FQ. *et al.*, 2006), the other one is based on normal mouse bone marrow endothelial cells (mECK36) transfected with a KSHV-infectious bacterial artificial

chromosome (KSHV-Bac36) (Mutlu AD *et al.*, 2007). These studies showed that in contrast to other virally induced tumors, KSHV tumor formation depends on both, latent and lytic viral gene expression.

For animal models, also several closely related viruses of the gamma-2 sublineage have been investigated to serve as tractable animal models of KSHV latency, such as rhesus rhadino virus (RRV), retroperitoneal fibrosis associated herpesvirus (RFHV), Herpesvirus saimiri (HVS), and murine gammaherpesvirus 68 (MHV68). The work on primate and murine homologues has contributed to our current understanding of KSHV.

Macaques are mainly infected with two different types of gammaherpesviruses, RRV and RFHV. RRV is closely related KSHV and is associated with the development of B cell hyperplasia and persistent lymphadenopathy resembling MCD in rhesus macaques, that are co-infected with simian immunodeficiency virus (SIV) (Urzechowska BU *et al.*, 2008). RFHV induces retroperitoneal fibrosis (RF) in animals that are immunodeficient. The spindle-shaped cells in these RF lesions express a LANA ortholog, but these cells are assigned to the mesenchymal rather than the endothelial lineage and are therefore not relevant to KS biology (Bruce AG *et al.*, 2006).

HVS was first isolated from healthy squirrel monkeys (*Saimiri sciureus*). When infecting its natural host, HVS infection does not cause any obvious pathological symptoms, reminiscent of other primate gamma-2 herpesviruses like HVA (herpesvirus ateles in New World primate host spider monkeys) (Abrecht JC, 2000). However, HVS infection of other New World primates, such as *Samuineus spp.* and *Callithrix spp.* results in fulminant lymphoproliferative disorders. But unlike KSHV, HVS establishes latency in T cells instead of B cells. It induces acute T-cell lymphomas and leukemia in New World monkeys and New Zealand white rabbits and can immortalize T cells both in vivo and in vitro (Medveczky MM. *et al.*, 1993).

Though MHV68 infection, as a mouse model, is not associated with KS-like and related diseases (Virgin HW, 1997), MHV68 has been invaluable, since many of the viral proteins show high sequence and functional homology to KSHV, such as viral encoded cyclin, which induces tumors in transgenic mice, analogous to KSHV. MHV68 will be discussed in further detail in the following chapter.

1.3 Murine gammaherpesvirus 68

Murine gammaherpesvirus 68 (MHV68/γHV68), also known as murine herpesvirus 4 (MHV4/MuHV4), is one of several closely related gamma-2 herpesviruses isolated from murid rodents in the late 1970s during field studies in Slovakia on the ecology of arboviruses (Blaskovic D *et al.*, 1980). It displays serological and biological properties with other isolates including MHV60, MHV72, which along with MHV68 were isolated from yellow-necked mice (*Apodemus flavicollis*) and bank voles (*Clethrionomys glareolus*). MHV76 and MHV78 were recovered from wood mice (*Apodemus flavicollis*) in the same locality. These herpesviruses appear to be widespread among rodent populations in Northern Europe, e.g. surveys estimate that up to 70% of bank voles and wood mice in the UK carry the virus in their respiratory tract. In addition, a MHV68-like virus, MHV-Brest, was more recently discovered in white-toothed shrews (*Crocidura russula*), a small insectivorous animals (Chastel C *et al.*, 1994). It remains unclear, whether these are all strains of the same virus or represent several distinct viruses. Over the last two decades, there has been an increasing interest in studying MHV68 infection of inbred strains of laboratory mice, hoping to gain better insights into KSHV and EBV infections in humans.

Like KSHV, MHV68 establishes latency predominately in B cells but has also been shown to establish latency in macrophages, dendritic cells, and epithelial cell lines derived from several mammalian species including humans. Additionally, MHV68 can establish acute and persistent infection in laboratory mice, and therefore provides a good compromise for a small animal model to address questions about gammaherpesvirus latency in the context of all viral genes as well as an intact immune response.

MHV68 consists of a long unique region (LUR), flanked by a variable number of GC-rich terminal repeat (TR) elements, a structure that is characteristic of several members of the gamma-2 herpesviruses. A single TR element consists of 1.2 kb and has a G/C content of 78%. The MHV68 LUR is approximately 118kb in length with an overall GC content of 46% and is predicted to encode approximately 80 ORFs, 63 of which are homologous to KSHV and HVS gene products (Virgin HW *et al.*, 1997). The comparison of the genomic organisation of MHV68 with other Rhadinoviruses, such as KSHV (see Figure 1-3) revealed large blocks of co-linearly arranged genes, interspersed with virus-specific ORFs, which are predicted to determine the particular biological properties of these viruses (Simas JP & Efstathiou S, 1998).

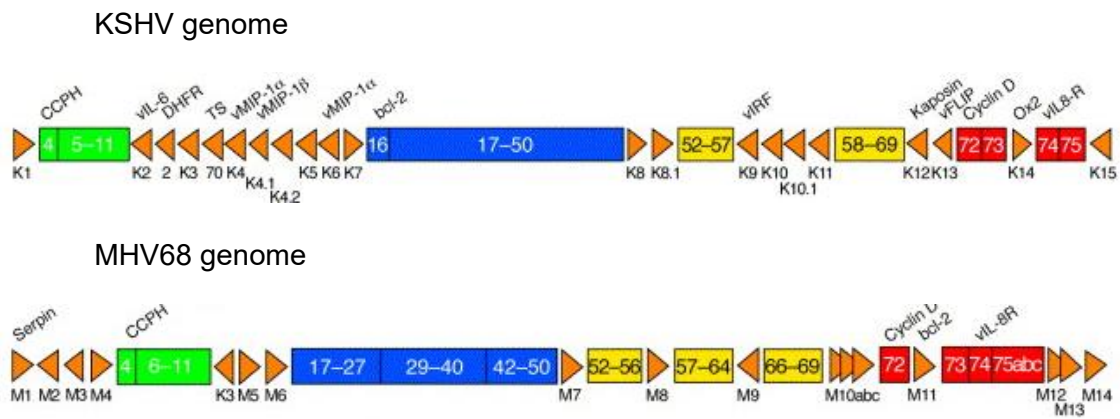


Figure 1-3. Comparison of the genomic structure of the Rhadinoviruses KSHV and MHV68 (modified from Simas JP & Efstathiou S, 1998).

Conserved gene blocks are displayed as boxes, interspersed with ORFs (arrows) that are largely unique to the virus; they contain several homologues to cellular genes. K, KSHV specific ORFs; M, MHV68 specific ORFs. Bcl-2, B cell lymphoma gene 2; CCPH, complement control protein homologue; DHFR, dihydrofolate reductase; TS, thymidylate synthetase; vIL6, viral interleukin 6; vIL8R, viral interleukin 8 receptor; vIRF, viral interferon-responsive factor; vFLIP, viral FLICE (caspase-8) inhibitory protein; vMIP-1a/b, viral macrophage inflammatory protein 1a/b.

Of the unique ORFs encoded by MHV68, M1 displays significant amino acid similarity to the poxvirus serpin family of proteins (SPI-1), which are known for their ability to irreversibly inhibit their target protease through conformational changes. M1 is not necessary for the establishment of latency, but it may regulate apoptosis or host inflammatory response (Simas JP & Efstathiou S, 1998). M2 is expressed during the lytic phase. Zinc finger antiviral protein (ZAP) is a host factor that binds to the mature mRNA of M2 to reduce its expression. Thereby it can inhibit the replication of the virus, suggesting an important role in the establishment and maintenance of viral latency (Xuan Y *et al.*, 2012). M3 codes for a chemokine-binding protein, which hinders chemokines in recruiting hematopoietic cells to sites of infection and inflammation trying to oppose the viral infection (van Berkel V *et al.*, 2000). M7 codes for the membrane protein gp150, which plays a key role in the attachment and fusion of the viral particle to host cell membrane. It is also considered a marker of late lytic replication (Simas JP & Efstathiou S, 1998).

MHV68 encodes 15 mature miRNAs, all of which are clustered at the 5' end of the genome. Uniquely, all MHV68 miRNAs are located downstream of viral tRNA-like elements (vtRNAs). KSHV and EBV miRNAs target transcripts are for example involved in immune recognition, apoptosis, and cell cycle pathways, and some gammaherpesvirus miRNAs can act as functional orthologs of host miRNAs. Feldman ER *et al.*, 2014, showed that MHV68 miRNAs were dispensable for short-term virus replication but were important for establishment of lifelong infection in the key virus reservoir of memory B

cells. Moreover, the MHV68 miRNAs were essential for the development of virus-associated pneumonia, implicating them as a critical component of gammaherpesvirus-associated disease.

A general feature of gammaherpesvirus genomes is the presence of cellular gene homologues that have been captured from host DNA relatively recently in evolutionary time. As in KSHV, they are involved in cell cycle and apoptosis regulation, cytokine signaling, and host immune suppression. MHV68 encoded genes with obvious cellular counterparts are for example a D-type cyclin (vCycD/ORF72) that, analogous to KSHV vcycD, is predicted to associate with and regulate the cyclin-dependent kinase cdk6 to promote cellular proliferation. Another example is a unique ORF, designated M11, which has some similarity to bcl-2 family members and is distantly related to the bcl-2 homologues encoded by KSHV and EBV, both of which have been shown to inhibit proliferation.

1.3.1 Pathogenesis of MHV68 infection

Primary infection of mice with MHV68 upon intranasal infection results in a productive infection of the lungs that lasts for about 10 days. Infectious virus is also detected in adrenal glands and heart tissue, indicating hematogenous spread, but is rarely detected in lymphoid tissue during acute infection (Sunil-Chandra NP. *et al.*, 1992). Productive infection is antagonised by the host immune response in a CD8 positive T-cell dependent manner around day 10 post infection, but MHV68 DNA is still detectable. It involves alveolar epithelial and mononuclear cells, which can be observed as interstitial pneumonia, with a portion of mice developing clinical disease (Ehtisham S *et al.*, 1993). Acute infection in the lung resolves within 10 to 12 days, followed by viremia and life-long latent infection that spreads the virus to the spleen. MHV68 has been detected in its latent form in B lymphocytes that are the main target for viral latency, as well as macrophages, and dendritic cells. The establishment of latency in lymphoid tissue is characterized by a transient phase of splenomegaly and lymph node enlargement. At two to three weeks post inoculation, the maximal number of splenocytes are latently infected. Thereafter the number of latently infected cells decreases until a steady state is reached (Sunhil-Chandra NP *et al.*, 1994). In B cell deficient mice, MHV68 cannot establish splenic latency, though MHV68 DNA was detectable in the lung even after resolution of the primary infection, suggesting B-lymphocytes to be the most important, if not the only, lymphatic reservoir for MHV68 infection in vivo (Usherwood EJ *et al.*, 1996). Interestingly, non-lymphatic lung cells of epithelial origin have been demonstrated to harbour latent

MHV68 (Stewart JP *et al.*, 1998), providing a possible explanation for MHV68 persistence in B cell deficient mice. Long-term persistent infection is associated with approximately 10% of the mice developing lymphoproliferative disease (LPD) and high-grade lymphomas (Sunhil-Chandra NP *et al.*, 1994).

The MHV68 infection of laboratory mice represents an amenable model system for the investigation of gammaherpesvirus pathogenesis and infection of humans and domestic animals. The availability of various gene-knockout mouse strains and the possibility of manipulating specific immune responses, facilitates the investigation of host immune responses. With the establishment of an MHV-68 bacterial artificial chromosome (BAC) and the fact that in vitro, MHV68 can lytically infect a variety of cell types, the efficient generation of mutant viruses has become possible (Adler H *et al.*, 2000). Additionally, virus deletion mutants allow the study of viral gene products and their role in acute and persisting infection.

1.3.2 Murine latency associated nuclear antigen

MHV68 encodes a homologue of LANA (ORF73) (Albrecht JC *et al.*, 1992; Virgin HW *et al.*, 1997) and for better understanding is now referred to as mLANA. The comparison of mLANA with homologues encoded by other members of the genus Rhadinovirus, reveals significant sequence homology, but is mainly concentrated to its C-terminus. mLANA is comprised of 314 amino acids, which is obviously smaller than KSHV LANA (kLANA) with 1162 amino acids, mainly due to the lack of internal acidic and glutamine-rich repeats present in kLANA (see Figure 1-4).

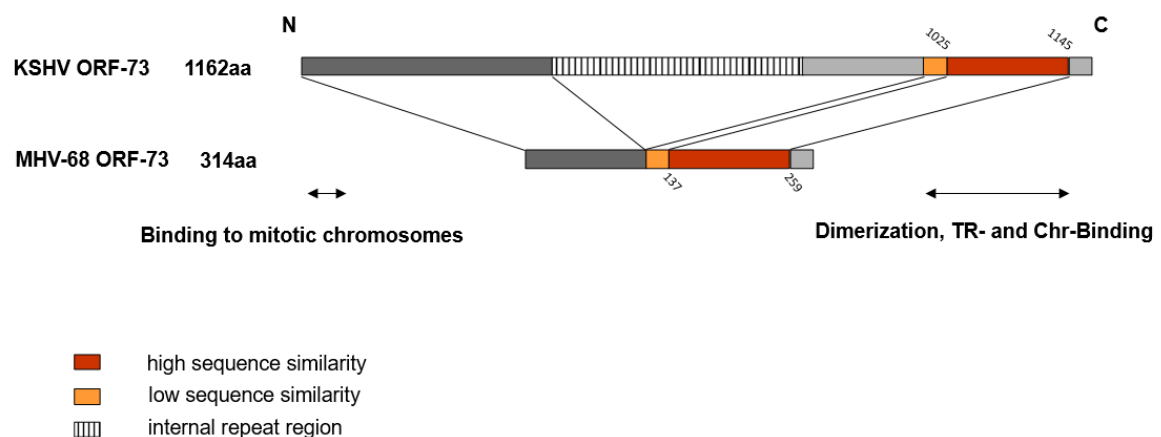


Figure 1-4. Sequence comparison of ORF73 proteins from KSHV and MHV68.

The LANA homologues also share functional and some structural similarity to the EBV encoded episome maintenance protein EBNA1, even though there is no obvious sequence homology. Alike EBNA1, the episome maintenance function of kLANA and possibly of the mLANA analogue is related to the attachment to host cell chromosomes, thereby ensuring an efficient partitioning of viral episomes to the daughter cells during mitosis of latently infected cells. Unlike EBNA1 that solely functions to replicate and support maintenance of the latent EBV episomes through interaction with the cis-acting element within the oriP sequence, kLANA and possibly also mLANA promote host cell proliferation (Moorman NJ *et al.*, 2003).

The transcription of mLANA is rather complex, with the distal terminal repeats of MHV68 constituting an important component of episomal persistence. In addition to one promoter directly upstream of murine ORF73, the murine TRs (mTRs), which are located more than 10kb distant from mLANA itself, contain two promoters capable of transcribing mLANA. The large mLANA mRNA is spliced starting from a 5' non-coding exon within the TRs to the right end of the LUR, and then across several ORFs (ORF75a-c and ORF74) to ORF73 (Coleman HM *et al.*, 2005).

There are some studies that identified murine ORF73 as an immediate-early lytic transcript (Rochford R *et al.*, 2001; Ebrahimi B *et al.*, 2003). Others groups suggested that, based on cDNA gene arrays, the ORF73 transcript is latently expressed in MHV68 infected S11 B cells, though it cannot be absolutely excluded that some of the latent S11 cells undergo lytic reactivation (Martinez-Guzman D *et al.*, 2003). Fowler P *et al.* (2003) studied mLANA deletion and frameshift mutants and revealed that mLANA is not required for efficient lytic replication in vitro or in vivo. However, a severe latency deficit was observed in splenocytes of mice infected with these mutants, suggesting a crucial role for mLANA in the establishment of latency and for viral persistence in the host. Similarly, Moorman NJ *et al.* (2003) constructed a mLANA stop mutant by introduction of a translation termination codon in the ORF73 of MHV68, revealing that this mutant virus replicated normally in vitro, in proliferating as well as quiescent murine fibroblasts. In contrast, the mutant virus exhibited delayed replication in the lungs of immunocompetent mice, as well as severe deficits in the establishment of splenic latency. By analogy with kLANA, which binds to the TRs, this fact would provide potential for transcriptional autoregulation (Garber AC *et al.*, 2002).

1.4 Dissertation objectives

The latency associated nuclear antigen of KSHV (kLANA), encoded by ORF73, is one of few KSHV genes expressed during latency, and is necessary and sufficient to mediate episome persistence. It shares to some extent sequence homology to the MHV68 encoded ORF73 (mLANA), which could potentially provide a suitable animal model to study gammaherpesvirus infection in its natural mouse host.

We therefore asked, if mLANA can resemble the function of kLANA as the episome maintenance protein for MVH68.

The first question addressed in this work was the identification of the murine terminal repeat elements (mTRs) as the *cis*-acting sequence for MHV68 episome maintenance, analogous to the function of TRs present in the KSHV genome (kTRs). Next, we asked whether mLANA can mediate episome persistence by acting on mTR DNA *in cis* and *in trans*. Since initial experiments with low level expression of mLANA driven by a CMV promoter only led to low levels of episome maintenance, we therefore designed constructs in which mLANA expression was driven by its natural promoters, located within the mTRs. We sought to enhance the level of mLANA expression, in an attempt to increase the efficiency of episome persistence in parallel.

Additionally, we wished to investigate the possibility of inter-species functionality of mLANA and kLANA for episome maintenance. We also asked if mTRs could serve as *cis*-acting element for kLANA, supporting episome persistence. Such findings could indicate that mLANA and kLANA are interchangeable, potentially leading to a chimeric mouse model.

2 References

- Adler H, Messerle M, Wagner M, and Koszinowski UH.** 2000. Cloning and mutagenesis of the murine gammaherpesvirus 68 genome as an infectious bacterial artificial chromosome. *J Virol* **74**:6964-6974.
- Ahmadpoor P.** 2009. Human herpesvirus-8 and Kaposi sarcoma after kidney transplantation: mechanisms of tumor genesis. *Iran J Kidney Dis* **3**:121-126.
- Albrecht JC.** 1992. Primary structure of the herpesvirus saimiri genome. *J Virol* **66**:5047-5058.
- Albrecht, JC, Nicholas J, Biller D, Cameron KR, Biesinger B, Newman C, Wittmann S, Craxton MA, Coleman H, and Fleckenstein B.** 1992. Primary structure of the herpesvirus saimiri genome. *J Virol* **66**:5047-5058.
- An FQ, Folarin HM, Compitello N, Roth J, Gerson SL, McCrae KR, Fakhari FD, Dittmer DP, and Renne R.** 2006. Long-term-infected telomerase immortalized endothelial cells: a model for Kaposi's sarcoma-associated herpesvirus latency in vitro and in vivo. *J Virol* **80**:4833–4846.
- Arvanitakis L, Mesri EA, Nador RG, Said JW, Asch AS, Knowles DM, and Cesarman E.** 1996. Establishment and Characterization of a Primary Effusion (Body Cavity-Based) Lymphoma Cell Line (BC-3) Harboring Kaposi's Sarcoma-Associated Herpesvirus (KSHV/HHV-8) in the Absence of Epstein-Barr Virus. *Blood* **88**:2648-2654.
- Ballestas ME, Chatis PA, and Kaye KM.** 1999. Efficient persistence of extrachromosomal KSHV DNA mediated by latency-associated nuclear antigen. *Science* **284**:641-644.
- Barbera AJ, Ballestas ME, and Kaye, KM.** 2004. The Kaposi's sarcoma-associated herpesvirus latency-associated nuclear antigen 1 N terminus is essential for chromosome association, DNA replication, and episome persistence. *J Virol* **78**:294-301.
- Barbera AJ, Chodaparambil JV, Kelley-Clarke B, Joukov V, Walter JC, Luger K, and Kaye KM.** 2006. The nucleosomal surface as a docking station for Kaposi's sarcoma herpesvirus LANA. *Science* **311**:856-861.
- Barozzi P, Luppi M, Facchetti F, Mecucci C, Alu M, Sarid R, Rasini V, Ravazzini L, Rossi E, Festa S, Crescenzi B, Wolf DG, Schulz TF, and Torelli G.** 2003. Post-transplant Kaposi sarcoma originates from the seeding of donor-derived progenitors. *Nat Med* **9**:554-561.
- Bastien N & McBride AA.** 2000. Interaction of the papillomavirus E2 protein with mitotic chromosomes. *Virology* **270**:124-134.
- Beral V and Newton R.** 1998. Overview of the epidemiology of immunodeficiency-associated cancers. *J Natl Cancer Inst Monogr*: 1-6
- van Berkel V, Barrett J, Tiffany HL, Fremont DH, Murphy PM, McFadden G, Speck SH, Virgin HW.** 2000. Identification of a gammaherpesvirus selective chemokine binding protein that inhibits chemokine action. *J Virol* **74**:6741-7.
- Blaskovic D, Stancekova M, Svobodova J, and Mistrikova J.** 1980. Isolation of five strains of herpesviruses from two species of free living small rodents. *Acta Virol* **24**:468. 1980.
- Boshoff C.** 2012. Ephrin receptor: a door to KSHV infection. *Nat Med*.**18**:861-863.
- Bowden RJ, Simas JP, Davis AJ, and Efstathiou S.** 1997. Murine gammaherpesvirus 68 encodes tRNA-like sequences which are expressed during latency. *J Gen Virol* **78**:1675-87.
- Brooks LA, Wilson AJ, and Crook T.** 1997. Kaposi's sarcoma-associated herpesvirus (KSHV)/human herpesvirus 8 (HHV8)—a new human tumour virus. *J Pathol* **182**:262.

- Bruce AG, Bakke AM, Bielefeldt-Ohmann H, Ryan JT, Thouless ME, Tsai CC, Rose TM.** 2006. High levels of retroperitoneal fibromatosis (RF)-associated herpesvirus in RF lesions in macaques are associated with ORF73 LANA expression in spindleoid tumour cells. *J Gen Virol* **87**:3529-38.
- Cai Q, Verma SC, Lu J, and Robertson ES.** 2010. Molecular biology of Kaposi's sarcoma-associated herpesvirus and related oncogenesis. *Adv Virus Res* **78**:87-142.
- Calderwood MA, Hall KT, Matthews DA, and Whitehouse A.** 2004. The herpesvirus saimiri ORF73 gene product interacts with host-cell mitotic chromosomes and self-associates via its C terminus. *J Gen Virol* **85**:147-153.
- Cathomas G.** 2003. Kaposi's sarcoma-associated herpesvirus (KSHV)/human herpesvirus 8 (HHV-8) as a tumour virus. *Herpes* **10**:72.
- Chang Y, Cesarman E, Pessin MS, Lee F, Culpepper J, Knowles DM, and Moore PS.** 1994. Identification of Herpesvirus-like DNA Sequences in AIDS-Associated Kaposi's Sarcoma. *Science* **266**:1865-1869.
- Chastel C, Beaucournu JP, Chastel O, Legrand MC, and Le Goff F.** 1994. A herpesvirus from an European shrew (*Crocidura russula*). *Acta Virol* **38**:309.
- Cesarman E, Chang Y, Moore PS, Said JW, and Knowles DM.** 1995. Kaposi's Sarcoma-Associated Herpesvirus-Like DNA Sequences in AIDS-Related Body-Cavity-Based Lymphomas. *NEJM* **332**:1186-1191.
- Chen T and Hudnall SD.** 2006. Anatomical mapping of human herpesvirus reservoirs of infection. *Mod. Pathol* **19**:726-737.
- Chiou CJ, Poole LJ, Kim PS, Ciufu DM, Cannon JS, Rhys CM, Alcendor DJ, Zong JC, Ambinder RF, Hayward GS.** 2002. Patterns of gene expression and a transactivation function exhibited by the vGCR (ORF74) chemokine receptor protein of Kaposi's sarcoma-associated herpesvirus. *J Virol* **76**:3421.
- Choi J, Means RE, Damania B, and Jung JU.** 2001. Molecular piracy of Kaposi's sarcoma associated herpesvirus. *Cytokine Growth Factor Rev* **12**:245.
- Coleman HM, Efsthathiou S, and Stevenson PG.** 2005. Transcription of the murine gammaherpesvirus 68 ORF73 from promoters in the viral terminal repeats. *J Gen Virol* **86**:561-574.
- Cotter MA & Robertson ES.** 1999. The latency-associated nuclear antigen tethers the Kaposi's sarcoma associated herpesvirus genome to host chromosomes in body cavity-based lymphoma cells. *Virology* **264**:254.
- Coscoy L & Ganem D.** 2000. Kaposi's sarcoma-associated herpesvirus encodes two proteins that block cell surface display of MHC class I chains by enhancing their endocytosis. *Proc Natl Acad Sci USA* **97**:8051-8056.
- Coscoy L & Ganem D.** 2001. A viral protein that selectively downregulates ICAM-1 and B7-2 and modulates T cell costimulation. *J Clin Invest* **107**:1599-1606.
- Coscoy L, Sanchez DJ, and Ganem D.** 2001. A novel class of herpesvirus-encoded membrane-bound E3 ubiquitin ligases regulates endocytosis of proteins involved in immune recognition. *J Cell Biol* **155**:1265-1273.
- Cotter MA & Robertson ES.** 1999. The latency-associated nuclear antigen tethers the Kaposi's sarcoma-associated herpesvirus genome to host chromosomes in body cavity-based lymphoma cells. *Virology* **264**:254-264.

- Dagna L, Broccolo F, Paties CT, Ferrarini M, Sarmati L, Praderio L, Sabbadini MG, Lusso P, and Malnati MS.** 2005. A relapsing inflammatory syndrome and active human herpesvirus 8 infection. *N Engl J Med* **353**:156.
- Dhar SK, Yoshida K, Machida Y, Khaira P, Chaudhuri B, Wohlschlegel JA, Leffak M, Yates J, and Dutta A.** 2001. Replication from oriP of Epstein-Barr virus requires human ORC and is inhibited by geminin. *Cell* **106**:287-296.
- Dittmer D, Lagunoff M, Renne R, Staskus K, Haase A, and Ganem D.** 1998. A cluster of latently expressed genes in Kaposi's sarcoma-associated herpesvirus. *J Virol* **72**:8309.
- Dittmer D, Stoddart C, Renne R, Linquist-Stepps V, Moreno ME, Bare C, McCune JM, and Ganem D.** 1999. Experimental transmission of Kaposi's sarcoma-associated herpesvirus (KSHV/HHV-8) to SCID-hu Thy/Liv mice. *J Exp Med* **190**:1857-68.
- Dourmishev LA, Dourmishev AL, Palmeri D, Schwartz RA, and Lukac DM.** 2003. Molecular Genetics of Kaposi's Sarcoma-Associated Herpesvirus (Human Herpesvirus 8) Epidemiology and Pathogenesis. *Microbiology and Molecular Biology Reviews* **67**:175-212.
- Dupin N, Fisher C, Kellam P, Ariad S, Tulliez M, Franck N, van Marck E, Salmon D, Gorin I, Escande JP, Weiss RA, Alitalo K, and Boshoff C.** 1999. Distribution of human herpesvirus-8 latently infected cells in Kaposi's sarcoma, multicentric Castleman's disease, and primary effusion lymphoma. *Proc Natl Acad Sci USA* **96**:4546.
- Duprez R, Lacoste V, Briere J, Couppie P, Frances C, Sainte-Marie D, Kassa-Kelembho E, Lando MJ, Essame Oyono JL, Nkegoum B, Hbid O, Mahe A, Lebbe C, Tortevoeye P, Huerre M, and Gessain A.** 2007. Evidence for a multiclonal origin of multicentric advanced lesions of Kaposi sarcoma. *J Natl Cancer Inst* **99**:1086-1094.
- Ebrahimi B, Dutia BM, Roberts KL, Garcia-Ramirez JJ, Dickinson P, Stewart JP, Ghazal P, Roy DJ, and Nash AA.** 2003. Transcriptome profile of murine gammaherpesvirus-68 lytic infection. *J Gen Virol* **84**:99-109.
- Ehtisham S, Sunil-Chandra NP, and Nash AA.** 1993. Pathogenesis of murine gammaherpesvirus infection in mice deficient in CD4 and CD8 T cells. *J Virol* **67**:5247-5252.
- Fejer G, Medveczky MM, Horvath E, Lane B, Chang Y, and Medveczky PG.** 2003. The latency-associated nuclear antigen of Kaposi's sarcoma-associated herpesvirus interacts preferentially with the terminal repeats of the genome in vivo and this complex is sufficient for episomal DNA replication. *J Gen Virol* **84**:1451-1462.
- Foreman KE, Friborg J, Chandran B, Katano H, Sata T, Mercader M, Nabel GJ, Nickoloff BJ.** 2001. Injection of human herpesvirus-8 in human skin engrafted on SCID mice induces Kaposi's sarcoma-like lesions. *J Dermatol Sci* **26**:182-93.
- Fowler P, Marques S, Simas JP, and Efstathiou S.** 2003. ORF73 of murine herpesvirus-68 is critical for the establishment and maintenance of latency. *J Gen Virol* **84**:3405-3416.
- Feldman ER, Kara M, Coleman CB, Grau KR, Oko LM, Krueger BJ, Renne R, van Dyk LF, Tibbetts SA.** 2014. Virus-encoded microRNAs facilitate gammaherpesvirus latency and pathogenesis in vivo. *M Bio* **53**:981-14.
- Friedman-Birnbaum R, Weltfreund S, and Katz I.** 1990. Kaposi's sarcoma: retrospective study of 67 cases with the classical form. *Dermatologica* **180**:13-17.
- Gaidano G, Cechova K, Chang Y, Moore PS, Knowles DM, and Dalla-Favera R.** 1996. Establishment of AIDS related lymphoma cell lines from lymphomatous effusions. *Leukemia* **10**:1237.

- Gao SJ, Kingsley L, Hoover DR, Spira TJ, Rinaldo CR, Saah A, Phair J, Detels R, Parry P, Chang, Y, and Moore PS.** 1996. Seroconversion to antibodies against Kaposi's sarcoma-associated herpesvirus-related latent nuclear antigens before the development of Kaposi's sarcoma. *N Engl J Med* **335**:233-241.
- Garber AC, Hu J, and Renne R.** 2002. Latency-associated nuclear antigen (LANA) cooperatively binds to two sites within the terminal repeat, and both sites contribute to the ability of LANA to suppress transcription and to facilitate DNA replication. *J Biol Chem* **277**:27401-11.
- Gessain A & Duprez R.** 2005. Spindle cells and their role in Kaposi's sarcoma. *Int J Biochem Cell Biol* **37**:2457-2465.
- Griffiths R & Whitehouse A.** 2007. Herpesvirus saimiri episomal persistence is maintained via interaction between open reading frame 73 and the cellular chromosome-associated protein MeCP2. *J Virol* **81**:4021-4032.
- Grundhoff A & Ganem D.** 2003. The Latency-Associated Nuclear Antigen of Kaposi's Sarcoma-Associated Herpesvirus Permits Replication of Terminal Repeat-Containing Plasmids. *J Virol* **77**:2779-2783.
- Hu J & Renne R.** 2005. Characterization of the minimal replicator of Kaposi's sarcoma-associated herpesvirus latent origin. *J Virol* **79**:2637.
- Hung SC, Kang MS, and Kieff E.** 2001. Maintenance of Epstein-Barr virus (EBV) oriP-based episomes requires EBV-encoded nuclear antigen-1 chromosome-binding domains, which can be replaced by high-mobility group-I or histone H1. *Proc Natl Acad Sci USA* **98**:1865-1870.
- Ilves I, Kivi S, and Ustav M.** 1999. Long-term episomal maintenance of bovine papillomavirus type 1 plasmids is determined by attachment to host chromosomes, which is mediated by the viral E2 protein and its binding sites. *J Virol* **73**:4404-4412.
- Iscovich J, Boffetta P, and Brennan P.** 1999. Classic Kaposi's sarcoma as a first primary neoplasm. *Int J Cancer* **80**:173-177.
- Ishido S, Choi JK, Lee BS, Wang C, DeMaria M, Johnson RP, Cohen GB, and Jung JU.** 2000. Inhibition of natural killer cell-mediated cytotoxicity by Kaposi's sarcoma-associated herpesvirus K5 protein. *Immunity* **13**:365-374.
- Jenner RG, Alba MM, Boshoff C, and Kellam P.** 2001. Kaposi's sarcoma-associated herpesvirus latent and lytic gene expression as revealed by DNA arrays. *J Virol* **75**:891-902.
- Jenner RG and Boshoff C.** 2002. The molecular pathology of Kaposi's sarcoma-associated herpesvirus. *Biochim. Biophys. Acta.* **1602**:1-22.
- Judde JG, Lacoste V, Briere J, Kassa-Kelembho E, Clyti E, Couppie P, Buchrieser C, Tulliez M, Morvan J, and Gessain A.** 2000. Monoclonality or oligoclonality of human herpesvirus 8 terminal repeat sequences in Kaposi's sarcoma and other diseases. *J Natl Cancer Inst* **92**:729-736.
- Katano H, Iwasaki T, Baba N, Terai M, Mori S, Iwamoto A, Kurata T, and Sata T.** 2000. Identification of antigenic proteins encoded by human herpesvirus 8 and seroprevalence in the general population and among patients with and without Kaposi's sarcoma. *J Virol* **74**:3478-3485.
- Kalt I, Masa SR, and Sarid R.** 2009. Linking the Kaposi's sarcoma-associated herpesvirus (KSHV/HHV-8) to human malignancies. *Methods Mol Biol* **471**:387-407.

- Kedes DH, Operskalski E, Busch M, Kohn R, Flood J, and Ganem D.** 1996. The seroepidemiology of human herpesvirus 8 (Kaposi's sarcoma-associated herpesvirus): distribution of infection in KS risk groups and evidence for sexual transmission. *Nat Med* **2**:918-924.
- Keller SA, Hernandez-Hopkins D, Vider J, Ponomarev V, Hyjek E, Schattner EJ, and Cesarman E.** 2006. NF-kappaB is essential for the progression of KSHV- and EBV-infected lymphomas in vivo. *Blood* **107**:3295-302.
- Kelley-Clarke B, Ballestas ME, Komatsu T, and Kaye KM.** 2007. Kaposi's sarcoma herpesvirus C-terminal LANA concentrates at pericentromeric and peri-telomeric regions of a subset of mitotic chromosomes. *Virology* **357**:149-157.
- Kelley-Clarke B, De Leon-Vazquez E, Slain K, Barbera AJ, and Kaye KM.** 2009. Role of Kaposi's sarcoma-associated herpesvirus C-terminal LANA chromosome binding in episome persistence. *J Virol* **83**:4326-4337.
- Komatsu T, Ballestas ME, Barbera AJ, Kelley-Clarke B, and Kaye, KM.** 2004. KSHV LANA1 binds DNA as an oligomer and residues N-terminal to the oligomerization domain are essential for DNA binding, replication, and episome persistence. *Virology* **319**:225-236.
- Krithivas A, Fujimuro M, Weidner M, Young BD, and Hayward SD.** 2002. Protein interactions targeting the latency-associated nuclear antigen of Kaposi's sarcoma-associated herpesvirus to cell chromosomes. *J Virol* **76**:11596-11604.
- Lan K, Koppers DA, Verma SC, Sharma N, Murakami M, and Robertson ES.** 2005. Induction of Kaposi's sarcoma-associated herpesvirus latency-associated nuclear antigen by the lytic transactivator RTA: A novel mechanism for establishment of latency. *J Virol* **79**:7453.
- Lehman CW & Botchan MR.** 1998. Segregation of viral plasmids depends on tethering to chromosomes and is regulated by phosphorylation. *Proc Natl Acad Sci* **95**:4338-4343.
- Lenette ET, Blackbourn DJ, and Levy JA.** 1996. Antibodies to human herpesvirus type 8 in the general population and in Kaposi's sarcoma patients. *Lancet* **348**:858.
- Martinez-Guzman D, Rickabaugh T, Wu TT, Brown H, Cole S, Song MJ, Tong L, and Sun R.** 2003. Transcription program of murine gammaherpesvirus 68. *J Virol* **77**:10488-10503.
- Mayama S, Cuevas LE, Sheldon J, Omar OH, Smith DH, Okong P, Silvel B, Hart CA, and Schulz TF.** 1998. Prevalence and transmission of Kaposi's sarcoma-associated herpesvirus (human herpesvirus 8) in Ugandan children and adolescents. *Int J Cancer* **77**:817-820.
- Means RE, Choi JK, Nakamura H, Chung YH, Ishido S, and Jung JU.** 2002. Immune evasion strategies of Kaposi's sarcoma-associated herpesvirus. *Curr Top Microbiol Immunol* **269**:187.
- Medveczky MM, Horvath E, Lund T, and Medveczky PG.** 1997. In vitro antiviral drug sensitivity of the Kaposi's sarcoma-associated herpesvirus. *AIDS* **11**:1327-32.
- Mesri EA, Cesarman E, and Boshoff C.** 2010. Kaposi's sarcoma and its associated herpesvirus. *Nat. Rev. Cancer* **10**:707-719.
- Molden J, Chang Y, You Y, Moore PS, and Goldsmith MA.** 1997. A Kaposi's sarcoma-associated herpesvirus encoded cytokine homolog (vIL-6) activates signaling through the shared gp130 receptor subunit. *J Biol Chem* **272**:19625.
- Moore PS, Gao SJ, Dominguez G, Cesarman E, Lungu O, Knowles DM, Garber R, Pellett PE, McGeoch DJ, and Chang Y.** 1996. Primary characterization of a herpesvirus agent associated with Kaposi's sarcomae. *J Virol* **70**:549-58.

- Moore PS & Chang Y.** 1998. Antiviral activity of tumor-suppressor pathways: clues from molecular piracy by KSHV. *Trends Genet* **14**:144-150.
- Moorman NJ, Willer DO, and Speck SH.** 2003. The gammaherpesvirus 68 latency-associated nuclear antigen homolog is critical for the establishment of splenic latency. *J Virol* **77**:10295-10303.
- Mutlu AD, Cavallin LE, Vincent L, Chiozzini C, Eroles P, Duran EM, Asgari Z, Hooper AT, La Perle KM, Hilsher C, Gao SJ, Dittmer DP, Rafii S, and Mesri EA.** 2007. *In vivo*-restricted and reversible malignancy induced by human herpesvirus-8 KSHV: a cell and animal model of virally induced Kaposi's sarcoma. *Cancer Cell* **11**:245–258.
- Orzechowska BU, Powers MF, Sprague J, Li H, Yen B, Searles RP, Axthelm MK, and Wong SW.** 2008. Rhesus macaque rhadinovirus-associated non-Hodgkin lymphoma: animal model for KSHV-associated malignancies. *Blood* **112**:4227–4234.
- Pan H, Zhou F, and Gao SJ.** 2004. Kaposi's sarcoma-associated herpesvirus induction of chromosome instability in primary human endothelial cells. *Cancer Res* **64**:4064.
- Parsons CH, Adang LA, Overdevest J, O'Connor CM, Taylor JR Jr, Camerini D, and Kedes DH.** 2006. KSHV targets multiple leukocyte lineages during long-term productive infection in NOD/SCID mice. *J Clin Invest* **116**:1963-73.
- Paulose-Murphy M, Ha NK, Xiang C, Chen Y, Gillim L, Yarchoan R, Meltzer P, Bittner M, Trent J, and Zeichner S.** 2001. Transcription program of human herpesvirus 8 (kaposi's sarcoma-associated herpesvirus), *J. Virol* **75**:4843–4853.
- Parravinci C, Corbellino M, Paulli M, Magrini U, Lazzarino M, Moore PS, and Chang Y.** 1997. Expression of a virus-derived cytokine, KSHV vIL-6, in HIV-seronegative Castleman's disease. *Am J Pathol* **151**:1517-1522.
- Pearce M, Matsumura S, and Wilson AC.** 2005. Transcripts encoding K12, v-FLIP, v-cyclin, and the microRNA cluster of Kaposi's sarcoma-associated herpesvirus originate from a common promoter. *J Virol* **79**:14457-14464.
- Penn I.** 1988. Secondary neoplasms as a consequence of transplantation and cancer therapy. *Cancer Detect Prev* **12**:39-57.
- Piolot T, Tramier M, Coppey M, Nicolas JC, and Marechal V.** 2001. Close but distinct regions of human herpesvirus 8 latency-associated nuclear antigen 1 are responsible for nuclear targeting and binding to human mitotic chromosomes. *J Virol* **75**:3948-3959.
- Platt GM, Simpson GR, Mitnacht S, and Schulz TF.** 1999. Latent nuclear antigen of Kaposi's sarcoma-associated herpesvirus interacts with RING3, a homolog of the *Drosophila* female sterile homeotic (fsh) gene. *J Virol* **73**:9789-9795.
- Raab MS, Albrecht JC, Birkmann A, Yaguboglu S, Lang D, Fleckenstein B, and Neipel F.** 1998. The immunogenic glycoprotein gp35-37 of human herpesvirus 8 is encoded by open reading frame K8.1. *J Virol* **72**:6725-6731.
- Renne R, Zhong W, Herndier B, McGrath M, Abbey N, Kedes D, and Ganem D.** 1996. Lytic growth of Kaposi's sarcoma-associated herpesvirus (human herpesvirus 8) in culture. *Nat Med* **2**:342–346.
- Rochford R, Lutzke ML, Alfinito RS, Clavo A, and Cardin RD.** 2001. Kinetics of murine gammaherpesvirus 68 gene expression following infection of murine cells in culture and in mice. *J. Virol.* **75**:4955-4963.
- Rossetto C, Gao Y, Yamboliev I, Papouskova I, and Pari G.** 2007. Transcriptional repression of K-Rta by Kaposi's sarcoma-associated herpesvirus K-bZIP is not required for oriLyt-dependent DNA replication. *Virology* **369**:340–350.

- Roizmann B, Desrosiers RC, Fleckenstein B, Lopez C, Minson AC, and Studdert MJ.** 1992. The family Herpesviridae: an update. The Herpesvirus Study Group of the International Committee on Taxonomy of Viruses. *Arch Virol* **123**:425-449.
- Roizman B & Pellett PE.** The family Herpesviridae: A Brief Introduction. In: Knipe DM, Howley PM, Griffin DE, Lamb RA, Martin, MA, Roizman B, and Straus SE. (ed.), *Virology*, 4th edition. 2002. Lippincott, Williams, and Wilkins, Philadelphia, PA: 2381-2397.
- Russo JJ, Bohenzky RA, Chien MC, Chen J, Yan M, Maddalena D, Parry JP, Peruzzi D, Eman IS, Chang Y, and Moore PS.** 1996. Nucleotide sequence of the Kaposi sarcoma-associated herpesvirus (HHV8). *PNAS* **93**:14862-14867.
- Samols MA, Hu J, Skalsky RL, and Renne, R.** 2005. Cloning and identification of a microRNA cluster within the latency-associated region of Kaposi's sarcoma-associated herpesvirus. *J Virol* **79**:9301-9305.
- Schwam DR, Luciano RL, Mahajan SS, Wong L, and Wilson AC.** 2000. Carboxy terminus of human herpesvirus 8 latency-associated nuclear antigen mediates dimerization, transcriptional repression, and targeting to nuclear bodies. *J Virol* **74**:8532-8540.
- Sears J, Ujihara M, Wong S, Ott C, Middeldorp J, and Aiyar A.** 2004. The amino terminus of Epstein-Barr Virus (EBV) nuclear antigen 1 contains AT hooks that facilitate the replication and partitioning of latent EBV genomes by tethering them to cellular chromosomes. *J Virol* **78**:11487-11505.
- Simas JP and Efstathiou S.** 1998. Murine gammaherpesvirus 68: a model for the study of gammaherpesvirus pathogenesis. *Trends Microbiol* **6**:276-82.
- Simpson GR, Schulz TF, Whitby D, Cook PM, Boshoff C, Rainbow L, Howard MR, Gao SJ, Bohenzky RA, Simmonds P, Lee C, De Ruiter A, Hatzakis A, Tedder RS, Weller IV, Weiss RA, and Moore PS.** 1996. Prevalence of Kaposi's sarcoma associated herpesvirus infection measured by antibodies to recombinant capsid protein and latent immunofluorescence antigen. *Lancet* **348**:1133-1138.
- Skalsky RL, Hu J, and Renne R.** 2007. Analysis of viral cis elements conferring Kaposi's sarcoma-associated herpesvirus episome partitioning and maintenance. *J Virol* **81**:9825.
- Soulier J, Grollet L, Oksenhendler E, Cacoub P, Cazals Hatem D, Babinet P, d'Agay MF, Clauvel JP, Raphael M and Degos L.** 1995. Kaposi's sarcoma-associated herpesvirus-like DNA sequences in multicentric Castlemann's disease. *Blood* **8**:1276-1280.
- Staskus KA, Zhong W, Gebhard K, Herndier B, Wang H, Renne R, Beneke J, Pudney J, Anderson DJ, Ganem D, and Haase AT.** 1997. Kaposi's sarcoma-associated herpesvirus gene expression in endothelial (spindle) tumor cells. *J Virol* **71**:715.
- Staudt MR, Kanan Y, Jeong JH, Papin JF, Hines-Boykin R, and Dittmer DP.** 2004. The tumor microenvironment controls primary effusion lymphoma growth in vivo. *Cancer Res* **64**:4790-9.
- Sun Q, Tsurimoto T, Juillard F, Li L, Li S, De León Vázquez E, Chen S, Kaye K.** 2014. Kaposi's sarcoma-associated herpesvirus LANA recruits the DNA polymerase clamp loader to mediate efficient replication and virus persistence. *Proc Natl Acad Sci USA* **111**:11816-21.
- Sunil-Chandra NP, Arno J, Fazakerley J, and Nash AA.** 1994. Lymphoproliferative disease in mice infected with murine gammaherpesvirus 68. *Am J Pathol* **145**:818-26.
- Sunil-Chandra NP, Efstathiou S, Arno J, and Nash AA.** 1992. Virological and pathological features of mice infected with murine gamma-herpesvirus 68. *J Gen Virol* **73**:2347-2356. 1992.
- Tye BK.** 1999. MCM proteins in DNA replication. *Annu Rev Biochem* **68**:649-686.

- Usherwood EJ, Stewart JP, Robertson K, Allen DJ, and Nash AA.** 1996. Absence of splenic latency in murine gammaherpesvirus 68-infected B cell-deficient mice. *J Gen Virol* **77**:2819-2825.
- Verma SC, Lan K, Choudhuri T, Cotter MA, and Robertson ES.** 2007. An autonomous replicating element within the KSHV genome. *Cell Host Microbe* **2**:106.
- Virgin HWt, Latreille P, Wamsley P, Hallsworth K, Weck E, Dal Canto AJ, and Speck SH.** 1997. Complete sequence and genomic analysis of murine gammaherpesvirus 68. *J Virol* **71**:5894-5904.
- Wabinga HR, Parkin DM, Wabwire-Mangen F, and Mugerwa JW.** 1993. Cancer in Kampala, Uganda, in 1989-91: changes in incidence in the era of AIDS. *Int J Cancer* **54**:26-36.
- Wang LX, Kang G, Kumar P, Lu W, Li Y, Zhou Y, Li Q, and Wood C.** 2014. Humanized-BLT mouse model of Kaposi's sarcoma-associated herpesvirus infection. *Proc Natl Acad Sci USA* **111**:3146-51.
- Wen KW & Damania B.** 2010. Kaposi sarcoma-associated herpesvirus (KSHV): molecular biology and oncogenesis. *Cancer Lett* **289**:140-150.
- West JT & Wood C.** 2003. The role of Kaposi's sarcoma-associated herpesvirus/human herpesvirus-8 regulator of transcription activation (RTA) in control of gene expression. *Oncogene* **22**:5150.
- Winceslaus J.** 1998. Regression of AIDS-related pleural effusion with HAART. Highly active antiretroviral therapy. *Int J STD AIDS* **9**:368-370.
- Wu H, Ceccarelli DF, and Frappier L.** 2000. The DNA segregation mechanism of Epstein-Barr virus nuclear antigen 1. *EMBO Reports* **1**:140-144.
- Xie J, Pan H, Yoo S, and Gao SJ.** 2005. Kaposi's sarcoma-associated herpesvirus induction of AP-1 and interleukin 6 during primary infection mediated by multiple mitogen-activated protein kinase pathways. *J Virol* **79**:15027.
- Xuan Y, Liu L, Shen S, Deng H, Gao G.** 2012. Zinc finger antiviral protein inhibits murine gammaherpesvirus 68 M2 expression and regulates viral latency in cultured cells. *J Virol* **86**:12431-4.
- Ziegler JL & Katongole-Mbidde E.** 1996. Kaposi's sarcoma in childhood: an analysis of 100 cases from Uganda and relationship to HIV infection. *Int J Cancer* **65**:200-203.

3 Murine Gammaherpesvirus 68 LANA Acts on Terminal Repeat DNA to Mediate Episome Persistence

Aline C. Habison^a, Chantal Beauchemin^a, J. Pedro Simas^b, Edward J. Usherwood^c,
and Kenneth M. Kaye^a

Murine Gammaherpesvirus 68 LANA Acts on Terminal Repeat DNA To Mediate Episome Persistence

Aline C. Habison,^a Chantal Beauchemin,^a J. Pedro Simas,^b Edward J. Usherwood,^c and Kenneth M. Kaye^a

Channing Laboratory and Departments of Medicine, Brigham and Women's Hospital and Harvard Medical School, Boston, Massachusetts, USA^a; Instituto de Microbiologia e Instituto de Medicina Molecular, Faculdade de Medicina, Universidade de Lisboa, Lisbon, Portugal^b; and Department of Microbiology and Immunology, Dartmouth Medical School, Lebanon, New Hampshire, USA^c

Murine gammaherpesvirus 68 (MHV68) ORF73 (mLANA) has sequence homology to Kaposi's sarcoma-associated herpesvirus (KSHV) latency-associated nuclear antigen (LANA). LANA acts on the KSHV terminal repeat (TR) elements to mediate KSHV episome maintenance. Disruption of mLANA expression severely reduces the ability of MHV68 to establish latent infection in mice, consistent with the possibility that mLANA mediates episome persistence. Here we assess the roles of mLANA and MHV68 TR (mTR) elements in episome persistence. mTR-associated DNA persisted as an episome in latently MHV68-infected tumor cells, demonstrating that the mTR elements can serve as a *cis*-acting element for MHV68 episome maintenance. In some cases, both control vector and mTR-associated DNAs integrated into MHV68 episomal genomes. Therefore, we also assessed the roles of mTRs as well as mLANA in the absence of infection. DNA containing both mLANA and mTRs in *cis* persisted as an episome in murine A20 or MEF cells. In contrast, mTR DNA never persisted as an episome in the absence of mLANA. mLANA levels were increased when mLANA was expressed from its native promoters, and episome maintenance was more efficient with higher mLANA levels. Increased numbers of mTRs conferred more efficient episome maintenance, since DNA containing mLANA and eight mTR elements persisted more efficiently in A20 cells than did DNA with mLANA and two or four mTRs. Similar to KSHV LANA, mLANA broadly associated with mitotic chromosomes but relocalized to concentrated dots in the presence of episomes. Therefore, mLANA acts on mTR elements to mediate MHV68 episome persistence.

Murine gammaherpesvirus 68 (MHV68 or murid herpesvirus 4) is a gamma-2 herpesvirus that was isolated from a naturally infected rodent, the bank vole (*Clethrionomys glareolus*) (7, 8). Similar to the case with other gamma-2 herpesviruses, following viral replication at the primary site of inoculation, latent, persistent MHV68 infection occurs. MHV68 predominantly latently infects B cells, but latent infection also occurs in epithelial cells, macrophages, and dendritic cells (22, 23, 46, 49, 59, 67). The establishment of latent infection in mice causes an infectious mononucleosis-like syndrome with lymphocyte activation (20).

MHV68 is genetically similar to other gammaherpesviruses, including the human Kaposi's sarcoma-associated herpesvirus (KSHV; also known as human herpesvirus 8 [HHV-8]) (a gamma-2 herpesvirus) and Epstein-Barr virus (EBV) (a gamma-1 herpesvirus), both of which are associated with human malignancies (26, 39, 53, 57). For example, the ~118-kb unique sequence of MHV68 features a GC content of 46% and contains ~1.2-kb terminal repeat (TR) elements that are 78% GC rich, while the KSHV genome contains an ~140-kb unique sequence with a GC content of 54% and 0.8-kb TR elements that are 85% GC rich (54, 64). Moreover, the ~80 open reading frames (ORFs) carried by the MHV68 genome are largely colinear with those of the genomes of KSHV, EBV, and other gammaherpesviruses, such as herpesvirus saimiri (HVS), a New World monkey virus (1). MHV68 infection of mice is often used as a tractable small-animal model for gammaherpesviruses and is particularly relevant for KSHV (24, 56, 58).

During latency, the gammaherpesvirus genome persists as a circularized, extrachromosomal episome (plasmid) (16, 17, 61). Therefore, in order to persist in proliferating cells, the episomal genomes must replicate and segregate to daughter nuclei. In latently infected cells, only a limited subset of genes is expressed (46,

57). Among them, ORF73 is known to be responsible for viral episome maintenance in at least two other gamma-2 herpesviruses, i.e., HVS and KSHV (3, 4, 10, 13, 63).

KSHV ORF73 encodes the latency-associated nuclear antigen (LANA) (54) (Fig. 1A). LANA is a 1,162-amino-acid viral protein that mediates KSHV episome persistence (3, 4). C-terminal LANA binds specific sequence in the KSHV TR element to mediate its replication, and this binding is essential for episome maintenance (4, 15, 21, 27, 28, 32, 33, 41, 45). In addition, N- and C-terminal LANA regions associate with mitotic chromosomes (5, 36, 37, 42, 44, 51, 69). N-terminal LANA attaches to mitotic chromosomes through binding of core histones H2A and H2B (6). Through simultaneous binding of KSHV DNA and chromosomes, LANA tethers the viral episome to mitotic host chromosomes to ensure efficient episome segregation to daughter nuclei during cellular division. Therefore, KSHV LANA allows genome persistence by mediating both viral DNA replication and segregation of episomes to progeny nuclei.

MHV68 ORF73 (mLANA) is homologous to KSHV LANA, particularly in the C-terminal domain (Fig. 1A). mLANA is comprised of 314 amino acids, which is considerably smaller than the 1,162-amino-acid KSHV LANA (64). Most of the difference in size is due to the absence of internal acidic and glutamine-rich repeat elements in mLANA. Recombinant MHV68 disrupted for

Received 27 June 2012 Accepted 13 August 2012

Published ahead of print 22 August 2012

Address correspondence to Kenneth M. Kaye, kkaye@rics.bwh.harvard.edu.

Copyright © 2012, American Society for Microbiology. All Rights Reserved.

doi:10.1128/JVI.01656-12

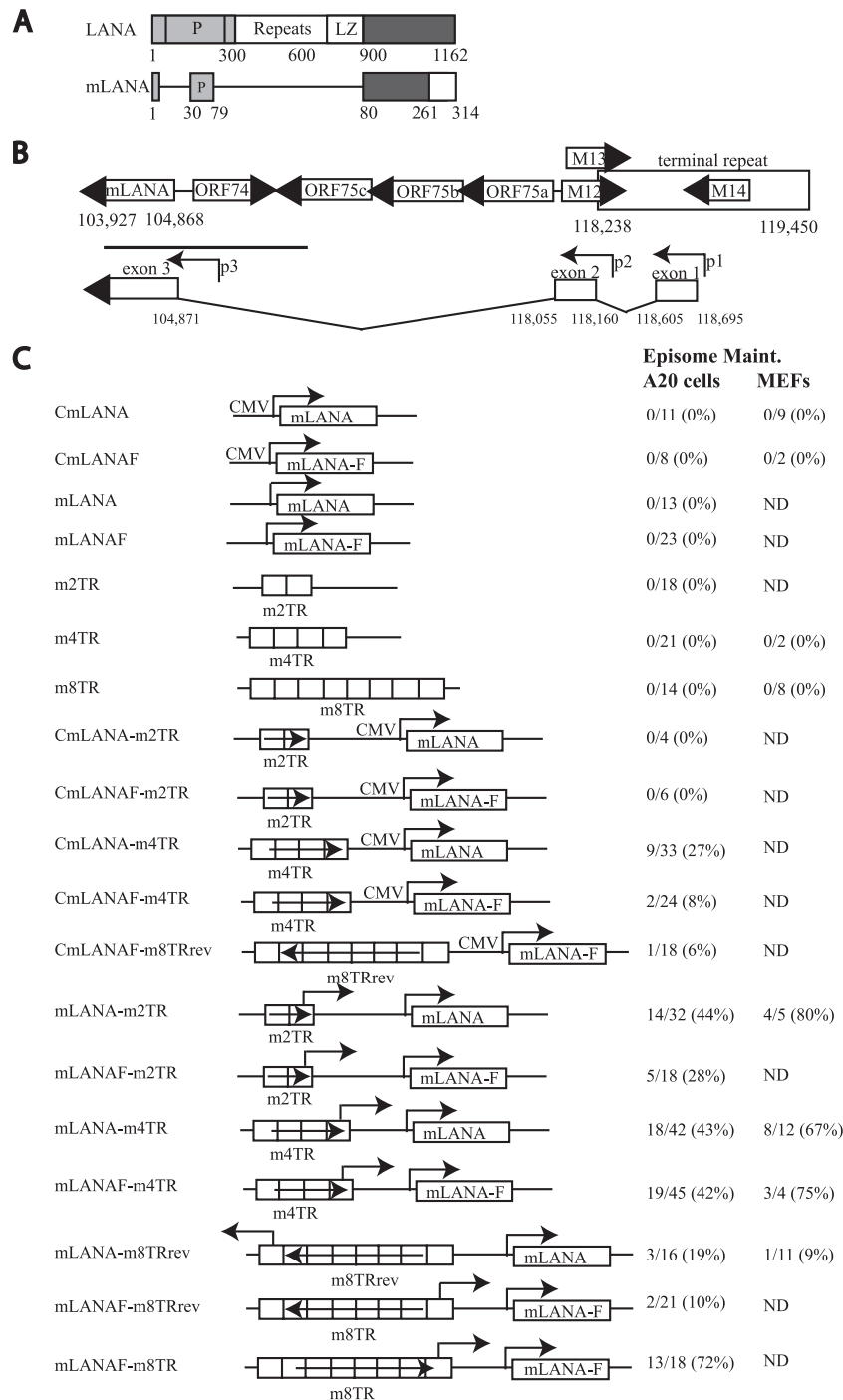


FIG 1 Schematic diagrams. (A) Comparison of KSHV LANA and mLANA. Homologous regions are shown with similar shading. Unshaded regions lack homology. The C-terminal domains (darkly shaded) share the highest level of homology. C-terminal KSHV LANA mediates self-association, DNA binding, and chromosome association. N-terminal KSHV LANA (residues 1 to 32) mediates chromosome association through interaction with histones H2A and H2B and includes a nuclear localization signal. Amino acid residues are indicated. P, proline-rich region; LZ, predicted leucine zipper. (B) Schematic diagram of mLANA transcription from the MHV68 genome. MHV68 ORFs are indicated. The three potential LANA promoters, p1, p2, and p3, are indicated. Genomic nucleotide positions are indicated for the terminal repeat, the mLANA ORF, and exons 1, 2, and 3 (2, 12). When expressed from an upstream mTR element, multiple exon 1 copies are present in transcripts. A second exon (not shown) in the mTR (located at positions 119,373 to 119,195) can be driven by promoter p2 from an upstream mTR element, and a single copy of this exon is then spliced to exon 1 copies (12, 34). The line drawn above exon 3 and promoter 3 and extending into ORF75c indicates the sequence upstream of mLANA included in the native promoter constructs used in this work. (C) Schematic diagrams of mLANA and mTR constructs used in this work. Promoters are indicated. One arrow is used in the mTRs to represent the two potential promoters present in each of the mTRs (see panel A and Discussion for details). Arrows within the mTR elements indicate the direction relative to mLANA. In the native genomic MHV68 orientation, the arrow points toward mLANA. Summaries of numbers of G418-resistant cell lines positive for episomes over the total number tested, with percentages in parentheses, are shown at right for A20 and MEF cells. ND, not determined.

mLANA expression is highly compromised in the ability to establish efficient latent infection and persistence in mice (25, 48, 50). These data are consistent with the possibility that mLANA may mediate episome persistence of MHV68 DNA. In addition, since LANA acts on the KSHV TRs to mediate episome persistence, it is possible that mLANA may act on the MHV68 TR (mTR) elements to mediate episome maintenance.

In this work, we evaluated whether mLANA acts on the mTR elements to mediate episome persistence of MHV68 DNA. We found that a plasmid containing mTR elements can persist as an episome in an MHV68-infected mouse tumor cell line. Furthermore, plasmids containing mLANA and mTR elements in *cis* were capable of persisting as episomes in uninfected cells. These findings indicate that mLANA acts on the MHV68 TR elements to maintain viral episomes, analogous to the effect of LANA on the KSHV TRs.

MATERIALS AND METHODS

Cell lines. A20 murine B lymphoma cells (40) were cultured in RPMI medium supplemented with 10% Fetalplex (Gemini) or bovine growth serum (BGS) (HyClone), beta mercaptoethanol, sodium pyruvate, Glutamax (Invitrogen), and 15 μ g/ml gentamicin. Baby hamster kidney (BHK) cells and mouse embryonic fibroblast (MEF) cells were maintained in Dulbecco's modified Eagle's medium (DMEM) supplemented with 10% BGS, beta mercaptoethanol, and 15 μ g/ml gentamicin. S11 cells (61) were maintained in RPMI medium supplemented with 20% BGS supplemented with beta mercaptoethanol.

Virus infection and purification. BHK21 cells at ~75% confluence in five 500-cm² cell culture dishes were infected with MHV68 at a multiplicity of infection of 0.001 in DMEM containing 2% Fetalplex (12 ml/dish) for 1 h at 37°C. Fifty milliliters of DMEM containing 10% Fetalplex was then added, and cells were incubated for 3 days, at which time plaques were evident. Cells were trypsinized, collected by centrifugation, and incubated in 1.5 ml RSB buffer (10 mM Tris-HCl, pH 7.5, 10 mM KCl, 1.5 mM MgCl₂) per plate, supplemented with 0.5% NP-40, for 10 min at 4°C. Centrifugation was then performed to remove nuclei, and the supernatant was collected. Centrifugation of the supernatant in microcentrifuge tubes was performed at 20,800 \times g for 2 h at 4°C. Pellets containing virus were resuspended in 400 μ l NTE buffer (100 mM NaCl, 10 mM Tris-HCl, pH 7.5, 1 mM EDTA) by sonication. SDS and additional EDTA were then added to final concentrations of 2.5% SDS and 10 mM EDTA, and incubation was performed for 5 min at 37°C. Virus DNA was purified using DNAzol (Invitrogen) according to the manufacturer's instructions.

Plasmids. MHV-68 TR (mTR) elements were cloned from purified MHV68 DNA. First, virus DNA was digested with Tsp509I, which digests frequently in the unique sequence but not in the mTRs. Subsequently, partial NotI digestion was performed. mTR elements each have one NotI site. Fragments containing two, four, and eight TR copies were gel purified and ligated into the NotI site of the pRepCK vector (4) to generate m2TR, m4TR, and m8TR, respectively (Fig. 1C).

Plasmids expressing mLANA from a cytomegalovirus (CMV) promoter were constructed. Linker NS contains NsiI and StuI sites and was generated by annealing the sequences NSfwd (TC GAG ATG CAT GCT CGA TAC AGC AGG CCT AAG G) and NSrev (GA TCC CTT AGG CCT GCT GTA TCG AGC ATG CAT C). Linker NS was then inserted into pRepCK, m2TR, m4TR, and m8TR, after digestion of each with XhoI and BamHI, to generate pRepCK-NS, m2TR-NS, m4TR-NS, and m8TR-NS, respectively. To generate pCMVFmLANA, mLANA was amplified from MHV68 DNA by using the primers mLANAfwd (CGC GGA TCC ATG CCC ACA TCC CCA CCG) and mLANArev1 (TCG ATA TCT TAT GTC TGA GAC CCT TGT CC), which add a BamHI site upstream of mLANA and an EcoRV site immediately downstream of mLANA. The PCR product was digested with BamHI and EcoRV and inserted into the BamHI and EcoRV sites of pCMV-3Tag-6 (Stratagene), resulting in pCMVFmLANA,

which contains a 3 \times FLAG tag upstream of mORF73. The 3 \times FLAG tag was then removed by digestion with BamHI and NotI, and the sites were blunted and ligated, resulting in pCMVmLANA. pCMVmLANA was digested with NsiI and PciI, releasing the CMVmLANA expression cassette, and this was inserted into the NsiI and StuI sites of pRepCK vector-NS, m2TR-NS, and m4TR-NS to generate CmLANA, CmLANA-m2TR, and CmLANA-m4TR, respectively. These constructs contain mLANA without an epitope tag driven by the CMV promoter and containing 0, 2, or 4 mTRs.

Constructs containing 3 \times C-terminal FLAG-tagged mLANA driven by a CMV promoter were generated. pCMVmLANAF was constructed in the same fashion as pCMVFmLANA, except that the PCR amplification of mLANA was performed with primers mLANAfwd and mLANArev2 (TCG ATA TCT GTC TGA GAC CCT TGT CC). mLANArev2 omits the native mLANA stop codon and contains an EcoRV site at its 5' end. The N-terminal 3 \times FLAG tag was removed with BamHI and NotI as described above. The 3 \times FLAG tag was PCR amplified from pCMV-3Tag-6 with oligonucleotides FLAG fwd (CGG ATA TCG CGG TGG CGG CCG CC) and FLAG rev (CCG GCT CGA GTT AGA ATT CCT GCA GCC CGG G), which add a stop codon immediately downstream of the 3 \times FLAG tag and EcoRV and XhoI sites at the 5' and 3' ends, respectively. The PCR product was digested with EcoRV and XhoI and inserted into the EcoRV and XhoI sites (of the vector polylinker) in pCMVmLANA, lacking the native stop codon, to generate pCMVmLANAF, which contains a C-terminal 3 \times FLAG epitope-tagged mLANA sequence driven by the CMV promoter. The CMV mLANA FLAG expression cassette was released by digestion with NsiI and PciI and inserted into the NsiI and StuI sites of pRepCK-NS, m2TR-NS, m4TR-NS, and m8TR-NS to generate CmLANAF, CmLANAF-m2TR, CmLANAF-m4TR, and CmLANAF-m8TRrev, respectively (Fig. 1C).

Plasmids containing mLANA driven from its native promoter were generated. Oligonucleotides m73fwd and m73rev were used to amplify the mLANA sequence, including 2,037 bp upstream of the mLANA open reading frame, from MHV68 DNA.

Oligonucleotide m73fwd (CAGCTCGAGATCCAGACTTTGGAGCA TATGTTT) contains an XhoI site at the 5' end, and oligonucleotide m73rev (CGCGGATCCTTATGTCTGAGACCCTTGTC) contains a BamHI site at its 5' end. The PCR product was digested with XhoI and BamHI, gel purified, and inserted into XhoI- and BamHI-digested pRepCK, m2TR, m4TR, and m8TR to generate mLANA, mLANA-m2TR, mLANA-m4TR, and mLANA-m8TRrev, respectively (Fig. 1C). To generate mLANA-m8TR, mLANA-2TR (Fig. 1C) was digested with NheI and XhoI to remove the mTR elements, and a linker containing the XhoI, NsiI, SacI, StuI, and NheI restriction sites was generated by annealing oligonucleotides NXfwd (CTAGGCTCGAGATGCATGAGCTCAGGCCTGCTA GCG) and NXrev (TCGACGCTAGCAGGCCTGAGCTCATGCATCTC GAGC) and inserted into the NheI and XhoI sites. The linker construction destroyed the original NheI and XhoI sites in the parent plasmid, and the inserted sites resulted in reversing the orientation of XhoI and NheI compared to the original vector. m8TR was digested with XhoI and NheI, removing the 8 mTR units, and these were inserted into the XhoI and NheI sites of the plasmid containing the linker to generate mLANA-m8TR, which contains the 8 mTR units in opposite orientation compared with mLANA-m8TRrev and results in the native genomic orientation of the mTRs relative to mLANA.

C-terminal mLANA FLAG epitope tags were inserted into constructs expressing mLANA from its native promoter. pCMVmLANAF (described above) was digested with PciI and PciI, releasing a C-terminal portion of the mLANAF expression cassette, and this fragment was inserted into PciI- and HpaI-digested mLANA, mLANA-m2TR, mLANA-m4TR, mLANA-m8TRrev, and mLANA-m8TR to generate mLANAF, mLANAF-m2TR, mLANAF-m4TR, mLANAF-m8TRrev, and mLANAF-m8TR, respectively (Fig. 1C). All PCR-amplified coding sequences were confirmed by sequencing. Clones were expanded in Stbl2 (Invitrogen)

bacteria for large-scale DNA preparations due to the greater stability of the repeat elements in these bacteria.

Episome maintenance assays. S11 cells were maintained in log-phase growth by reseeding at 0.2×10^6 cells/ml for three consecutive days. A total of 10×10^6 cells were transfected by electroporation with 35 μ g of m4TR, m8TR, or vector (pRepCK) in 400 μ l, using a BTX Electrosquare Porator T820 electroporation system, pulsing the cells once at 200 V for 65 milliseconds. Immediately after transfection, cells were supplemented with 0.5 ml of medium in the cuvette and incubated at room temperature for 10 min. Cells were then transferred to T25 flasks in 5 ml medium. At 3 days posttransfection, cells were seeded at 10,000 or 1,000 cells per well in 96-well plates in medium containing G418 (400 μ g/ml) (Gemini). G418-resistant cells were then expanded in preparation for detection of episomes.

A20 cells were kept in log-phase growth by reseeding at 0.3×10^6 cells/ml for three consecutive days. A total of 10×10^6 A20 cells were transfected with 35 μ g vector (pRepCK), mLANA, CmLANA, mLANAF, CmLANAF, m2TR, m4TR, m8TR, m73-m2TR, mLANA-m4TR, mLANA-m8TR, mLANA-m8TRrev, mLANAF-m2TR, mLANAF-m4TR, mLANAF-m8TR, mLANAF-m8TRrev, CmLANA-m2TR, CmLANA-m4TR, CmLANAF-m2TR, CmLANAF-m4TR, or CmLANAF-m8TRrev in 400 μ l by electroporation using a BTX Electrosquare Porator T820 electroporation system, pulsing the cells once at 225 or 250 V for 65 milliseconds. After transfection, cells were treated similarly to S11 cells, except that at 72 h posttransfection cells were seeded at 1,000, 100, or 10 cells per well in medium containing G418 (400 μ g/ml) (Gemini) and G418-resistant cells expanded.

MEF cells were transfected with 2 μ g of mLANA, m8TR, mLANA-m8TRrev, mLANA-m2TR, mLANA-m4TR, or mLANAF-m4TR in 6-cm dishes at about 75% confluence, using Effectene transfection reagent (Qiagen) according to the manufacturer's instructions. Two days after transfection, cells were trypsinized, counted, and seeded at 10,000 or 50,000 cells in a 15-cm dish. The next day, cells were rinsed with phosphate-buffered saline, and fresh medium containing G418 (1,000 μ g/ml) (Gemini) was added. G418-resistant clones were picked and transferred to 12-well plates for expansion.

Gardella analysis (29) was performed on G418-resistant clones. Cells were loaded into gel wells composed of agarose containing DNase-free protease (Sigma) and sodium dodecyl sulfate. *In situ* lysis of cells occurs as electrophoresis begins in Tris-borate-EDTA buffer. DNA was then transferred to a nylon membrane and detected with a 32 P-labeled probe. Probes were DpnI digested prior to radiolabeling, except for the mLANA probe, which was a PCR product amplified using the mLANAFwd and mLANArev1 oligonucleotide primers and was not digested prior to radiolabeling.

Western blots. A20 cells were transfected as described above. Extract from 0.25×10^6 cells was loaded into each lane. Proteins were resolved by SDS-PAGE in 8% polyacrylamide gels, transferred to nitrocellulose, and detected with anti-FLAG antibody conjugated to horseradish peroxidase (HRP) (Sigma), used at a 1:750 dilution, or mouse anti-tubulin monoclonal antibody B-5-1-2 (Sigma), used at a 1:1,000 dilution. Incubation with secondary anti-mouse HRP-conjugated antibody followed by chemiluminescence was performed to detect anti-tubulin antibody.

Fluorescence microscopy. For metaphase spreads, MEF cells were grown in six-well dishes to 80% confluence and then incubated overnight in 1 μ g/ml of colcemid (Calbiochem) to induce metaphase arrest. Colcemid-treated cells were swollen in hypotonic buffer for 20 min (1% sodium citrate, 10 mM CaCl₂, 10 mM MgCl₂), spread onto slides by the cytospin method (Thermoshandon), fixed for 10 min in 4% paraformaldehyde (Polysciences) in phosphate-buffered saline, and permeabilized for 5 min in 0.5% Triton X-100 in phosphate-buffered saline. To detect FLAG epitope-tagged mLANA, cell spreads were incubated with M2 anti-FLAG monoclonal antibody (Sigma) at a 1:750 dilution. Secondary anti-mouse-Alexa Fluor 488 (Molecular Probes) was used to detect M2. Cells were counterstained with propidium iodide (Molecular Probes) (1 μ g/ml) to

detect DNA, and coverslips were applied with Aqua-Poly mounting reagent (Polysciences). Microscopy was performed with a Zeiss Axioskop microscope, PCM2000 hardware, and C-imaging software (Compix, Inc.).

RESULTS

The MHV68 TR elements act in *cis* to mediate episome persistence. Since the TR elements are the *cis*-acting sequence for KSHV episome maintenance, we assessed whether the mTR elements are the *cis*-acting element for MHV68. KSHV LANA acts on the KSHV TR elements to mediate episome persistence. mLANA is homologous to LANA (Fig. 1A) and is critical for establishment of viral latency in mice. We hypothesized that the mTR elements might have a role in episome maintenance similar to that of the KSHV TRs.

We assayed whether MHV68 TR DNA can mediate extrachromosomal persistence of DNA in murine B lymphoma S11 cells. Most S11 cells are latently infected with MHV68, although some S11 cells contain virus undergoing lytic replication. In latently infected cells, MHV68 persists as a multicopy episome (61). Therefore, the necessary factors responsible for MHV68 episome persistence are expressed in these cells. If the mTRs are the *cis*-acting sequence for episome persistence, then DNA containing the mTR sequence is expected to be capable of persisting as an episome in S11 cells. m8TR (contains eight copies of the MHV68 TR element), m4TR (contains four copies of mTR), or vector alone was transfected into S11 cells. Cells were then seeded into microtiter plates at 10,000 or 1,000 cells per well and placed under G418 selection, for which resistance is encoded on the plasmid. In at least three experiments, outgrowth of G418-resistant cells transfected with m8TR was robust and occurred in all 96 wells in the plates seeded with 10,000 cells per well and in an average of 20 wells in the plates seeded with 1,000 cells per well. Outgrowth was also robust in cells transfected with m4TR, and an average of 86 wells were positive for outgrowth at 10,000 cells per well and 7 wells were positive at 1,000 cells per well. In contrast, after transfection with the vector control, which lacks mTR elements, outgrowth occurred in only an average of 9 wells and 1 well after seeding at 10,000 and 1,000 cells per well, respectively. These outgrowth data indicate that mTR DNA persists more efficiently than the vector in S11 cells. The observed enhanced persistence could be due to maintenance of mTR DNA as episomes or to increased efficiency of integration of mTR DNA.

To assess the presence of m8TR episomal DNA, Gardella gel analyses were performed on G418-resistant cell lines. In Gardella gels (29), live cells are loaded into gel wells and lysed immediately at the start of the gel run. Episomes as large as several hundred kilobases can migrate into the gel, while chromosomal DNA remains at the gel origin. Episomes are then detected by Southern blotting. S11 cells (Fig. 2A, lanes 1, 11, and 20) contain episomes but were not detected because the probe consisted of vector only, which does not share sequence with MHV68. After 90 days of G418 selection, m8TR episomes were detected in 11 (Fig. 2A, lanes 4, 6 to 10, 14, 15, and 17 to 19) of 16 lanes. In a total of two experiments, 26 of 35 G418-resistant cell lines contained episomes. In addition, three of six m4TR-transfected, G418-resistant cell lines had episomes (data not shown). The episomes generally migrated much slower than covalently closed circular plasmid DNA (Fig. 2A, lane 2, faster-migrating band), consistent with recombination events. Selection of enlarged KSHV episomes is fre-

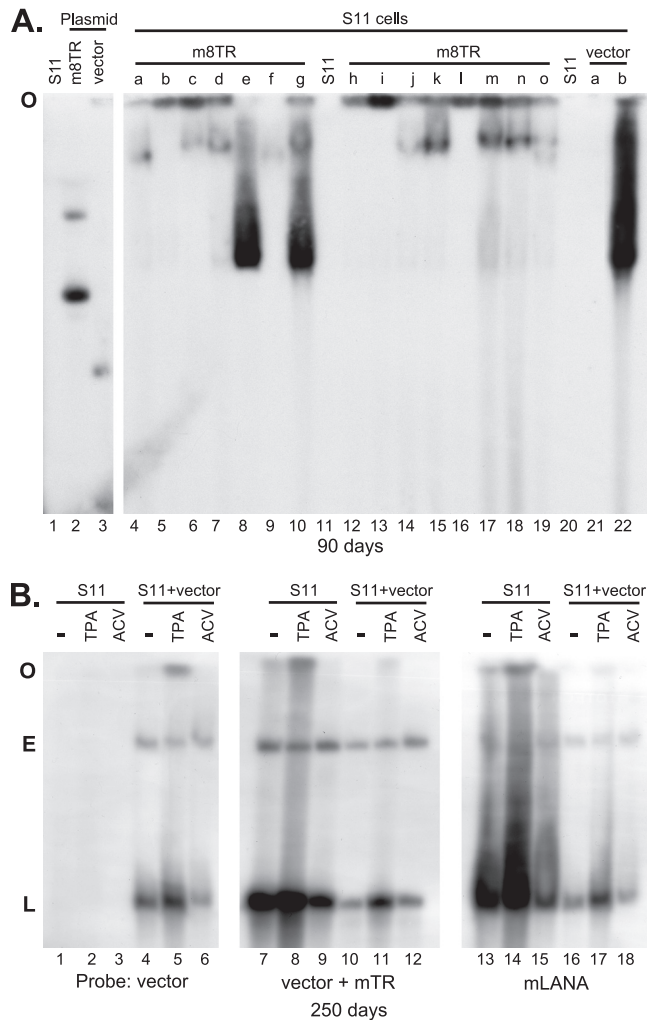


FIG 2 mTR DNA persists as an episome in S11 cells. m8TR or pRepCK vector was transfected into MHV68-infected S11 cells. Seventy-two hours later, cells were seeded into microtiter plates at 10,000 cells/well or 1,000 cells/well and placed under G418 selection. G418-resistant cells were expanded and assessed for episomes by use of Gardella gels. This figure is representative of two experiments. (A) Gardella gel containing S11 cells (lanes 1, 11, and 20), naked m8TR (lane 2) or pRepCK (lane 3) plasmid DNA, m8TR-transfected, G418-resistant S11 cells (lanes 4 to 10 and 12 to 19), and vector-transfected, G418-resistant S11 cells (lanes 21 and 22). A total of $\sim 1.5 \times 10^6$ cells was loaded in each lane. G418-resistant cell lines were taken from plates seeded with 10,000 cells per well (lanes 17 to 19, 21, and 22) or 1,000 cells per well (lanes 4 to 10 and 12 to 16). The Gardella gel analysis was performed after 90 days of G418 selection. The faster-migrating signal for m8TR (lane 2) or vector (lane 3) is circular covalently closed DNA. The blot was probed with ^{32}P -radiolabeled pRepCK vector DNA. (B) S11 cells (lanes 1 to 3, 7 to 9, and 13 to 15) and a vector-transfected, G418-resistant S11 cell line (lanes 4 to 6, 10 to 12, and 16 to 18) that contained episomal DNA were assessed after treatment with TPA or acyclovir (ACV). The experiment was performed after 250 days of G418 selection. Probes consisted of vector (lanes 1 to 6), m8TR plasmid (which includes both mTR and vector sequences) (lanes 7 to 12), and the mLANA ORF (lanes 13 to 18). For lanes 1 to 6, 1.5×10^6 cells were loaded per lane; for lanes 7 to 12, 0.15×10^6 cells were loaded per lane; and for lanes 13 to 18, 1.5×10^6 cells were loaded per lane. Fewer cells were used with the mTR probe due to the greater sensitivity of detection resulting from the number of repeated mTR elements in MHV68. The gel origin (O) and S11 episomal (E) and linear (L) forms (due to MHV68 lytic replication) are indicated.

quently observed in KSHV episome maintenance assays and is due to recombination events resulting in increased numbers of TR elements in episomes. Therefore, MHV68 TR DNA can persist as episomes in cells latently infected with MHV68.

Integration of transfected DNA into MHV68. Unexpectedly, one of the two G418-resistant cell lines transfected with vector, which lacks TR sequence, had large amounts of extrachromosomal DNA (Fig. 2A, lane 22). In fact, extrachromosomal signals in vector-transfected S11 cells were observed for 3 of 6 G418-resistant cell lines tested in a total of two experiments. Since the vector lacks mTR DNA and any MHV68 sequence, it was expected that integration into host cell chromosomes would be required to allow persistence of DNA and that transfected DNA would not persist as an episome. Notably, two of the G418-resistant cell lines containing m8TR episomes (Fig. 2A, lanes 8 and 10) also had large amounts of extrachromosomal DNA, which ran in a similar pattern on the gel compared with that of the vector-transfected cell line (Fig. 2A, lane 22). Of the 35 G418-resistant cell lines transfected with m8TR, this finding of large amounts of extrachromosomal DNA was observed in 5 cell lines and in 1 of 6 G418-resistant cell lines transfected with m4TR (Fig. 2 and data not shown).

One possible explanation for the vector being maintained as an episome was that the vector had integrated into MHV68 genomes, which are episomal. To test this possibility, the Southern blot was stripped of signal and reprobed for a sequence present in MHV68 but not the transfected mTR DNA. Strikingly, overlay of the two films demonstrated complete signal overlap for the cell line containing extrachromosomal vector (data not shown). Notably, the two cell lines containing m8TR DNA in a pattern similar to that of the extrachromosomal vector noted above also had a confluence of signals when the films were overlaid (data not shown). These results are consistent with integration of vector and m8TR DNAs into MHV68 genomes in these G418-resistant cell lines.

Since the integration of vector lacking any MHV68 DNA into MHV68 episomal genomes was an unexpected event, we further investigated this finding. S11 cells or a G418-resistant S11 cell line transfected with vector (lacking mTR DNA) but containing extrachromosomal vector DNA was assessed after 250 days of G418 selection. Cells were treated with 20 ng/ml tetradecanoyl phorbol acetate (TPA) or 100 μM acyclovir for 48 h. TPA induces lytic infection, while acyclovir inhibits lytic infection. As expected, probing with vector did not detect a signal in S11 cells (Fig. 2B, lanes 1 to 3), since the probe lacks MHV68 sequence. However, the vector probe detected episomal (E) (Fig. 2B, lane 4) and linear (L) (Fig. 2B, lane 4) DNA (from lytic infection) in the G418-resistant cells containing vector episomal DNA. Incubation with TPA increased the vector-containing linear, replicating DNA signal (Fig. 2B, lane 5) but not the episomal signal, which is the expected effect on S11 virus, since TPA induces lytic replication. In contrast, treatment with acyclovir decreased the amount of linear, replicating DNA but not the episomal signal (Fig. 2B, lane 6), which is the expected effect on MHV68 infection. A Gardella gel with the same cell lines was also probed with mLANA, which is present in MHV68 but not in the vector, to detect MHV68 DNA. In both S11 cells and G418-resistant, vector-transfected S11 cells, similar patterns of increasing linear DNA after TPA treatment and decreased linear DNA after acyclovir treatment were observed (Fig. 2B, lanes 13 to 18).

Simultaneous probing of a Gardella gel with sequences specific for both vector and mTRs detected the same episomal and linear

replicating DNA patterns with TPA and acyclovir. No additional bands or doublets were detected in the cells containing episomal vector DNA compared with the S11 cells (Fig. 2B, lanes 7 to 12). This finding strongly indicates that both probes detected the same bands. Overall, these findings are consistent with vector integration into MHV68 episomal genomes in some G418-resistant S11 cell lines. Furthermore, these results suggest that some G418-resistant m8TR cell lines (such as in Fig. 2A, lanes 8 and 10) also have integration of transfected vector into episomal MHV68 genomes. Importantly, however, most G418-resistant cell lines transfected with m8TR did not have an overlap of signal when probed for mLANA compared with the vector probe. This result is therefore consistent with independent episome persistence of the transfected m8TR DNA in these lines.

CMV promoter-driven mLANA acts on mTR DNA in *cis* to mediate low levels of episome persistence. Since m8TR and m4TR persisted as episomes in S11 cells, we wished to investigate whether mLANA acts on mTR DNA to mediate episome maintenance analogous to the KSHV LANA function. To test this possibility, we constructed plasmids containing CMV promoter-driven mLANA or mLANA with a C-terminal FLAG tag (mLANAF), and also plasmids containing two, four, or eight mTR elements (termed CmLANA-m2TR, CmLANAF-m2TR, CmLANA-m4TR, CmLANAF-m4TR, or CmLANAF-m8TRrev). As controls, we generated plasmids containing only mLANA (termed CmLANA or CmLANAF) or used m2TR, m4TR, and m8TR, which contain only TR elements. Uninfected mouse A20 B lymphoma cells were transfected with m2TR, m4TR, m8TR, CmLANA, CmLANAF, CmLANA-m2TR, CmLANAF-m2TR, CmLANA-m4TR, CmLANAF-m4TR, or CmLANAF-m8TRrev. Cells were seeded into microtiter plates at 3 days posttransfection and placed under G418 selection, against which resistance is encoded by the plasmid vector. G418-resistant cell outgrowth was similar for each of the transfections containing mTR DNA, whether or not mLANA was present in *cis*. After transfection with mTR-containing DNA, nearly all 96 wells were positive for outgrowth in plates seeded at 1,000 cells/well, ~10 to 30 wells were positive after seeding at 100 cells per well, and ~0 to 5 wells were positive after seeding at 10 cells per well. G418-resistant cell outgrowth for the CmLANA or CmLANAF transfections was lower, at ~50 positive wells for plates seeded at 1,000 cells/well, ~10 positive wells after seeding at 100 cells per well, and ~0 to 2 wells after seeding at 10 cells per well. The comparable rates of G418-resistant cell outgrowth with mTR transfections, regardless of the presence of mLANA, were consistent with either an absence of mLANA episome maintenance or episome maintenance occurring at a rate similar to that of integration.

G418-resistant cells were expanded and assessed by Gardella gel analysis for the presence of episomes. m2TR-transfected cells (Fig. 3B, lanes 10 to 13), m4TR-transfected cells (Fig. 3A, lanes 5 and 6), and m8TR-transfected cells (Fig. 3B, lanes 31 to 34), which contain mTR elements but not the mLANA sequence, did not contain episomes. Similarly, cells transfected with CmLANA (Fig. 3A, lanes 21 to 24 and 33) or CmLANAF (Fig. 3B, lanes 19 to 22), which contain the mLANA sequence but do not have mTR elements, also did not contain any episomes. Therefore, no episomes were present when either mLANA was present without mTR elements or mTR elements were present without mLANA.

G418-resistant cells transfected with DNA containing both mLANA and mTRs were also assessed for the presence of episomes. CmLANAF-m2TR, which contains FLAG-tagged mLANA

and two mTRs, had no episomes in six G418-resistant cell lines (Fig. 3B, lanes 13 to 18). Similarly, cells transfected with CmLANA-m2TR, which contains mLANA without an epitope tag and two mTRs, had no episomes in four G418-resistant cell lines (data not shown). However, CmLANA-m4TR, which contains mLANA and four mTR elements (Fig. 3A, lanes 7 to 20 and 27 to 32), had episomal DNA in four lanes (Fig. 3A, lanes 9, 27, 28, and 30), and in a total of two experiments, CmLANA-m4TR-transfected cells had episomes in 9 of 33 (27%) G418-resistant cell lines. In addition, CmLANAF-m4TR, which contains FLAG-tagged mLANA and four mTR elements, had episomal DNA in one lane (Fig. 3B, lane 5), and in a total of two experiments, CmLANAF-m4TR had episomes in 2 of 24 (8%) G418-resistant cell lines. CmLANAF-m8TRrev had episomes in 1 (Fig. 3B, lane 29) of 18 (6%) G418-resistant cell lines (Fig. 3B, lanes 25 to 30, and data not shown). Therefore, when mLANA expressed from a CMV promoter was present in *cis* with 4 or 8 mTR elements, episomes were present in a small percentage of G418-resistant cell lines. This finding is consistent with mLANA acting on mTR elements to mediate low-efficiency episome persistence.

The native mLANA promoter drives higher-level mLANA expression than the CMV promoter. We reasoned that a low expression level of mLANA might have been responsible for the low efficiency of episome persistence and therefore assessed mLANA expression levels driven by either the CMV promoter or the native mLANA promoter. CmLANAF, CmLANAF-m2TR, CmLANAF-m4TR, and CmLANAF-m8TRrev, which have mLANA driven by the CMV promoter, were transfected into A20 cells and analyzed for mLANA expression by immunoblotting with anti-FLAG antibody. CmLANAF-m4TR (Fig. 4, lanes 3 and 14) expressed mLANA at a higher level than did CmLANAF (Fig. 4, lane 5) or CmLANAF-m2TR (Fig. 4, lane 4). CmLANAF-m4TR mLANA expression (Fig. 4, lanes 3 and 14) was also higher than that of CmLANAF-m8TRrev (Fig. 4, lane 15). It is possible that the higher expression level from CmLANAF-m4TR accounted for its higher efficiency of episome persistence than that of CmLANAF-m2TR or CmLANAF-m8TRrev (Fig. 3).

mLANAF, mLANAF-m2TR, mLANAF-m4TR, and mLANAF-m8TRrev each have mLANA driven by its native promoter sequence and were also tested for mLANA expression levels. Three native promoters have been described for mLANA, including one immediately upstream of mLANA and two within the mTR elements (2, 12). The orientation of the mTR elements in relation to mLANA in mLANAF-m2TR and mLANAF-m4TR is the same as in genomic MHV68, but it is reversed in mLANAF-m8TRrev. mLANAF (Fig. 4, lane 10) expressed mLANA at a similar level to those of mLANAF-m8TRrev (Fig. 4, lane 7) and CmLANAF (Fig. 4, lane 5). mLANAF-m2TR (Fig. 4, lane 9) and mLANAF-m4TR (Fig. 4, lane 8) expressed mLANA at substantially higher levels than those of mLANAF and mLANAF-m8TRrev. The expression level for mLANAF-m4TR was higher than that for mLANAF-m2TR, as evident in the 10-s exposure (Fig. 4, middle panel, lanes 8 and 9, respectively). Therefore, the presence of upstream mTR elements in the native genomic orientation relative to mLANA substantially enhances mLANA expression, and the level of expression is much greater than that driven by the CMV promoter. Furthermore, four upstream mTR elements were more efficient than two mTR elements in driving mLANA expression.

Native promoter-driven mLANA maintains mTR episomes with enhanced efficiency. Since higher mLANA expression oc-

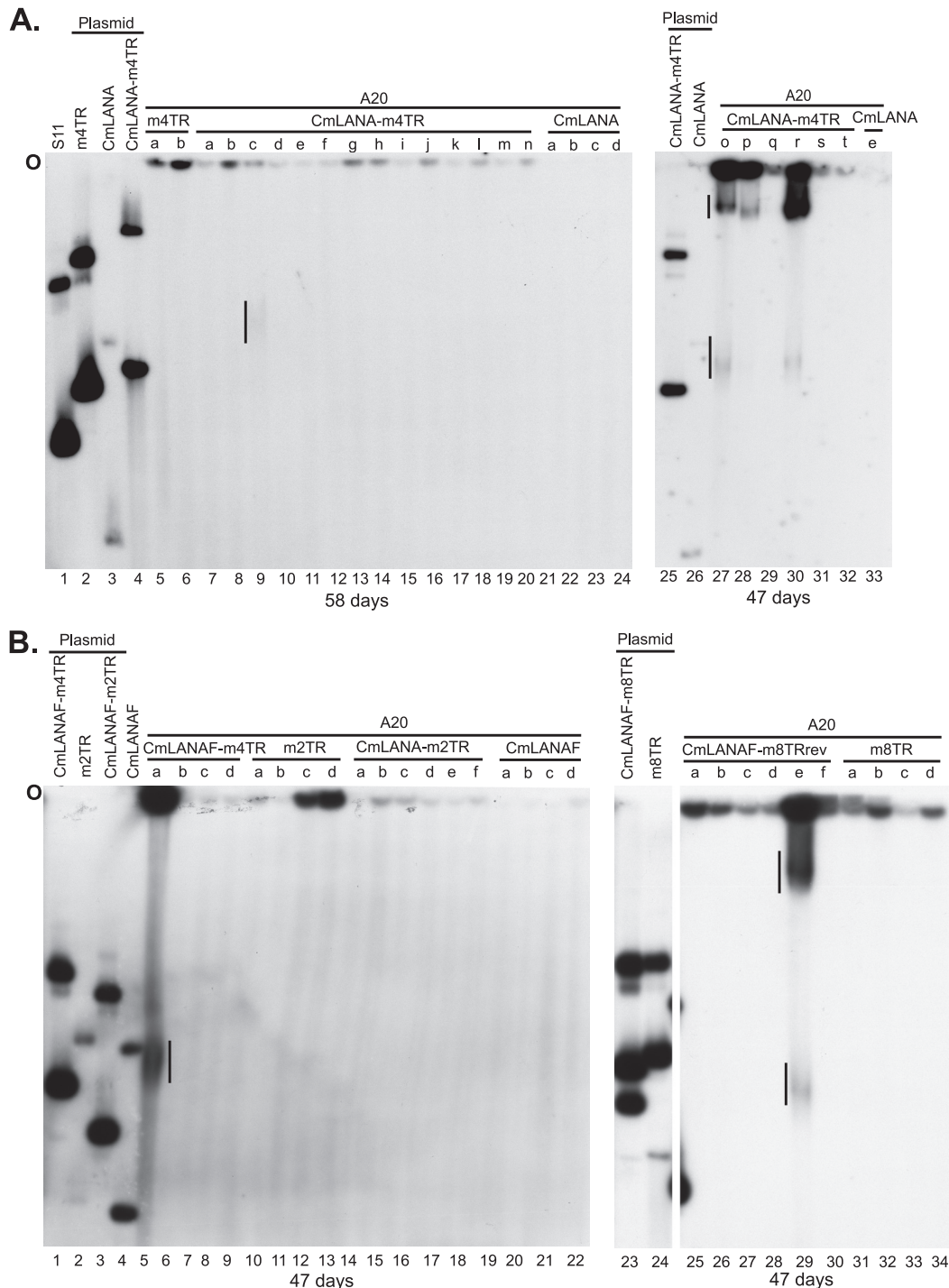


FIG 3 CMV promoter-driven mLANA in *cis* with mTR elements persists in episomal form at low efficiency. A20 cells were transfected with plasmids containing CMV promoter-driven mLANA and mTR elements or with mTR DNA. Seventy-two hours later, cells were seeded in microtiter plates at 1,000, 100, or 10 cells/well and placed under G418 selection. A total of 2×10^6 to 3×10^6 A20 cells was loaded per lane in Gardella gels, and 1.5×10^5 S11 cells were loaded per lane. (A) Gardella gel containing S11 cells (lane 1), naked m4TR DNA (lane 2), naked CmLANA DNA (lanes 3 and 26), naked CmLANA-m4TR plasmid DNA (lanes 4 and 25), m4TR-transfected, G418-resistant A20 cells (lanes 5 and 6), CmLANA-m4TR-transfected, G418-resistant A20 cells (lanes 7 to 20 and 27 to 32), and CmLANA-transfected, G418-resistant A20 cells (lanes 21 to 24 and 33). G418-resistant cell lines were taken from plates seeded with 1,000 cells per well (lanes 22 and 24) or 100 cells per well (lanes 5 to 21, 23, 27 to 33). (B) Gardella gel containing naked CmLANA-m4TR (lane 1), naked m2TR (lane 2), naked CmLANAF (lane 4), naked CmLANAF-m4TR (lanes 5 to 8), m2TR (lanes 9 to 12), CmLANAF-m2TR (lanes 13 to 18), CmLANAF (lanes 19 to 22), CmLANAF-m8TR (lane 23), and naked m8TR (lane 24) plasmid DNA, as well as G418-resistant A20 cells transfected with CmLANAF-m4TR (lanes 5 to 8), m2TR (lanes 9 to 12), CmLANAF-m2TR (lanes 13 to 18), CmLANAF (lanes 19 to 22), CmLANAF-m8TRrev (lanes 25 to 30), or m8TR (lanes 31 to 34). G418-resistant cell lines were taken from plates seeded with 100 cells per well (lanes 5 to 8, 10 to 12, 15 to 18, 20 to 22, and 30 to 34) or 10 cells per well (lanes 9, 13, 14, 19, and 25 to 29). The gel origin (O) is indicated. The number of days of G418 selection is shown below each panel. For naked plasmid DNA, the fastest-migrating signal is circular covalently closed DNA. Blots were probed with ^{32}P -radiolabeled m8TR DNA. Vertical lines indicate migration locations of episomal DNA.

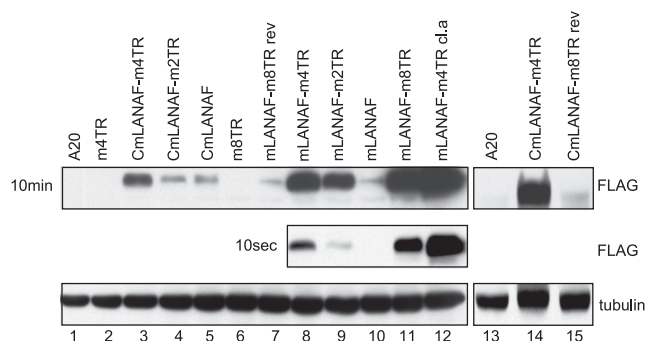


FIG 4 mLANA levels after transfection of different expression vectors. A20 cells were transfected with the indicated plasmids and harvested for immunoblotting 72 h later, except for the sample in lane 12. The gel shows A20 cells (lanes 1 and 13) and A20 cells transfected with m4TR (lane 2), CmLANAF-m4TR (lanes 3 and 14), CmLANAF-m2TR (lane 4), CmLANAF (lane 5), m8TR (lane 6), mLANAF-m8TRrev (lane 7), mLANAF-m4TR (lane 8), mLANAF-m2TR (lane 9), mLANAF (lane 10), mLANAF-m8TR (lane 11), or CmLANAF-m8TRrev (lane 15). Lane 12 contains mLANA-m4TR c.l.a., which is the G418-resistant cell line containing episomes shown in Fig. 5A, lane 8. The bottom panel shows a tubulin immunoblot for the same cells. A total of 0.25×10^6 cells was loaded in each lane. The middle panel shows a shorter exposure (10 s) of lanes 8 to 12 than the 10-min exposure for these lanes in the top panel. The top right panel shows a 20-min exposure. This figure is representative of at least two experiments.

curs from the native promoter than from the CMV promoter, we assessed whether episome maintenance is enhanced when native promoter-driven mLANA is oriented in *cis* with mTR elements. mLANAF, m4TR, and mLANAF-m4TR were each transfected into A20 cells, seeded into microtiter plates at a density of 1,000 cells per well, 100 cells per well, or 10 cells per well, and placed under G418 selection. For m4TR and mLANAF-m4TR, G418-resistant outgrowth occurred in nearly all wells seeded at 1,000 cells per well, in ~ 15 wells seeded at 100 cells/well, and in ~ 2 wells seeded at 10 cells/well. This pattern of similar G418-resistant cell outgrowth after transfection of all mTR-containing DNA constructs in both the presence and absence of mLANA continued in subsequent experiments. In comparison, mLANAF G418-resistant cell outgrowth occurred in only ~ 30 wells seeded at 1,000 cells/well, ~ 2 wells seeded at 100 cells/well, and 0 wells seeded at 10 cells/well. The higher rate of G418-resistant cell outgrowth for cells transfected with mTR-containing DNA than that for cells in the absence of mTR DNA provided evidence for a higher rate of integration of mTR-containing plasmids into the host genome. Since there was no increase in the G418 outgrowth rate with mLANA and mTRs expressed in *cis*, results were consistent with either a lack of episome persistence or an efficiency of episome persistence that was no higher than that of integration.

G418-resistant cell lines were expanded and assessed for the presence of episomes by Gardella gel analysis at 47 days postselection. As expected, neither m4TR (Fig. 5A, lanes 5 to 7), which lacks mLANA, nor mLANAF (Fig. 5A, lanes 22 to 24), which lacks mTR elements, had episomes. In contrast, mLANAF-m4TR persisted as episomal DNA in 10 (Fig. 5A, lanes 8 to 10, 12 to 16, 19, and 21) of 14 lanes. Notably, most of the episomal signal migrated much more slowly than the covalently closed circular mLANAF-m4TR plasmid (Fig. 5A, lane 3, bottom band) and even slower than episomal MHV68 from infected S11 cells (Fig. 5A, lane 1, upper band), consistent with selection for recombination into very large

episomes. In two experiments, mLANAF-m4TR had episomes in 19 of 45 (42%) G418-resistant cell lines. Furthermore, in two additional experiments, mLANA-m4TR, which is similar to mLANAF-m4TR except that mLANA lacks a C-terminal epitope tag, episomes were present in 18 of 42 (43%) G418-resistant cell lines (data not shown). Since mLANAF-m4TR persisted as episomal DNA with an efficiency similar to that of mLANA-m4TR, the C-terminal FLAG tag did not adversely affect mLANA function.

To assess the long-term stability of the episomes, selected G418-resistant cell lines were again assayed by Gardella gel analysis after 173 days of selection. All five cell lines (Fig. 5B, lanes 8 to 14) continued to stably maintain episomal mLANAF-m4TR DNA. Therefore, episomes were stable for at least ~ 6 months in continuous culture.

mLANA expression was assessed in these G418-resistant cell lines. As expected, no signal was detected in m4TR (Fig. 5C, lanes 1, 13, and 14)-transfected cell lines, since this plasmid lacks mLANA. mLANAF expression was detected in only one (Fig. 5C, lane 21) of three (Fig. 5C, lanes 11, 12, 20, and 21) mLANAF-transfected, G418-resistant cell lines and was expressed at a relatively low level. In contrast, mLANAF expression was detected in all mLANAF-m4TR cell lines (Fig. 5C, lanes 2 to 10 and 15 to 18) and was robust in all lines except for one that contained very low levels of episomes (Fig. 5A, lane 21). For this cell line, mLANAF could be detected only on longer exposure (Fig. 5C, middle panel, lane 19). It is interesting that robust mLANAF expression (Fig. 5C, lanes 5, 15, 16, and 18) was present even in cell lines that lacked episomes (Fig. 5A, lanes 11, 17, 18, and 20) when the plasmid was integrated.

We observed that A20 cells expressing mLANA proliferated at a lower rate than that of cells that did not express mLANA, suggesting that mLANA may exert growth-inhibitory effects. Therefore, it is possible that when cell outgrowth is robust in nearly all wells, such as after plating 1,000 cells/well after transfection of mTR-containing plasmids, cells with integrated plasmid and lacking mLANA expression may overgrow those cells which contain episomes and express mLANA. However, in these experiments, Gardella gel analyses were generally done from plates seeded with 100 cells/well that had low levels of G418-resistant outgrowth, in which outgrowth is expected to be nearly clonal.

The presence of two or eight mTR elements instead of four mTR elements in *cis* with mLANA was also assessed with regard to episome maintenance. In three experiments, mLANA-m2TR (without an epitope tag) had episomes in 14 of 32 (44%) G418-resistant cell lines, while in two experiments, mLANAF-2mTR (containing a FLAG tag) had episomes in 5 of 18 (28%) cell lines (data not shown). These rates of episome persistence were very similar to those with four mTRs (42% for mLANAF-m4TR and 43% for mLANA-m4TR). mLANA-m8TRrev-transfected, G418-resistant cell lines contained episomes in only 3 (Fig. 5D, lanes 7, 8, and 14) of 12 (Fig. 5D, lanes 3 to 14) cell lines. In two experiments, mLANA-m8TRrev had episomes in 3 of 16 (19%) G418-resistant cell lines, and the signal was very weak in two of the lanes (Fig. 5D, lanes 7 and 14). Two additional experiments assessing mLANAF-m8TRrev (containing an mLANA FLAG epitope tag) had episomes in 2 of 21 (10%) G418-resistant cell lines. Therefore, mLANA-m8TRrev and mLANAF-m8TRrev had lower efficiencies of episome persistence than vectors containing two or four copies of mTR. This lower efficiency was likely due to lower

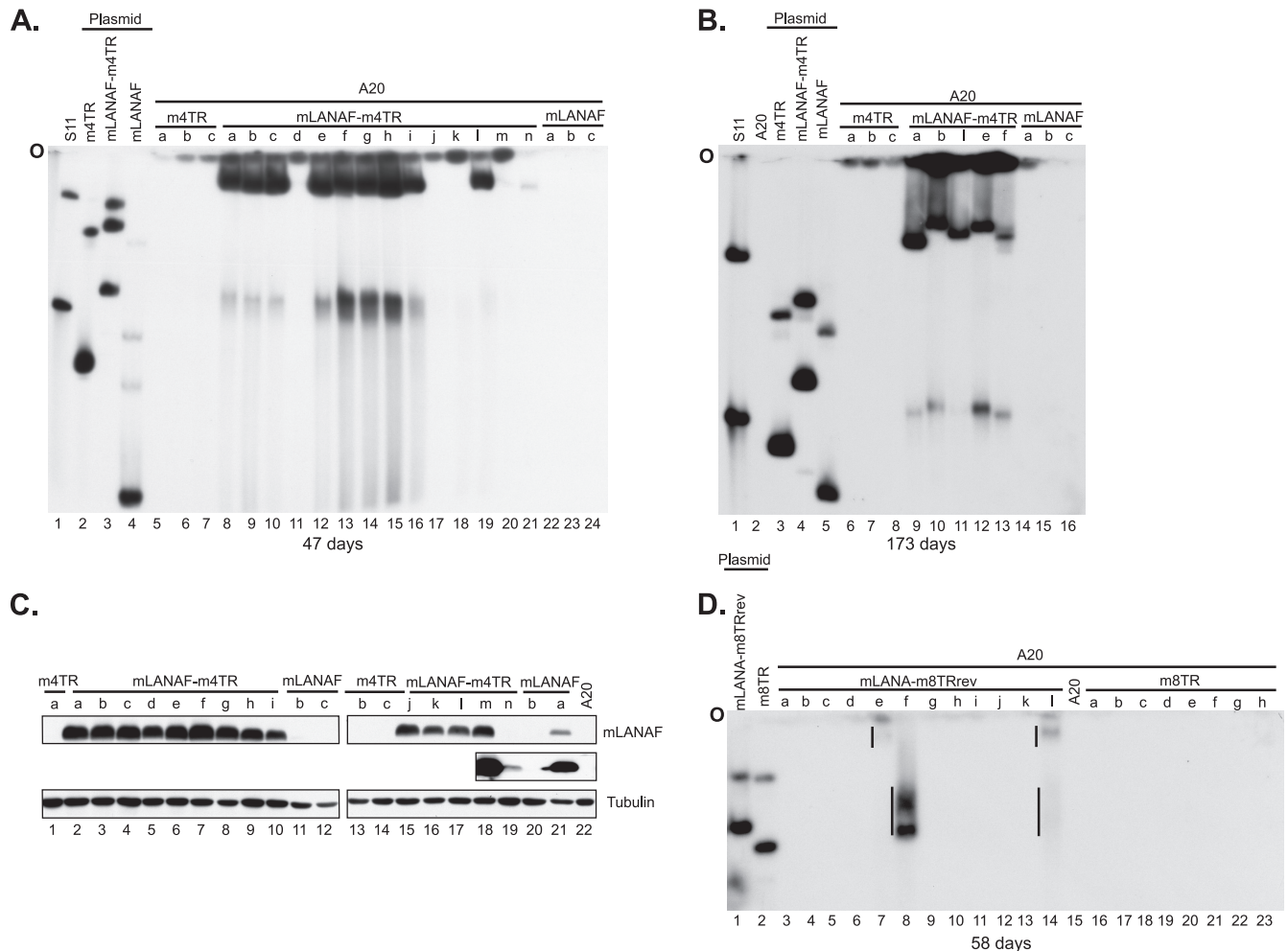


FIG 5 Native promoter-driven mLANA in *cis* with mTR elements persists in episomal form with increased efficiency. A20 cells were transfected with plasmids containing native promoter-driven mLANA with mTR elements or with mTR DNA. Seventy-two hours later, cells were seeded into microtiter plates at 1,000, 100, or 10 cells/well and placed under G418 selection. A total of 2×10^6 to 3×10^6 cells was loaded per lane for Gardella gels. (A) Gardella gel containing S11 cells (lane 1), naked m4TR plasmid DNA (lane 2), naked mLANAF-m4TR plasmid DNA (lane 3), naked mLANAF plasmid DNA (lane 4), G418-resistant, m4TR-transfected A20 cells (lanes 5 to 7), G418-resistant, mLANAF-m4TR-transfected A20 cells (lanes 8 to 21), and G418-resistant, mLANAF-transfected A20 cells (lanes 22 to 24). G418-resistant cell lines were taken from plates seeded with 1,000 cells per well (lanes 22 to 24), 100 cells per well (lanes 5 to 11 and 17 to 20), or 10 cells per well (lanes 12 to 16 and 21). (B) Gardella gel containing S11 cells (lane 1), A20 cells (lane 2), naked m4TR DNA (lane 3), naked mLANAF-m4TR DNA (lane 4), naked mLANAF DNA (lane 5), and A20 cells after 173 days of G418 selection (lanes 6 to 16). Letters above the lanes correspond to the same letters in panel A. (C) Immunoblot of mLANA G418-resistant cell lines from panel A. Lane letters correspond to the same letters as in panel A. Lanes 11 and 20 contain cells from the same G418-resistant “b” cell line. A total of 0.25×10^6 cells was loaded per lane. The middle panel shows a longer exposure for lanes 18 to 22. The bottom panel shows a tubulin immunoblot. (D) Gardella gel containing naked mLANA-m8TRrev DNA (lane 1), naked m8TR DNA (lane 2), G418-resistant, mLANA-m8TRrev-transfected A20 cells (lanes 3 to 14), A20 cells (lane 15), and G418-resistant, m8TR-transfected A20 cells (lanes 16 to 23). G418-resistant cell lines were taken from plates seeded with 1,000 cells per well (lanes 3 to 21) or 100 cells per well (lanes 22 and 23). The figure is representative of at least two experiments. Numbers of days of G418 selection are indicated below the panels. The faster-migrating bands in S11 lanes are linear MHV68 genomic DNA from cells undergoing lytic infection, and the slower-migrating band is episomal MHV68. The fastest-migrating bands in naked DNA lanes are circular covalently closed DNA. Blots in panels A, B, and D were probed with ^{32}P -radiolabeled m8TR DNA. Vertical lines in panel D indicate episomal DNA.

mLANA expression from this construct, which has the mTRs reversed from their native orientation relative to mLANA (Fig. 4, lane 7). In the absence of mLANA (Fig. 5D, lanes 16 to 23), no episomes were observed. Therefore, episome persistence occurred only when mLANA and mTRs were together in *cis*, and episome persistence was more efficient at higher mLANA expression levels.

mLANA maintains mTR episomes in MEF cells. Since mLANA in *cis* with mTRs persisted as episomal DNA in A20 B lymphoma cells, we assessed if mLANA could also maintain episomes in another cell type. Therefore, MEF cells were trans-

fected with mLANA, mLANAF, m4TR, m8TR, mLANA-m2TR, mLANA-m4TR, mLANA-8TRrev, or mLANAF-m4TR and placed under G418 selection. G418-resistant colonies were expanded independently and assessed by Gardella gel analysis for the presence of episomes. As expected, the mLANA (Fig. 6B, lanes 5 to 8), mLANAF (Fig. 6C, lanes 12 and 13), m4TR (Fig. 6C, lanes 6 and 7), and m8TR (Fig. 6A, lanes 18 to 24, and B, lane 13) cell lines did not contain episomes. mLANA-m2TR contained episomes in 4 of 5 lanes (80%) (Fig. 6B, lanes 14, 15, 17, and 18), mLANA-m4TR had episomes in 8 of 12 lanes (67%) (Fig. 6A, lanes 12 to 14,

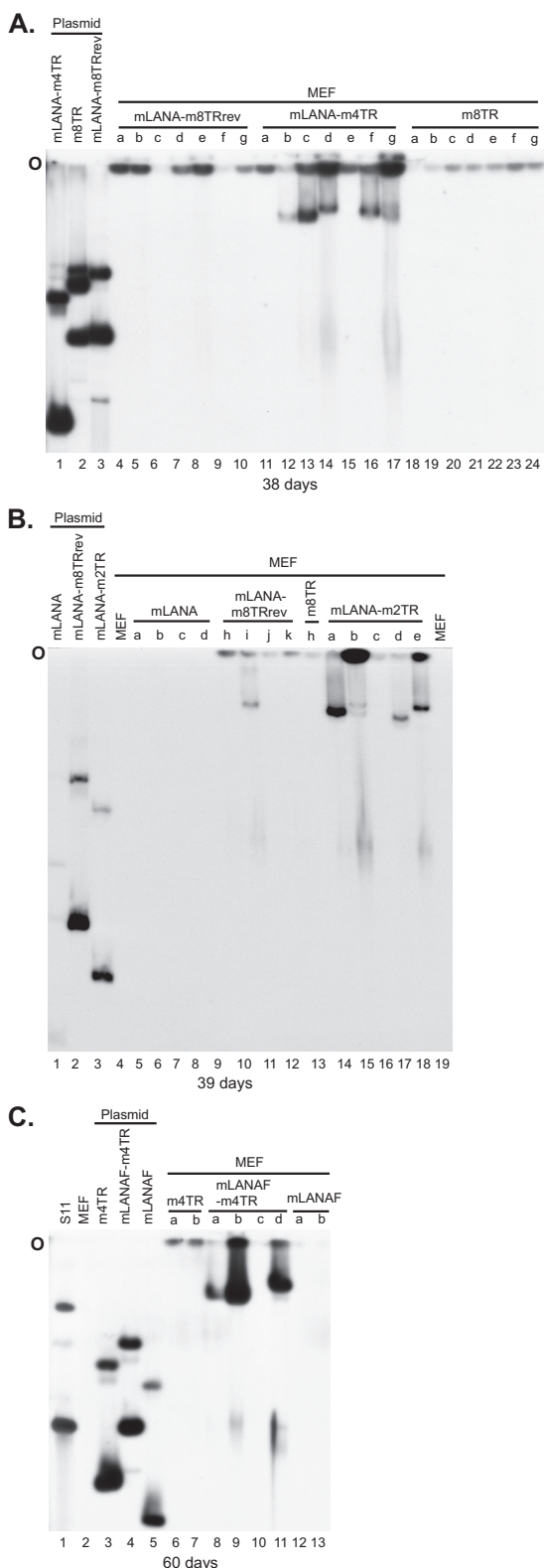


FIG 6 mLANA in *cis* with mTR elements persists in episomal form in MEF cells. MEF cells were transfected with plasmids containing native promoter-driven mLANA in *cis* with mTR elements or mTR elements alone. Forty-eight hours later, cells were trypsinized, reseeded into 15-cm dishes, and placed under G418 selection. (A) Gardella gel containing naked mLANA-m4TR DNA (lane 1), naked m8TR DNA (lane 2), naked mLANA-m8TRrev DNA (lane 3),

16, and 17, and data not shown), mLANA-m8TRrev contained episomes in 1 (Fig. 6B, lane 10) of 11 lanes (9%) (Fig. 6A, lanes 4 to 10, and B, lanes 9 to 12), and mLANAF-m4TR had episomes in 3 of 4 lanes (75%) (Fig. 6C, lanes 8, 9, and 11). Western blot analysis of mLANAF protein expression demonstrated that the mLANAF-m4TR-transfected cell line lacking episomes (Fig. 6C, lane 10) expressed mLANAF at a robust level that was only slightly lower than that of cells containing episomes (Fig. 6C, lanes 8, 9, and 11), while cells transfected with mLANAF without mTRs had significantly reduced or no mLANAF expression (data not shown). These expression patterns were similar to those in A20 cells (Fig. 5C). The lower rate of episome persistence for mLANA-m8TRrev was similar to that in A20 cells and was likely due to lower mLANA protein expression. As observed in A20 cells, MEF cells expressing mLANA proliferated at a lower rate than that of MEF cells not expressing mLANA. Therefore, mLANA acts on mTR DNA to mediate episome persistence in MEF cells.

Native genomic orientation of eight mTR elements in *cis* with mLANA increases episome persistence efficiency. We investigated whether the native genomic orientation of eight mTRs in *cis* with mLANA would affect the efficiency of episome maintenance, since mLANA-m8TRrev, in which the mTR orientation is reversed, was less efficient than mLANA in *cis* with only two or four mTRs in both A20 and MEF cells. Therefore, we generated mLANAF-m8TR, which contains eight mTR elements in native genomic orientation upstream of mLANA (Fig. 1C). Transfection of mLANAF-m8TR (Fig. 4, lane 11) into A20 cells demonstrated substantially more mLANA expression than that of mLANAF-m8TRrev (Fig. 4, lane 7), and the level was somewhat higher than that of mLANAF-m4TR (Fig. 4, middle panel, lane 8). The expression level of mLANAF-m8TR was only slightly lower than the expression level of mLANA in a G418-resistant cell line maintaining mLANAF-m4TR episomes (Fig. 4, middle panel, lane 12).

We assessed the ability of mLANAF-m8TR to persist as an episome. mLANAF-m8TR, m8TR, and mLANAF were each transfected into A20 cells, plated in microtiter plates, and selected for G418 resistance. As expected, m8TR (Fig. 7A, lanes 6 and 7) and mLANAF (Fig. 7A, lanes 22 and 23) did not have episomes. In contrast, mLANAF-m8TR had episomal DNA in 9 (Fig. 7A, lanes 9 to 11, 14 to 16, 18 to 19, and 21) of 15 (Fig. 7A, lanes 8 to 21) cell lines. In two experiments, mLANAF-m8TR had episomes in 13 of 18 (72%) cell lines. This episome maintenance efficiency was substantially higher than that of mLANAF-m8TRrev (10%) or mLANA-m8TRrev (19%) and was even higher than that of mLANA in native orientation with two or four mTRs in A20 cells

G418-resistant, mLANA-m8TRrev-transfected MEF cells (lanes 4 to 10), G418-resistant, mLANA-m4TR-transfected MEF cells (lanes 11 to 16), and G418-resistant, m8TR-transfected MEF cells (lanes 19 to 24). (B) Gardella gel containing naked mLANA DNA (lane 1), naked mLANA-m8TRrev DNA (lane 2), naked mLANA-m2TR DNA (lane 3), MEF cells (lanes 4 and 19), G418-resistant, mLANA-transfected MEF cells (lanes 5 to 8), G418-resistant, mLANA-m8TRrev-transfected MEF cells (lanes 9 to 12), G418-resistant, m8TR-transfected MEF cells (lane 13), and mLANA-m2TR-transfected MEF cells (lanes 14 to 18). (C) Gardella gel containing S11 cells (lane 1), MEF cells (lane 2), naked m4TR DNA (lane 3), naked mLANAF-m4TR DNA (lane 6), naked mLANAF DNA (lane 5), G418-resistant, m4TR-transfected MEF cells (lanes 6 and 7), G418-resistant, mLANAF-m4TR-transfected MEF cells (lanes 8 to 11), and G418-resistant, mLANAF-transfected MEF cells (lanes 12 and 13). A total of $\sim 1 \times 10^6$ MEF cells was loaded per lane in Gardella gels. Numbers of days of G418 selection are indicated at the bottom of panels. Blots were probed with ^{32}P -radiolabeled m8TR DNA.

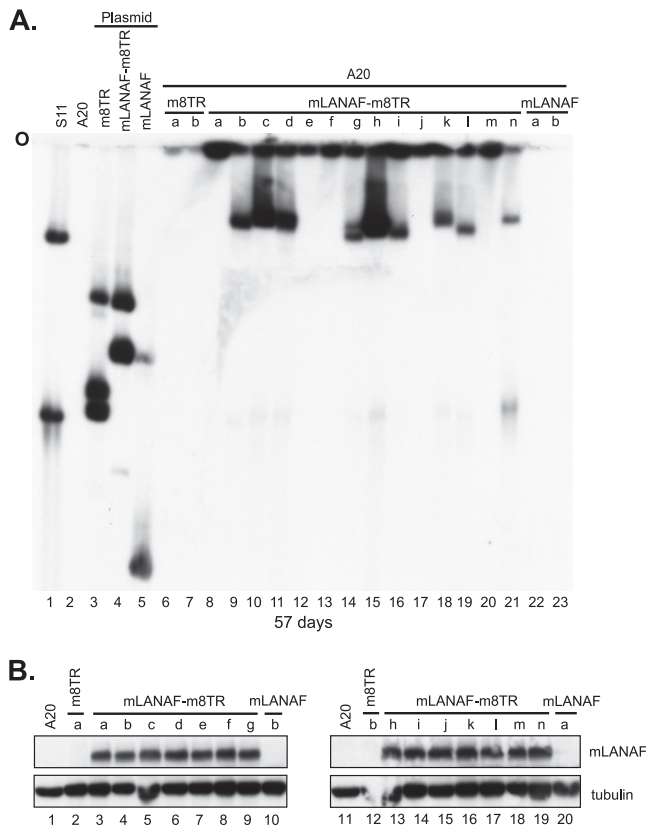


FIG 7 mLANA in *cis* with mTR elements in native orientation enhances episome persistence. (A) Gardella gel containing S11 cells (lane 1), A20 cells (lane 2), naked m8TR DNA (lane 3), naked mLANA F-m8TR DNA (lane 4), mLANAF (lane 5), G418-resistant, m8TR-transfected A20 cells (lanes 6 and 7), G418-resistant, mLANAF-m8TR-transfected A20 cells (lanes 8 to 21), and G418-resistant, mLANAF-transfected A20 cells (lanes 22 and 23). G418-resistant cell lines were taken from plates seeded with 1,000 cells per well (lanes 22 and 23), 100 cells per well (lanes 6 to 18), or 10 cells per well (lanes 19 to 21). A total of $\sim 1.5 \times 10^6$ cells was loaded per lane. The number of days of G418 selection is shown at the bottom. The blot was probed with ^{32}P -radiolabeled m8TR DNA. (B) Immunoblot of mLANAF and tubulin for cells in panel A. Letters above lanes correspond to the same letters in panel A.

(Fig. 1C). Therefore, native orientation of the eight mTR elements substantially increased both mLANA expression and episome persistence.

Immunoblot analysis demonstrated that mLANA was expressed at robust levels in all mLANAF-m8TR cell lines (Fig. 7B, lanes 3 to 9 and 13 to 19). Even cell lines lacking episomes (Fig. 7B, lanes 3, 7 to 8, 15, and 18), which therefore contained integrated plasmid, expressed mLANA, similar to the findings with integrated mLANAF-m4TR (Fig. 5C). Notably, cell lines transfected with mLANAF, which contains the native mLANA promoter immediately upstream of mLANA but no mTR elements, did not express mLANA (Fig. 7B, lanes 10 and 20).

mLANA redistributes and concentrates to dots along mitotic chromosomes in the presence of episomes. mLANA was detected in MEF cells (Fig. 8) containing mLANAF-m4TR episomes (cell line from Fig. 6C, lane 11) and in MEF cells deficient in episomes, for which no episomes were detected on Gardella gel analysis (cell line from Fig. 6C, lane 10). In episome-deficient cells (Fig. 8A to D), mLANAF (green) was distributed broadly throughout the nu-

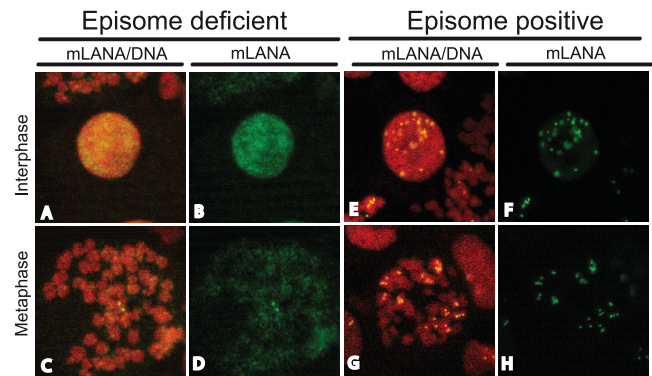


FIG 8 mLANA concentrates to dots along mitotic chromosomes in the presence of episomes but is broadly distributed along chromosomes in episome-deficient cells. mLANAF was detected in MEF cells deficient for episomes (A to D; cells from Fig. 6C, lane 10) or in MEF cells containing mLANAF-m4TR episomes (E to H; cells from Fig. 6C, lane 11). Cells were in interphase (A, B, E, and F) or metaphase (C, D, G, and H). Overlay of green (mLANAF) with red (DNA) generates yellow. Panels C and D contain two mitotic cells. The two paired dots in panels C and D are likely due to the presence of rare episomes that were not detected by the Gardella gel. Brightness and contrast were uniformly adjusted for some panels from the same field by use of Adobe Photoshop. Magnification, $\times 630$.

cleus (red) in interphase and over mitotic chromosomes (red) (overlay of green and red generates yellow). In contrast, in the presence of episomes (Fig. 8E to H), mLANAF (green) was concentrated to dots both in interphase and along mitotic chromosomes (red) (overlay of green and red generates yellow). Therefore, in the presence of episomes, mLANA relocated to dots along mitotic chromosomes.

DISCUSSION

This work demonstrates that mLANA acts on the mTR elements to mediate episome persistence. DNA containing mTR elements persisted as episomes in latently MHV68-infected S11 cells, indicating that the *cis*-acting element for episome persistence is located in the mTRs. Furthermore, plasmids containing mLANA expression cassettes and mTR elements in *cis* were capable of persisting as episomes in both murine A20 B lymphoma cells and MEF cells. In contrast, neither mTR elements nor mLANA alone ever persisted as episomal DNA, consistent with a requirement for both factors for episomal maintenance.

These findings follow earlier work which suggested an episome maintenance role for mLANA. LANA is the episome maintenance protein for KSHV and acts on KSHV TR DNA to maintain episomes (3–5, 14). Similarly, HVS LANA binds to and acts on HVS TR elements to mediate episome persistence (10, 11, 13, 30, 31, 63, 68). mLANA is the MHV68 positional homolog for both KSHV and HVS LANA proteins and also shares sequence homology with these proteins. Furthermore, studies which abolished mLANA expression by introduction of specific mutations demonstrated that mLANA is critical for MHV68's ability to establish latent infection in mice (25, 48). Notably, later work showed that MHV68 lacking mLANA expression could persist at low levels in murine splenocytes, especially after intraperitoneal injection. However, MHV68 was unable to reactivate from splenocytes, and no episomal DNA could be detected in the latently infected cells. This finding was consistent with either integration into host chromosomes or

maintenance of DNA in a linear state, therefore indicating a role for mLANA in the formation or maintenance of episomes (50).

Initial experiments transfecting mTR plasmids into S11 cells were consistent with the mTRs acting as the *cis*-acting element for episome persistence but were complicated by the finding of vector integration into MHV68 episomal genomes in some G418-resistant cell lines. Furthermore, some of the transfected mTR plasmids that persisted as episomes were also integrated into MHV68 genomes. The mTR plasmids contain homologous mTR sequences, which may have facilitated recombination of the transfected plasmid into the mTR elements of MHV68 genomes. However, the integration of nonhomologous pRepCK vector DNA into episomal viral episomes was highly unexpected. S11 cells contain ~40 MHV68 genomes per cell (61). The MHV68 genome is comprised of ~120 kb of unique sequence, plus an unknown number of mTR elements (64). Assuming an mTR copy number of ~40, similar to that in KSHV, the total MHV68 genome consists of ~170 kb. Therefore, there are $\sim 7 \times 10^6$ bp of MHV68 per S11 cell, compared with 2.5×10^9 bp of cell DNA (66), so MHV68 accounts for only ~0.3% of the total DNA present in the cell. The finding that 3 of 6 (50%) G418-resistant cell lines had vector integrated into MHV68 episomes indicates a >150-fold higher rate of integration than expected if integration were completely stochastic. It is possible that integration occurred in cells undergoing lytic replication, which contained increased levels of MHV68 DNA and therefore increased the possibility of integration. Virions released from these dying cells may then have superinfected latently infected cells to form episomes. Although we do not know if the site of integration in MHV68 is the same for each G418-resistant line, it is possible that MHV68 may contain a certain sequence, perhaps the mTR elements, that is highly prone to recombination.

Gardella gel analyses demonstrated that episomes with mLANA and mTRs migrated much more slowly than the input plasmids (Fig. 2, 3, 5, 6, and 7), consistent with recombination events leading to substantial size increases. In fact, much of the episomal signal migrated slower than the ~170-kb MHV68 episomes in S11 cells (Fig. 5 to 7). We previously observed similar increases in episome size in KSHV LANA episome maintenance, due to TR duplication and generation of input plasmids into multimers (4, 18). It is likely that there is strong selection for recombination events leading to increased numbers of mTR elements and/or an increased copy number of the mLANA expression cassette. If MHV68 contains ~40 TR elements (similar to KSHV) and therefore represents an optimal number for episome maintenance, recombination events leading to larger numbers of mTRs (up to ~40 copies) may occur.

Although MHV68 ORF74 and the C-terminal portion of ORF75C are included in the upstream sequence of the mLANA constructs containing the native promoter sequence (Fig. 1B), it is highly unlikely that either exerts a role in episome persistence. Most importantly, episome persistence occurred in the absence of ORF74 and truncated ORF75C with plasmids containing CMV-driven mLANA and mTRs (Fig. 3). Though episome maintenance efficiency was lower with CMV-driven mLANA, this finding correlated with a lower level of mLANA expression from these constructs. In addition, both mLANAF-m8TRrev (Fig. 5 and 6) and mLANAF-8TR (Fig. 7) contain the same mLANA upstream sequence yet had substantially different episome maintenance efficiencies (Fig. 1C). The difference between these two plasmids is only the orientation of the mTR elements in relation to the

mLANA cassette, which resulted in much higher mLANA expression for mLANAF-8TR, with a concomitant increase in episome maintenance efficiency. Furthermore, ORF75C is severely truncated, while ORF74 is a plasma membrane protein homologous to KSHV ORF74, which is a G protein-coupled receptor (65), and its plasma membrane location is not compatible with episome maintenance function.

The presence of the mTR elements in genomic orientation substantially enhanced mLANA expression (Fig. 4, 5, and 7). At least three promoters for mLANA have been described (Fig. 1B). Two are located within the terminal repeat elements, with one either completely (12) or partially (2) contained in the left half of the mTR and one in the right half of the mTR (2, 12). A third promoter is located just proximal to mLANA (12). In addition, the mTR element has enhancer activity for the promoter in the left half of the mTR (2), while the left end of the unique sequence of the MHV68 genome (which was not present in the constructs used here) has enhancer activity for the promoter in the right half of the mTR (12). Since the addition of the mTR elements in native orientation to mLANA substantially enhanced its expression (Fig. 4), it is likely that an mTR promoter was driving the enhanced mLANA expression. It is also possible that the mTR provided enhancer activity to the promoter immediately upstream of mLANA, although the orientation dependence of the mTR elements, in which expression was enhanced only in the native, not reverse, genomic orientation relative to mLANA in the constructs containing eight mTR elements, makes this scenario less likely. When expressed from MHV68, mLANA transcripts contain up to three 5'-untranslated exons, including one at the right end of the unique MHV68 genome and up to two different exons from within the mTR elements (2, 12, 34) (Fig. 1B). Since the unique sequence at the right end of the MHV68 genome is absent in the constructs used here, this exon would be omitted in our experiments when transcription occurs from the mTRs. We observed increased mLANA expression with a higher mTR copy number (Fig. 4), and this could be consistent with multiple active mTR promoters being active and/or increased numbers of mTR enhancer elements acting on the mTR promoter(s). Notably, the splice acceptor site just upstream of the mLANA ORF is present in the constructs with the native upstream mLANA sequence but absent in the CMV promoter constructs, so splicing to this site can occur only in those constructs where the native sequence is present. It is possible that the increased expression of mLANA from the CMV promoter in the presence of four upstream mTR elements (Fig. 4) could be due to mTR enhancer activity or a cryptic splice acceptor site resulting in the mTR promoter driving expression. The generally low expression level from the CMV promoter observed here could possibly be improved with a stronger Kozak consensus sequence.

Transcription of mLANA has several notable differences from that of KSHV LANA. In contrast to the mLANA promoters, the KSHV LANA promoter is located only immediately upstream of the LANA ORF, and there are not additional promoters in the KSHV TR elements. Of note, the promoter for the KSHV K1 gene does extend into the TR, but this is located in the opposite orientation from that of LANA to drive K1 expression at the extreme left end of the KSHV genome (9, 62). In addition, the KSHV LANA transcript is polycistronic and includes two additional ORFs, those of v-cyclin and v-FLIP, while the MHV68 transcript contains only the mLANA ORF (19, 55, 60). Another distinguish-

ing feature between KSHV and MHV68 is that the LANA promoter is activated by LANA (35, 52), while mLANA modestly downregulates the mLANA promoters (12). Also, KSHV ORF50, the lytic switch protein, activates the LANA promoter (43, 47), while mORF50 represses the promoter immediately upstream of mLANA and has little effect on the mTR promoters (12).

In comparison with KSHV LANA, the efficiency of mLANA episome persistence in these experiments appears to be relatively low. The highest efficiency of episome persistence in A20 cells occurred with mLANAF-8TR, for which 72% of G418-resistant cell lines contained episomes, and this efficiency was lower when plasmids contained only four or two mTR elements. Episome maintenance efficiency was somewhat higher in MEF cells than in A20 cells (up to 80% of mLANA-m2TR G418-resistant cell lines had episomes), although this finding was based on assessment of relatively few cell lines. Notably, the absence of episomes was not always due to a loss of mLANA expression, since mLANA continued to be expressed even in the absence of detectable episomes (Fig. 5 and 7). In contrast, in similar experiments with KSHV LANA constructs containing a LANA expression cassette with eight TR elements in *cis*, 100% of G418-resistant cell lines contained episomes (our unpublished data). It is possible that more mTR elements may be present in the MHV68 genome than the ~40 elements in KSHV, and therefore more mTR elements may be necessary for efficient episome persistence. KSHV LANA is a larger protein than MHV68 LANA and may have evolved to be more efficient in its episome persistence.

This work demonstrates that mLANA is nuclear and associates with mitotic chromosomes (Fig. 8). The pattern of distribution is very similar to that of KSHV LANA. In the absence of episomes, LANA distributes broadly throughout interphase nuclei and over mitotic chromosomes. However, when KSHV episomes are present, LANA is concentrated at dots at the sites of KSHV DNA both in interphase and along mitotic chromosomes (3, 5, 6, 14, 36, 38, 42, 51). mLANA was broadly distributed throughout the nucleus and over mitotic chromosomes in episome-deficient cells but was concentrated at dots in interphase nuclei and along mitotic chromosomes in episome-containing cells. It is likely that mLANA concentrates at sites of MHV68 episomes. This finding supports the hypothesis that mLANA directly tethers MHV68 episomes to mitotic chromosomes to allow for efficient segregation to daughter nuclei, similar to the tethering mechanism of KSHV LANA (3, 14). This mechanism of bridging episomes to chromosomes has also been proposed for HVS LANA (11, 13, 63). It is likely that mLANA attaches to episomes through direct binding of mTR DNA, similar to KSHV and HVS LANAs (4, 13, 15, 21, 28, 63, 68).

In summary, this work demonstrates that mLANA acts on MHV68 mTR DNA to mediate episome persistence. These results suggest that mLANA tethers mTR DNA to mitotic chromosomes to efficiently segregate MHV68 DNA into progeny nuclei. Future work is necessary to understand the molecular mechanisms underlying this process and to better understand the similarities and differences between KSHV and MHV68 LANA functions.

ACKNOWLEDGMENTS

This work was supported by grants from the National Cancer Institute (CA082036) (K.M.K.) and the U.S. Department of Defense (PR093491) (K.M.K.), by a collaborative supplement from the National Cancer Institute (CA103642) (E.J.U. and K.M.K.), by the Harvard Medical School-Portugal Program in Translational Research and Information (J.P.S. and

K.M.K.), and by the Fonds de Recherche en Santé du Québec (FRSQ) and the Canadian Institutes of Health Research (CIHR) (C.B.).

REFERENCES

- Albrecht JC. 1992. Primary structure of the herpesvirus saimiri genome. *J. Virol.* 66:5047–5058.
- Allen RD, 3rd, Dickerson S, Speck SH. 2006. Identification of spliced gammaherpesvirus 68 LANA and v-cyclin transcripts and analysis of their expression in vivo during latent infection. *J. Virol.* 80:2055–2062.
- Ballestas ME, Chatis PA, Kaye KM. 1999. Efficient persistence of extra-chromosomal KSHV DNA mediated by latency-associated nuclear antigen. *Science* 284:641–644.
- Ballestas ME, Kaye KM. 2001. Kaposi's sarcoma-associated herpesvirus latency-associated nuclear antigen 1 mediates episome persistence through cis-acting terminal repeat (TR) sequence and specifically binds TR DNA. *J. Virol.* 75:3250–3258.
- Barbera AJ, Ballestas ME, Kaye KM. 2004. The Kaposi's sarcoma-associated herpesvirus latency-associated nuclear antigen 1 N terminus is essential for chromosome association, DNA replication, and episome persistence. *J. Virol.* 78:294–301.
- Barbera AJ, et al. 2006. The nucleosomal surface as a docking station for Kaposi's sarcoma herpesvirus LANA. *Science* 311:856–861.
- Blasdel K, et al. 2003. The wood mouse is a natural host for murid herpesvirus 4. *J. Gen. Virol.* 84:111–113.
- Blaskovic D, Stancekova M, Svobodova J, Mistrikova J. 1980. Isolation of five strains of herpesviruses from two species of free living small rodents. *Acta Virol.* 24:468.
- Bowser BS, DeWire SM, Damania B. 2002. Transcriptional regulation of the K1 gene product of Kaposi's sarcoma-associated herpesvirus. *J. Virol.* 76:12574–12583.
- Calderwood M, White RE, Griffiths RA, Whitehouse A. 2005. Open reading frame 73 is required for herpesvirus saimiri A11-S4 episomal persistence. *J. Gen. Virol.* 86:2703–2708.
- Calderwood MA, Hall KT, Matthews DA, Whitehouse A. 2004. The herpesvirus saimiri ORF73 gene product interacts with host-cell mitotic chromosomes and self-associates via its C terminus. *J. Gen. Virol.* 85:147–153.
- Coleman HM, Efstathiou S, Stevenson PG. 2005. Transcription of the murine gammaherpesvirus 68 ORF73 from promoters in the viral terminal repeats. *J. Gen. Virol.* 86:561–574.
- Collins CM, Medveczky MM, Lund T, Medveczky PG. 2002. The terminal repeats and latency-associated nuclear antigen of herpesvirus saimiri are essential for episomal persistence of the viral genome. *J. Gen. Virol.* 83:2269–2278.
- Cotter MA, 2nd, Robertson ES. 1999. The latency-associated nuclear antigen tethers the Kaposi's sarcoma-associated herpesvirus genome to host chromosomes in body cavity-based lymphoma cells. *Virology* 264:254–264.
- Cotter MA, 2nd, Subramanian C, Robertson ES. 2001. The Kaposi's sarcoma-associated herpesvirus latency-associated nuclear antigen binds to specific sequences at the left end of the viral genome through its carboxy-terminus. *Virology* 291:241–259.
- Decker LL, et al. 1996. The Kaposi sarcoma-associated herpesvirus (KSHV) is present as an intact latent genome in KS tissue but replicates in the peripheral blood mononuclear cells of KS patients. *J. Exp. Med.* 184:283–288.
- Delecluse HJ, Bartnizke S, Hammerschmidt W, Bullerdiek J, Bornkamm GW. 1993. Episomal and integrated copies of Epstein-Barr virus coexist in Burkitt lymphoma cell lines. *J. Virol.* 67:1292–1299.
- De Leon Vazquez E, Kaye KM. 2011. The internal Kaposi's sarcoma-associated herpesvirus LANA regions exert a critical role on episome persistence. *J. Virol.* 85:7622–7633.
- Dittmer D, et al. 1998. A cluster of latently expressed genes in Kaposi's sarcoma-associated herpesvirus. *J. Virol.* 72:8309–8315.
- Doherty PC, Christensen JP, Belz GT, Stevenson PG, Sangster MY. 2001. Dissecting the host response to a gamma-herpesvirus. *Philos. Trans. R. Soc. Lond. B Biol. Sci.* 356:581–593.
- Fejer G, et al. 2003. The latency-associated nuclear antigen of Kaposi's sarcoma-associated herpesvirus interacts preferentially with the terminal repeats of the genome in vivo and this complex is sufficient for episomal DNA replication. *J. Gen. Virol.* 84:1451–1462.
- Fickenscher H, Fleckenstein B. 2001. Herpesvirus saimiri. *Philos. Trans. R. Soc. Lond. B Biol. Sci.* 356:545–567.

23. Flano E, Husain SM, Sample JT, Woodland DL, Blackman MA. 2000. Latent murine gamma-herpesvirus infection is established in activated B cells, dendritic cells, and macrophages. *J. Immunol.* 165:1074–1081.
24. Flano E, Woodland DL, Blackman MA. 2002. A mouse model for infectious mononucleosis. *Immunol. Res.* 25:201–217.
25. Fowler P, Marques S, Simas JP, Efstathiou S. 2003. ORF73 of murine herpesvirus-68 is critical for the establishment and maintenance of latency. *J. Gen. Virol.* 84:3405–3416.
26. Ganem D. 2007. Kaposi's sarcoma-associated herpesvirus, p 2847–2888. *In* Knipe DM, Howley PM (ed), *Fields virology*, vol 2. Lippincott Williams & Wilkins, Philadelphia, PA.
27. Garber AC, Hu J, Renne R. 2002. Latency-associated nuclear antigen (LANA) cooperatively binds to two sites within the terminal repeat, and both sites contribute to the ability of LANA to suppress transcription and to facilitate DNA replication. *J. Biol. Chem.* 277:27401–27411.
28. Garber AC, Shu MA, Hu J, Renne R. 2001. DNA binding and modulation of gene expression by the latency-associated nuclear antigen of Kaposi's sarcoma-associated herpesvirus. *J. Virol.* 75:7882–7892.
29. Gardella T, Medveczky P, Sairenji T, Mulder C. 1984. Detection of circular and linear herpesvirus DNA molecules in mammalian cells by gel electrophoresis. *J. Virol.* 50:248–254.
30. Griffiths R, Harrison SM, Macnab S, Whitehouse A. 2008. Mapping the minimal regions within the ORF73 protein required for herpesvirus saimiri episomal persistence. *J. Gen. Virol.* 89:2843–2850.
31. Griffiths R, Whitehouse A. 2007. Herpesvirus saimiri episomal persistence is maintained via interaction between open reading frame 73 and the cellular chromosome-associated protein MeCP2. *J. Virol.* 81:4021–4032.
32. Grundhoff A, Ganem D. 2003. The latency-associated nuclear antigen of Kaposi's sarcoma-associated herpesvirus permits replication of terminal repeat-containing plasmids. *J. Virol.* 77:2779–2783.
33. Hu J, Garber AC, Renne R. 2002. The latency-associated nuclear antigen of Kaposi's sarcoma-associated herpesvirus supports latent DNA replication in dividing cells. *J. Virol.* 76:11677–11687.
34. Husain SM, et al. 1999. Murine gammaherpesvirus M2 gene is latency-associated and its protein a target for CD8(+) T lymphocytes. *Proc. Natl. Acad. Sci. U. S. A.* 96:7508–7513.
35. Jeong JH, et al. 2004. Regulation and auto-regulation of the promoter for the latency-associated nuclear antigen (LANA) of Kaposi's sarcoma-associated herpesvirus. *J. Biol. Chem.* 279:16822–16831.
36. Kelley-Clarke B, Ballestas ME, Komatsu T, Kaye KM. 2007. Kaposi's sarcoma herpesvirus C-terminal LANA concentrates at pericentromeric and peri-telomeric regions of a subset of mitotic chromosomes. *Virology* 357:149–157.
37. Kelley-Clarke B, et al. 2007. Determination of Kaposi's sarcoma-associated herpesvirus C-terminal latency-associated nuclear antigen residues mediating chromosome association and DNA binding. *J. Virol.* 81:4348–4356.
38. Kelley-Clarke B, De Leon-Vazquez E, Slain K, Barbera AJ, Kaye KM. 2009. Role of Kaposi's sarcoma-associated herpesvirus C-terminal LANA chromosome binding in episome persistence. *J. Virol.* 83:4326–4337.
39. Kieff ED, Rickinson AB. 2007. Epstein-Barr virus and its replication, p 2603–2654. *In* Knipe DM, et al (ed), *Fields virology*, vol 2. Lippincott Williams & Wilkins, Philadelphia, PA.
40. Kim KJ, Kanellopoulos-Langevin C, Merwin RM, Sachs DH, Asofsky R. 1979. Establishment and characterization of BALB/c lymphoma lines with B cell properties. *J. Immunol.* 122:549–554.
41. Komatsu T, Ballestas ME, Barbera AJ, Kelley-Clarke B, Kaye KM. 2004. KSHV LANA1 binds DNA as an oligomer and residues N-terminal to the oligomerization domain are essential for DNA binding, replication, and episome persistence. *Virology* 319:225–236.
42. Krithivas A, Fujimuro M, Weidner M, Young DB, Hayward SD. 2002. Protein interactions targeting the latency-associated nuclear antigen of Kaposi's sarcoma-associated herpesvirus to cell chromosomes. *J. Virol.* 76:11596–11604.
43. Lan K, et al. 2005. Induction of Kaposi's sarcoma-associated herpesvirus latency-associated nuclear antigen by the lytic transactivator RTA: a novel mechanism for establishment of latency. *J. Virol.* 79:7453–7465.
44. Lim C, Seo T, Jung J, Choe J. 2004. Identification of a virus trans-acting regulatory element on the latent DNA replication of Kaposi's sarcoma-associated herpesvirus. *J. Gen. Virol.* 85:843–855.
45. Lim C, Sohn H, Lee D, Gwack Y, Choe J. 2002. Functional dissection of latency-associated nuclear antigen 1 of Kaposi's sarcoma-associated herpesvirus involved in latent DNA replication and transcription of terminal repeats of the viral genome. *J. Virol.* 76:10320–10331.
46. Marques S, Efstathiou S, Smith KG, Haury M, Simas JP. 2003. Selective gene expression of latent murine gammaherpesvirus 68 in B lymphocytes. *J. Virol.* 77:7308–7318.
47. Matsumura S, Fujita Y, Gomez E, Tanese N, Wilson AC. 2005. Activation of the Kaposi's sarcoma-associated herpesvirus major latency locus by the lytic switch protein RTA (ORF50). *J. Virol.* 79:8493–8505.
48. Moorman NJ, Willer DO, Speck SH. 2003. The gammaherpesvirus 68 latency-associated nuclear antigen homolog is critical for the establishment of splenic latency. *J. Virol.* 77:10295–10303.
49. Nash AA, Dutia BM, Stewart JP, Davison AJ. 2001. Natural history of murine gamma-herpesvirus infection. *Philos. Trans. R. Soc. Lond. B Biol. Sci.* 356:569–579.
50. Paden CR, Forrest JC, Moorman NJ, Speck SH. 2010. Murine gamma-herpesvirus 68 LANA is essential for virus reactivation from splenocytes but not long-term carriage of viral genome. *J. Virol.* 84:7214–7224.
51. Pilot T, Tramier M, Coppey M, Nicolas JC, Marechal V. 2001. Close but distinct regions of human herpesvirus 8 latency-associated nuclear antigen 1 are responsible for nuclear targeting and binding to human mitotic chromosomes. *J. Virol.* 75:3948–3959.
52. Renne R, et al. 2001. Modulation of cellular and viral gene expression by the latency-associated nuclear antigen of Kaposi's sarcoma-associated herpesvirus. *J. Virol.* 75:458–468.
53. Rickinson AB, Kieff ED. 2007. Epstein-Barr virus, p 2655–2700. *In* Knipe DM, et al (ed), *Fields virology*, vol 2. Lippincott Williams & Wilkins, Philadelphia, PA.
54. Russo JJ, et al. 1996. Nucleotide sequence of the Kaposi sarcoma-associated herpesvirus (HHV8). *Proc. Natl. Acad. Sci. U. S. A.* 93:14862–14867.
55. Sarid R, Flore O, Bohenzky RA, Chang Y, Moore PS. 1998. Transcription mapping of the Kaposi's sarcoma-associated herpesvirus (human herpesvirus 8) genome in a body cavity-based lymphoma cell line (BC-1). *J. Virol.* 72:1005–1012.
56. Simas JP, Efstathiou S. 1998. Murine gammaherpesvirus 68: a model for the study of gammaherpesvirus pathogenesis. *Trends Microbiol.* 6:276–282.
57. Speck SH, Ganem D. 2010. Viral latency and its regulation: lessons from the gamma-herpesviruses. *Cell Host Microbe* 8:100–115.
58. Speck SH, Virgin HW. 1999. Host and viral genetics of chronic infection: a mouse model of gamma-herpesvirus pathogenesis. *Curr. Opin. Microbiol.* 2:403–409.
59. Stewart JP, Usherwood EJ, Ross A, Dyson H, Nash T. 1998. Lung epithelial cells are a major site of murine gammaherpesvirus persistence. *J. Exp. Med.* 187:1941–1951.
60. Talbot SJ, Weiss RA, Kellam P, Boshoff C. 1999. Transcriptional analysis of human herpesvirus-8 open reading frames 71, 72, 73, K14, and 74 in a primary effusion lymphoma cell line. *Virology* 257:84–94.
61. Usherwood EJ, Stewart JP, Nash AA. 1996. Characterization of tumor cell lines derived from murine gammaherpesvirus-68-infected mice. *J. Virol.* 70:6516–6518.
62. Verma SC, Lan K, Choudhuri T, Robertson ES. 2006. Kaposi's sarcoma-associated herpesvirus-encoded latency-associated nuclear antigen modulates K1 expression through its cis-acting elements within the terminal repeats. *J. Virol.* 80:3445–3458.
63. Verma SC, Robertson ES. 2003. ORF73 of herpesvirus saimiri strain C488 tethers the viral genome to metaphase chromosomes and binds to cis-acting DNA sequences in the terminal repeats. *J. Virol.* 77:12494–12506.
64. Virgin HW, IV, et al. 1997. Complete sequence and genomic analysis of murine gammaherpesvirus 68. *J. Virol.* 71:5894–5904.
65. Wakeling MN, Roy DJ, Nash AA, Stewart JP. 2001. Characterization of the murine gammaherpesvirus 68 ORF74 product: a novel oncogenic G protein-coupled receptor. *J. Gen. Virol.* 82:1187–1197.
66. Waterston RH, et al. 2002. Initial sequencing and comparative analysis of the mouse genome. *Nature* 420:520–562.
67. Weck KE, Kim SS, Virgin HI, Speck SH. 1999. Macrophages are the major reservoir of latent murine gammaherpesvirus 68 in peritoneal cells. *J. Virol.* 73:3273–3283.
68. White RE, Calderwood MA, Whitehouse A. 2003. Generation and precise modification of a herpesvirus saimiri bacterial artificial chromosome demonstrates that the terminal repeats are required for both virus production and episomal persistence. *J. Gen. Virol.* 84:3393–3403.
69. Wong LY, Matchett GA, Wilson AC. 2004. Transcriptional activation by the Kaposi's sarcoma-associated herpesvirus latency-associated nuclear antigen is facilitated by an N-terminal chromatin-binding motif. *J. Virol.* 78:10074–10085.

4 Cross-species conservation of episome maintenance provides a basis for in vivo investigation of Kaposi's sarcoma herpes virus LANA

Aline C. Habison¹✉, Marta Pires de Miranda²✉, Chantal Beauchemin¹, Min Tan¹, Sofia A. Cerqueira², Bruno Correia³, Rajesh Ponnusamy³, Edward J. Usherwood⁴, Colin E. McVey³, J. Pedro Simas^{23*}, and Kenneth M. Kaye^{13*}

RESEARCH ARTICLE

Cross-species conservation of episome maintenance provides a basis for in vivo investigation of Kaposi's sarcoma herpesvirus LANA

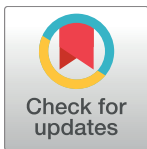
Aline C. Habison¹✉, Marta Pires de Miranda²✉, Chantal Beauchemin¹, Min Tan¹, Sofia A. Cerqueira², Bruno Correia³, Rajesh Ponnusamy³, Edward J. Usherwood⁴, Colin E. McVey³, J. Pedro Simas^{2†*}, Kenneth M. Kaye^{1‡*}

1 Departments of Medicine, Brigham and Women's Hospital, Harvard Medical School, Boston, Massachusetts, United States of America, **2** Instituto de Medicina Molecular, Faculdade de Medicina, Universidade de Lisboa, Lisboa, Portugal, **3** Instituto de Tecnologia Química e Biológica António Xavier, Universidade Nova de Lisboa, Oeiras, Portugal, **4** Department of Microbiology and Immunology, Geisel School of Medicine at Dartmouth, Lebanon, New Hampshire, United States of America

✉ These authors contributed equally to this work.

‡ JPM and KMK are joint senior authors.

* kkaye@bwh.harvard.edu (KMK); psimas@medicina.ulisboa.pt (JPS)



OPEN ACCESS

Citation: Habison AC, de Miranda MP, Beauchemin C, Tan M, Cerqueira SA, Correia B, et al. (2017) Cross-species conservation of episome maintenance provides a basis for in vivo investigation of Kaposi's sarcoma herpesvirus LANA. *PLoS Pathog* 13(9): e1006555. <https://doi.org/10.1371/journal.ppat.1006555>

Editor: Sankar Swaminathan, University of Utah, UNITED STATES

Received: May 9, 2017

Accepted: July 27, 2017

Published: September 14, 2017

Copyright: © 2017 Habison et al. This is an open access article distributed under the terms of the [Creative Commons Attribution License](https://creativecommons.org/licenses/by/4.0/), which permits unrestricted use, distribution, and reproduction in any medium, provided the original author and source are credited.

Data Availability Statement: All relevant data are within the paper and its Supporting Information files.

Funding: This work was supported in part by National Institutes of Health grants CA082036 (NCI), DE025208, and DE024971 (both NIDCR), to KMK, FCT PTDC/IMI-MIC/0980/2014 to JPS, FCT Harvard Medical School Portugal Program in Translational Research (HMSP-ICT/0021/2010) to JPS, KMK, CEM, Instituto de Medicina Molecular

Abstract

Many pathogens, including Kaposi's sarcoma herpesvirus (KSHV), lack tractable small animal models. KSHV persists as a multi-copy, nuclear episome in latently infected cells. KSHV latency-associated nuclear antigen (kLANA) binds viral terminal repeat (kTR) DNA to mediate episome persistence. Model pathogen murine gammaherpesvirus 68 (MHV68) mLANA acts analogously on mTR DNA. kLANA and mLANA differ substantially in size and kTR and mTR show little sequence conservation. Here, we find kLANA and mLANA act reciprocally to mediate episome persistence of TR DNA. Further, kLANA rescued mLANA deficient MHV68, enabling a chimeric virus to establish latent infection in vivo in germinal center B cells. The level of chimeric virus in vivo latency was moderately reduced compared to WT infection, but WT or chimeric MHV68 infected cells had similar viral genome copy numbers as assessed by immunofluorescence of LANA intranuclear dots or qPCR. Thus, despite more than 60 Ma of evolutionary divergence, mLANA and kLANA act reciprocally on TR DNA, and kLANA functionally substitutes for mLANA, allowing kLANA investigation in vivo. Analogous chimeras may allow in vivo investigation of genes of other human pathogens.

Author summary

KSHV latently infects cells and persists as a multi-copy, nuclear episome. KSHV LANA (kLANA) maintains episomes by acting on viral terminal repeat (kTR) elements. Model pathogen MHV68 mLANA acts analogously on mTR DNA. To date, KSHV investigation has been limited by lack of a tractable, small animal model. Here, we find that despite 60

Directors Fund to JPS, and iNOVA4Health Research Unit (LISBOA-01-0145-FEDER-007344) FCT/FEDER (PT2020 Partnership Agreement) to CEM. M.P.M is supported by a fellowship from Fundação para a Ciência e Tecnologia (FCT), Portugal. The funders had no role in study design, data collection and analysis, decision to publish, or preparation of the manuscript.

Competing interests: The authors declare no competing interests exist.

Ma of evolutionary divergence, kLANA and mLANA exhibit inter-species functionality, acting reciprocally on TR DNA to mediate episome persistence. Further, kLANA rescued mLANA deficient MHV68, allowing chimeric virus to establish latent infection in vivo. The level of in vivo latency was moderately lower for kLANA chimeric virus compared to that of WT, but chimeric and WT virus infected cells had similar virus genome copy numbers. These results now provide a tractable model to investigate kLANA in vivo. This chimeric approach has the potential to be broadly applied to other small animal models for human pathogens.

Introduction

Kaposi's sarcoma-associated herpesvirus (KSHV), a gamma-2 herpesvirus, is the etiologic agent of Kaposi's sarcoma, primary effusion lymphoma, and multicentric Castleman's disease[1–5]. KSHV infection of tumor cells is predominantly latent. During latent infection, KSHV persists as a nuclear, multi-copy, extrachromosomal, circular episome[6]. To persist in proliferating cells, genomes must replicate with each cell division and segregate to progeny nuclei.

The latency-associated nuclear antigen (kLANA) (Fig 1A) is one of a small subset of KSHV genes expressed in latency. LANA acts on KSHV terminal repeat (kTR) DNA to mediate episome persistence[7,8], for which it is essential[9]. N-terminal LANA binds histones H2A/H2B on the nucleosome surface to attach to mitotic chromosomes[10], and C-terminal LANA DNA binding domain (DBD) simultaneously binds adjacent LANA binding sites (LBSs) within TR DNA, to form a molecular tethering apparatus which ensures genomes are segregated to daughter cell nuclei following mitosis[8,11–14]. LANA also mediates KSHV DNA replication and exerts important transcriptional and growth effects[11,15–25].

Although KSHV infection is naturally limited to humans, the pursuit of a small animal model of infection to study pathogenesis has been a longstanding goal in the field and has been accomplished in several models of immune compromised mice. KSHV injection into SCID mice implanted with human fetal thymus and liver grafts led to lytic and latent infection with B cells most commonly infected[26], while injection into NOD/SCID mice resulted in latent and lytic gene expression over several months with infection of multiple cell types including B cells[27]. Oral, intraperitoneal or vaginal inoculation into a humanized NOD/SCID/IL2rgamma mouse implanted with human fetal liver and thymus permitted KSHV infection of B cells and macrophages[28]. These models are advantageous in allowing direct investigation of KSHV, but are limited by their requirement for immune suppressed mice.

Murine gamma-2 herpesvirus 68 (MHV68 or murid herpesvirus 4) infection of laboratory mice provides a complementary, well-characterized model for gammaherpesvirus investigation. After intranasal inoculation, MHV68 undergoes lytic infection in the lungs, disseminates to lymphoid organs where it establishes latency in the spleen, and drives proliferation of germinal center (GC) B cells[29–31]. MHV68 shares sequence homology and has a genome that is generally colinear with KSHV[32]. MHV68 encodes a LANA homolog (mLANA), which is smaller than kLANA but has a conserved C-terminal DNA binding domain (Fig 1A). Analogous to kLANA, mLANA acts on mTR DNA to mediate episome persistence[33]. Consistent with its central role in episome persistence, mLANA is essential for efficient establishment of MHV68 latency in vivo[34–36].

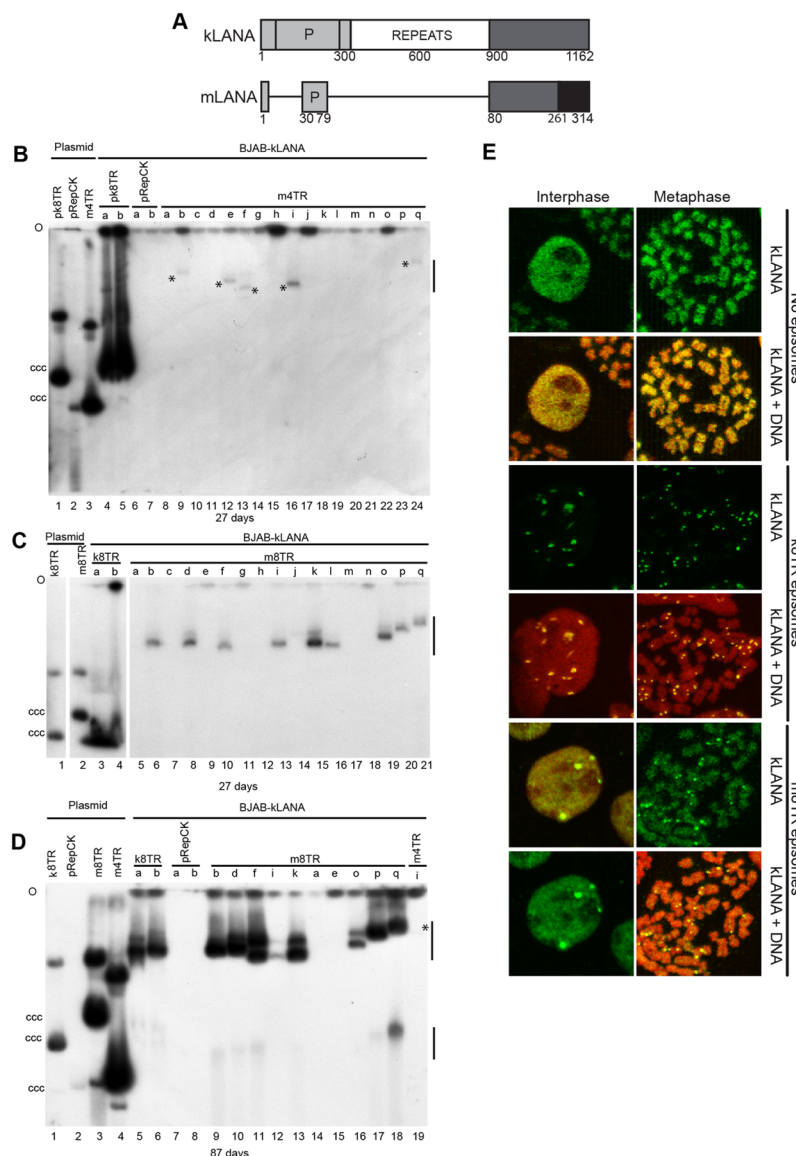


Fig 1. kLANA mediates mTR episome persistence. (A) Schematic of kLANA and mLANA. Homologous regions are indicated in grey shading. White and black regions share no homology. Amino acid residue numbers are indicated. P, proline-rich. Gardella gels after transfection of m4TR (B) or m8TR (C) DNA. Blots in B and C were probed with ^{32}P -pRepCK DNA. (D) Gardella gel after 87 days of indicated cell lines from panels B and C. Blot was probed with ^{32}P -m8TR DNA. Days of G418 selection are below each panel. O, gel origin; ccc plasmid DNA is indicated. Lanes contain 1.5×10^6 cells. Vertical lines at right (panels B, C, E) indicate positions of episomal bands. Asterisks indicate faint episomal bands. (E) Immune fluorescence for kLANA. m8TR cells are from cell line d (panels C, D). Brightness and contrast were uniformly adjusted in panels from the same field and red signal was uniformly enhanced for k8TR panels using Adobe Photoshop. Magnification, 630x.

<https://doi.org/10.1371/journal.ppat.1006555.g001>

In this work, we investigated the possibility of inter-species functionality between MHV68 and KSHV LANA for episome maintenance. We found that kLANA can support episome persistence of plasmids containing mTR elements and similarly, mLANA can support episome persistence of kTR plasmids. Further, we found that a chimeric MHV68, expressing kLANA, but not mLANA, was capable of establishing latent infection in splenic GC B cells, thus providing a model for kLANA investigation in vivo.

Results

KSHV LANA acts on mTRs to establish episome persistence

Since KSHV and MHV68 LANAs share homology (Fig 1A), we assessed if kLANA can mediate episome persistence of MHV68 TR (mTR) elements. We transfected DNA (encoding G418 resistance) containing 8 (m8TR), 4 (m4TR), or 2 (m2TR) MHV68 TR copies, 8 KSHV TR (pk8TR) copies, or vector (pRepCK) into human BJAB B lymphoma cells stably expressing kLANA (BJAB-kLANA). k8TR exhibited much higher outgrowth from kLANA expressing cells as compared with control BJAB cells (S1 Table). The higher outgrowth is due to the much higher efficiency of kLANA mediated episome persistence compared with integration. Similarly, m8TR, m4TR, and m2TR G418 resistant outgrowth was also increased in BJAB-kLANA cells compared with BJAB cells, consistent with possible kLANA mediated episome persistence.

G418 resistant cell lines were expanded and assessed for the presence of episomes by Gardella gels. In Gardella gels, live cells are loaded into gel wells, and lysed *in situ*. During electrophoresis, chromosomal DNA remains at the gel origin, whereas episomal DNA as large as several hundred kilobases migrates into the gel. As expected, BJAB-kLANA cells transfected with pk8TR showed strong episomal signal in all tested cell lines (Fig 1B–1D)(Table 1). Also, as expected, BJAB-kLANA cells transfected with vector pRepCK, which does not contain TR sequence, lacked episomes (Fig 1B and 1D). Transfection of m2TR DNA into BJAB-kLANA cells resulted in only one of 31 (3%) G418 resistant cell lines with episomes (Table 1). After transfection of m4TR DNA into BJAB-kLANA cells and G418 selection for 27 days, episomes were detected in five (Fig 1B, indicated with asterisks) of 17 lanes, and in three experiments, 12 of 37 (32%) G418 resistant cell lines contained episomes. The episomal signal was substantially weaker for the m4TR episomes compared to the pk8TR episomal DNA (Fig 1B, compare

Table 1. Episome maintenance of mTR or kTR DNA in mLANA or kLANA expressing cells.

Cell line	Transfected DNA	Episome positive (%) ¹
BJAB-kLANA ²	pk8TR	19/19 (100%)
BJAB-kLANA	m2TR	1/31 (3%)
BJAB-kLANA	m4TR	12/37 (32%)
BJAB-kLANA ²	m8TR	19/50 (38%)
BJAB-kLANA ²	pRepCK	0/16 (0%)
BJAB	m2TR	0/7 (0%)
BJAB	m4TR	0/9 (0%)
BJAB	m8TR	0/14 (0%)
A20-mLANAF(A) ³	m4TR-P	5/20 (25%)
A20-mLANAF(B) ⁴	m4TR-P	48/83 (58%)
A20-mLANAF(B)	pRepCK-P	0/21 (0%)
A20 ³	m4TR-P	0/34 (0%)
A20-mLANAF(A)	pk8TR-P	2/3 (67%)
A20-mLANAF(B)	pk8TR-P	27/29 (93%)
A20	pk8TR-P	0/10 (0%)

¹ Fractions indicate number of cell lines containing episomes divided by the total number of cell lines assayed by Gardella analyses; percentages are in parenthesis.

²Data from three experiments

³Data from two experiments.

⁴Data from five experiments.

<https://doi.org/10.1371/journal.ppat.1006555.t001>

pk8TR with m4TR lanes), indicating less episomal DNA in these cells. For m8TR DNA, episomes were detected in 10 of 17 lanes (Fig 1C), and in three experiments, 19 of 50 (38%) of G418 resistant cell lines had episomes. Although the m8TR episomal signal was weaker compared to that of the pk8TR cells (Fig 1C), there was substantially more m8TR episomal signal compared to that of m4TR (Fig 1B). Probe used in Fig 1B and 1C detected only vector backbone and therefore the efficiency of detection for all plasmids was the same. In general, mTR episomes migrated much more slowly than the ccc plasmid DNA (e.g. Fig 1B, lane 3 or Fig 1C, lane 2), and also more slowly than most pk8TR episomal DNA at 27 days of selection. The large, recombinant episomes were due to recombination events, and were primarily comprised of input plasmids arranged in tandem head to tail multimers, with expansion and contraction of tandem mTRs also occurring (S1 Text, S1 and S2 Figs). Therefore, kLANA can mediate episome persistence of mTR DNA and the efficiency of episome persistence is greater with higher mTR copy number.

We investigated kLANA's ability to maintain mTR episomes over a longer time period. Of four cell lines (Fig 1B, cell lines b, e, f, i) that initially had m4TR episomes after 27 days of G418 selection, three (Fig 1B, cell lines b, e, f) no longer contained episomes after ~2 months in continuous culture and the fourth m4TR cell line (Fig 1B, cell line i) had lost nearly all episomal DNA after 87 days of G418 selection (Fig 1D, lane 19, asterisk indicates faint band). In contrast, eight G418 resistant m8TR cell lines containing episomal DNA at 27 days continued to maintain m8TR episomal DNA after 87 days of selection (Fig 1D), while, as expected two cell lines which lacked episomes at 27 days, cell lines a and e, remained negative. Therefore, kLANA acts on m8TR DNA to mediate longterm episome persistence for at least ~3 months whereas m4TR episomal DNA was lost over time.

kLANA redistributes and concentrates to dots along mitotic chromosomes in the presence of mTR episomes

kLANA was detected in BJAB cells expressing kLANA either in the presence or absence of episomes that had been under G418 selection for over three months. Both interphase and metaphase arrested cells were assessed (Fig 1E). As expected, in the absence of episomes, kLANA (green) distributed broadly throughout the nucleus (red) in interphase (overlay of red and green generates yellow) and over mitotic chromosomes (red). In contrast, kLANA (green) concentrated to dots both in interphase nuclei (red), and along mitotic chromosomes (red) in cells containing k8TR episomes. Previous work demonstrated that each kLANA dot colocalizes with an episome[7]. In cells with m8TR episomes (from Fig 1C and 1D, cell line d used as a representative example), kLANA concentrated to dots in interphase and along mitotic chromosomes (red), but some kLANA also broadly distributed throughout the nucleus in interphase and broadly along mitotic chromosomes. In addition, there were generally fewer kLANA dots in cells with m8TR compared with k8TR, consistent with fewer m8TR episomes per cell. Therefore, kLANA relocated to dots in both k8TR and m8TR cells, although the relocation was less pronounced in cells with m8TR episomes compared with k8TR episomes.

mLANA acts *in trans* on kTR DNA to mediate episome persistence

Since kLANA mediated episome persistence of mTR DNA, we asked if mLANA can mediate episome persistence of k8TR DNA. mLANA acts on mTRs to mediate episome persistence when both are *in cis*[33], and we first performed experiments that demonstrated mLANA also acts *in trans* to mediate persistence (S3 Fig, S2 Text). To assess if mLANA mediates episome persistence of kTR DNA, pk8TR-P or pRepCK-P vector (encoding puromycin resistance) was transfected into murine A20 cells or A20 cells expressing mLANAF. As expected, puromycin

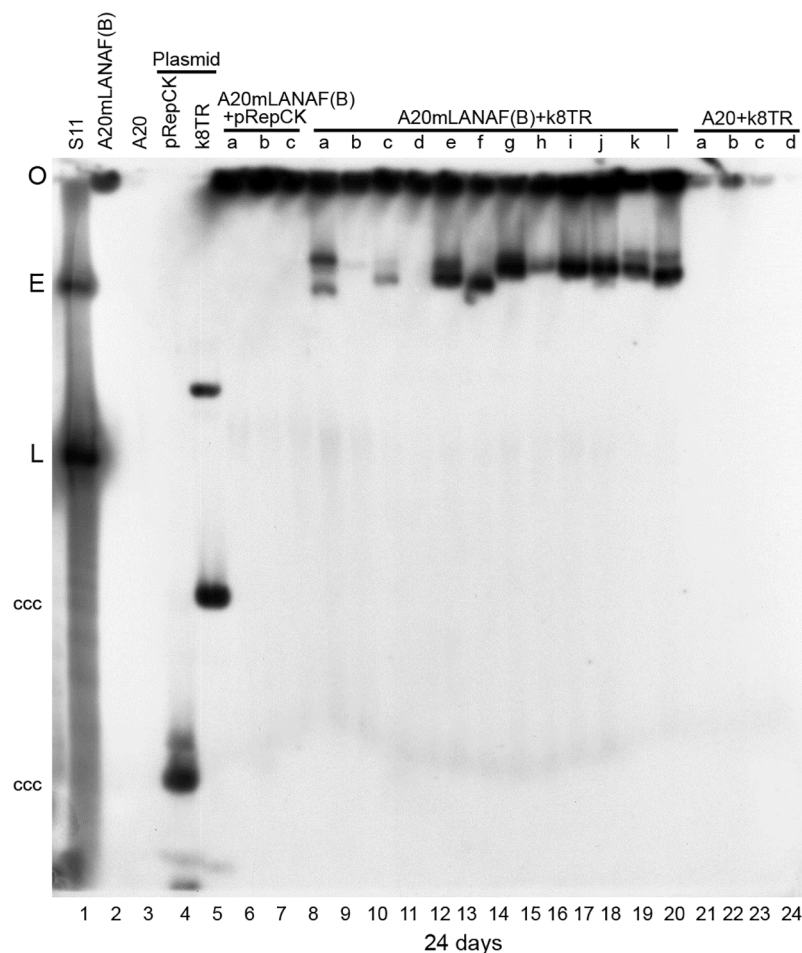


Fig 2. mLANA mediates kTR episome persistence. Gardella gel after transfection of A20 or A20/mLANA cells with pRepCK vector or k8TR DNA. Lanes contain $2-3 \times 10^6$ cells. Gel was performed at 24 days of puromycin selection. Blot was probed with ^{32}P -pk8TR DNA. O, gel origin; E, S11 episomes; L, S11 linear genomes due to lytic replication; ccc plasmid DNA is indicated.

<https://doi.org/10.1371/journal.ppat.1006555.g002>

resistant outgrowth was low after transfection of vector pRepCK-P or pk8TR-P into A20 cells (S1 Table). In contrast, transfection of pk8TR-P into A20-mLANAF cells resulted in much higher outgrowth, consistent with episome maintenance.

Cells were assessed by Gardella gel for episomes. As expected, mLANA expressing cells transfected with vector control or A20 cells transfected with k8TR-P lacked episomes (Fig 2). In contrast, after transfection of pk8TR-P into A20-mLANAF(B) cells, 11 of 12 (Fig 2) cell lines had episomes and in a total of 4 experiments, 27 of 29 (93%) of puromycin resistant cells contained episomes (Table 1). Therefore, mLANA mediates episome persistence of k8TR DNA at relatively high efficiency. Consistent with these results, and with those that showed kLANA mediates episome persistence of mTR DNA (Fig 1), we found that kLANA and mLANA bind reciprocally to each other's TR DNA recognition sequences (S3 Text, S4 Fig).

Generation of kLANA-MHV68 chimeric viruses

Since kLANA supported episome maintenance of mTR DNA, we asked if kLANA can functionally replace mLANA in MHV68 to support infection in vivo. The kLANA ORF and

5' UTR, but not the kLANA promoter[37], were inserted into MHV68 at the mLANA locus. The mORF72 (noncoding) exon, which overlaps with N-terminal mLANA, was retained to preserve splicing events important for expression of mORF72 and LANA. Thus, kLANA expression is driven by native mLANA promoters (Fig 3A)[38,39] in the absence of mLANA. The resulting chimeric virus was termed v-kLANA. We also engineered viruses with mutations in kLANA that abolish nucleosome binding (termed v-8A10, where LANA residues $_{8LRS10}$ were mutated to $_{8AAA10}$)[40] or LANA DNA binding (termed v- $\Delta_{1007-21}$, where residues 1007 to 1021 were deleted) [41] (Fig 3A). These mutations abolish kLANA episome persistence [40,41]. All kLANA-MHV68 recombinants were generated in backgrounds of wild type MHV68 or yellow fluorescent protein (yfp) MHV68[42].

Lytic replication of kLANA MHV68 viruses

mLANA promoters are predicted to drive transcription of transgenic kLANA during lytic replication in vitro, as they do for mLANA and mORF72[38,43]. We assessed LANA expression after infecting BHK-21 cells with MHV68 (v-WT), v-kLANA, v-8A10, or v- $\Delta_{1007-21}$. As expected, v-WT expressed mLANA, which distributed broadly throughout the nucleus (Fig 3B and S5A Fig, top panels)[43]. kLANA or kLANA mutants distributed similarly to mLANA (Fig 3B and S5A Fig, bottom panels) after infection with the chimeric viruses. Immunoblots confirmed mLANA or kLANA expression after infection with WT or chimeric viruses (Fig 3C, S5B Fig). The multiple kLANA bands are due to alternative initiation of translation and an alternative poly adenylation signal[44,45]. vCyclin (ORF72) and M3 (a chemokine binding protein expressed in lytic infection) levels were similar for v-WT and chimeric viruses (Fig 3C, S5B Fig), indicating preserved expression and comparable infection levels.

Growth kinetics of v-kLANA, v-8A10, or v- $\Delta_{1007-21}$ in BHK-21 cells infected at MOI of 0.01 was similar to that of v-WT virus (Fig 3D and S5C Fig). To assess lytic replication in vivo, we inoculated by intranasal (i.n.) route C57 BL/6 mice with 10^4 PFU of v-WT or v-kLANA virus and determined lung titers. While titers of all viruses were similar at day 3 (S5D Fig), at day 7 after infection titers were slightly lower for v-kLANA viruses, particularly for the kLANA mutants, compared to v-WT (Fig 3E and S5D Fig). At day 14 no virus was detected in the lungs (S5D Fig). The reduction of titers at day 7 indicates that kLANA cannot fully replace mLANA during lytic replication in vivo, and disruption of kLANA N-terminal chromosome binding or C-terminal DNA binding affected this phase of infection.

kLANA rescues MHV68 in vivo latent infection in the absence of mLANA

To assess if kLANA can support MHV68 latent infection in vivo we assessed viral latency in spleens of mice infected with v-WT or kLANA chimeric virus. To identify latently infected splenocytes at day 14 after infection (the peak of latent infection), cells were incubated with BHK cells (permissive for lytic infection) to detect virus produced after lytic reactivation. As expected, splenocytes from v-WT infected mice produced virions. Splenocytes from v-kLANA infected mice also produced virus, although titers were 2 to 2 1/2-log lower than those of v-WT infected animals (Fig 4A). In striking contrast, no detectable reactivating virus was observed in the v-8A10 or v- $\Delta_{1007-21}$ infection groups (Fig 4A).

We also investigated the frequency of infected cells by limiting dilution PCR, in total splenocytes or in germinal centre (GC) B cells, since this approach directly indicates numbers of latently infected cells in the absence of a requirement for lytic reactivation. The frequency of latently infected splenocytes or GC B cells for v-kLANA was ~1 log lower compared to that of v-WT. In direct contrast, latently infected cells were at much lower levels for v-8A10 or v- $\Delta_{1007-21}$ (Fig 4B).

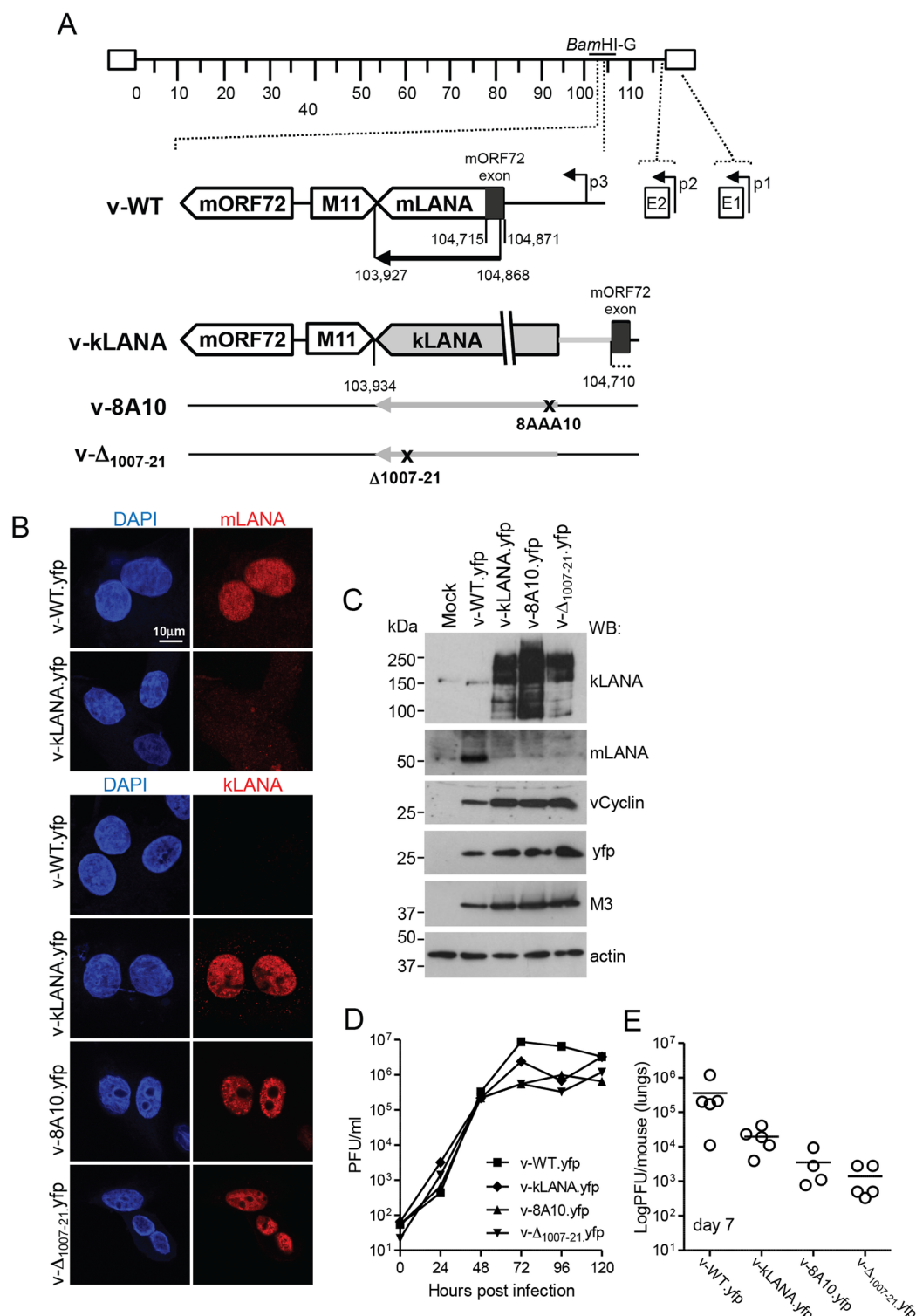


Fig 3. Generation and lytic growth of MHV68 chimeric viruses. (A) Schematic diagram. The kLANA cassette was inserted between the M11 stop codon and the mORF72 exon in place of MHV68 103,935–104,709, which includes most of the mLANA ORF. p1, p2, p3, are mLANA promoters[38,39]. The mORF72 noncoding exon (black) is located within the mLANA coding region. The E2 splice acceptor site (nt 104,871) and the mORF72 exon splice donor site (nt 104,715) were left intact to ensure expression of kLANA and mORF72. The mLANA start codon and three downstream ATGs were mutated to ATT to prevent initiation of translation (indicated by black

dots). The BamHI-G fragment (genomic nt 101,653–106,902) is indicated. mLANA ORF, nt 104,868–103,927. (B) Confocal immunofluorescence detection of mLANA (top panels) or kLANA (lower panels) from yfp viruses. Magnification 630x. (C) Immunoblot of viral proteins. (D) Growth curves of virus in BHK-21 cells after infection with 0.01 PFU/cell. There was no significant difference between infection groups ($p > 0.05$ using one-way non-parametric ANOVA Kruskal-Wallis). (E) Lung virus titers 7 days after infection with 10^4 PFU of the indicated viruses. Circles represent titers of individual mice ($n = 19$). Bars indicate the mean. v- Δ 1007-21.yfp had significantly lower titers than v-WT.yfp ($**p < 0.01$, using one-way non-parametric ANOVA Kruskal-Wallis followed by Dunn's multiple comparison test). There were no other statistically significant differences between groups.

<https://doi.org/10.1371/journal.ppat.1006555.g003>

We assessed the possibility that the reduction in v-kLANA latent infection at day 14 could be due to differing kinetics of infection of v-kLANA compared to v-WT by examining levels of latency at days 11 and 21. Results demonstrated that v-kLANA latent infection was similarly reduced compared to v-WT at days 11 and 21, indicating a consistent deficiency over time rather than differing infection kinetics (S6 Fig). We also asked if the lower level of latently infected splenocytes might be due to v-kLANA's reduced lytic replication in the lungs. However, after intraperitoneal infection, which bypasses the lungs to provide virus access to the spleen, latent infection remained lower for v-kLANA compared to v-WT (S6A and S6B Fig).

We assessed latent infection and GC B cell populations in the spleen by flow cytometry 14 days after infection with WT or kLANA yfp viruses. The percentage of B cells that were GC B cells varied between ~3–6% among infection groups (Fig 4C). Total number of GC B cells was slightly higher in mice infected with WT when compared to kLANA, and significantly lower numbers were observed for the kLANA mutants compared to v-WT (Fig 4C, right panel). This result is not unexpected, in light of results in Fig 4A and 4B since the magnitude of GC B cell amplification after MHV68 infection correlates with latent virus load[46]. The frequency of GC B cells that were infected was determined from YFP expression. Mean percent of YFP⁺ GC B cells was 5.8% for v-WT.yfp and 1.4% for v-kLANA.yfp infected mice (Fig 4D, right panel). Mice infected with the kLANA mutant yfp viruses had over 10-fold lower percent of YFP⁺ GC B cells compared with v-kLANA.yfp (Fig 4D). About 80% of v-WT.yfp infected cells infected had a GC phenotype. Similarly, ~60% of v-kLANA.yfp infected cells had a GC phenotype (Fig 4E, right panel). In contrast, of the very few infected YFP⁺ B cells in the v-8A10.yfp and v- Δ 1007-21.yfp groups, only small percentages, 14% and 22%, respectively, were GC B cells (Fig 4E, right panel). Thus, kLANA largely rescued MHV68 in vivo latency in the absence of mLANA, whereas kLANA containing mutations that abolish episome persistence did not.

kLANA chimeric virus persists at WT levels in latently infected cells

To further investigate v-kLANA latency we assessed kLANA expression in vivo. We first confirmed latent v-kLANA infection in spleen sections by detection of MHV68 miRNAs 1–6, which are expressed in latently infected cells[30]. As expected, signal was detected in v-kLANA infected mice, although in fewer cells compared to v-WT (Fig 5A). LANA concentrates to dots at sites of episomal DNA in nuclei of latently infected cells[7]. kLANA was detected by immunohistochemistry, sometimes as nuclear dots, in adjacent sections in B cell follicles of v-kLANA mice (Fig 5B, arrow). mLANA distributed similarly in nuclear dots in v-WT sections (Fig 5C). We also detected LANA dots by immunofluorescence in v-WT (Fig 5D) or v-kLANA (Fig 5E) infected B cell follicles.

We quantified the number of nuclear dots since LANA concentrates to dots at viral episomes, and each dot therefore indicates a viral genome. Since entire nuclei were rarely present in sections, we counted the number of dots per nuclear volume across confocal z-stacks. The concentration of mLANA or kLANA dots was similar, with means of 8.2 (range 2.2–21.0) and 7.7 (range 1.3 to 21.8) dots per $100\mu\text{m}^3$, respectively (Fig 5F). Considering a 4:1 nucleus-

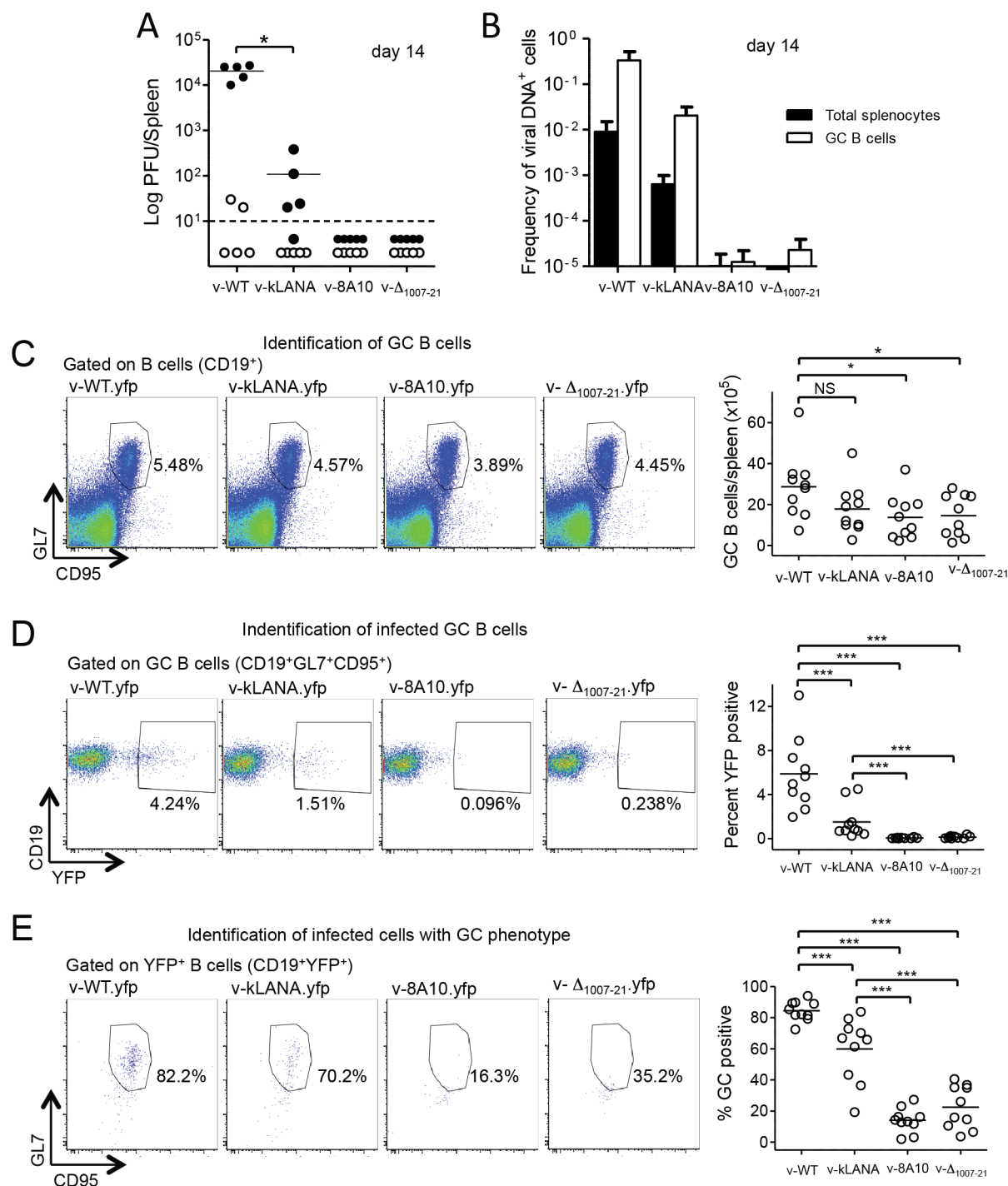


Fig 4. v-KLANA latent infection. Viral latency in spleens of C57 BL/6 mice 14 days after i.n. infection with 10^4 PFU of the indicated viruses. (A) Latent titers determined by co-culture reactivation assay (closed circles) and titers of pre-formed infectious virus by plaque assay (open circles). Circles are titers of individual mice. Bars indicate mean and dashed line shows the limit of assay detection. v-kLANA titers were significantly lower than v-WT (Mann-Whitney test). $*p < 0.05$. (B) Quantification of viral DNA-positive cells in total splenocytes and in sorted GC B cells (CD19⁺CD95⁺GL7⁺). Data are from pools of five spleens per group. Bars are frequency of viral DNA-positive cells. Error bars indicate 95% confidence intervals. (C-E) Flow cytometry analyses. Representative FACS plots from individual mice are shown in left panels. Quantification graphs in which each point represents an individual mouse are shown at the right. Bars are mean values. Data were combined from 2 independent experiments with 5 mice in each group. (C) Total number of GC B cells (CD19⁺CD95⁺GL7⁺). NS, not significant; $*p < 0.05$ using the Mann-Whitney test. (D) Percentage of GC B cells that were YFP positive. (E) Percentage of YFP positive cells that were GC B cells. $***p < 0.001$ in (D) and (E) using the Mann-Whitney test.

<https://doi.org/10.1371/journal.ppat.1006555.g004>

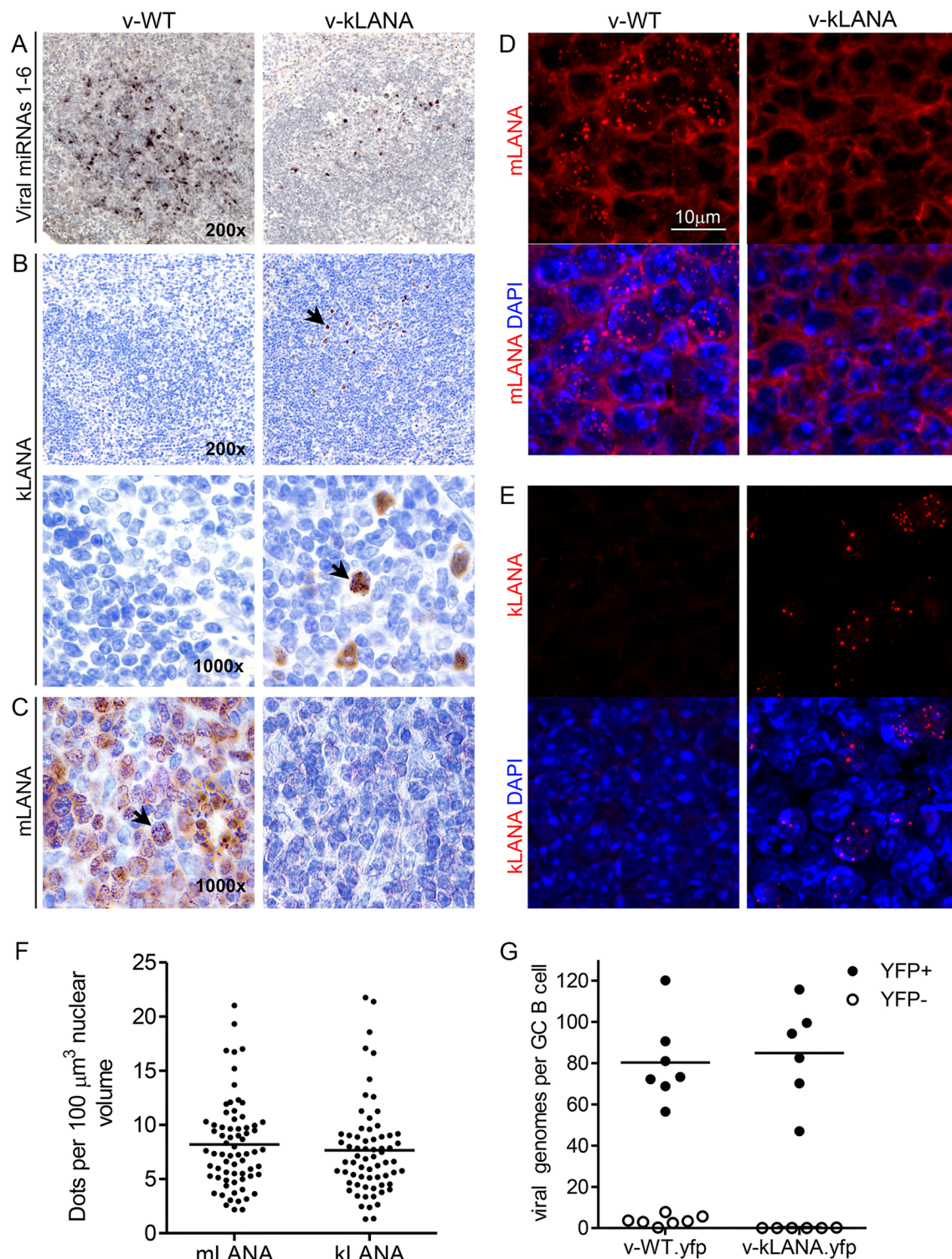


Fig 5. mLANA and kLANA expression in vivo. Spleen sections of mice infected with 10^4 PFU of v-WT or v-kLANA for 14 days. (A) In situ hybridization (brown) with probes for viral miRNAs 1–6. Sections were counter stained with Mayer's Haemalum. (B, C) Detection of kLANA (B) and mLANA (C) by immunohistochemistry in sections adjacent to those shown in panel A. Arrows in panel B indicate the same kLANA positive cell. Arrow in panel C indicates a mLANA positive cell. Sections were counterstained with haematoxylin. No kLANA signal was detected in sections stained only with secondary antibody. (D, E) mLANA and kLANA nuclear dots detected by indirect immunofluorescence. Images are maximum intensity projections of

Z-stacks acquired over the thickness of the spleen sections. No dots were observed in unstained sections or with secondary antibody alone. Magnification 630x. (F) Quantification of mLANA ($n = 69$ nuclei from 3 mice) or kLANA ($n = 67$ nuclei from 3 mice) dots per $100 \mu\text{m}^3$ nuclear volume. Bars indicate means. The number of dots per volume was not significantly different between v-WT and v-kLANA mice (Mann-Whitney test, $p > 0.05$). (G) Viral genomes in FACS sorted YFP⁺ and YFP⁻ GC B cells from spleens of v-WT.yfp ($n = 7$) and v-kLANA.yfp ($n = 6$) infected mice. Circles represent individual mice. Bars indicate means. There was no significant difference between the two infection groups (Mann-Whitney test, $p > 0.05$).

<https://doi.org/10.1371/journal.ppat.1006555.g005>

cytoplasm volume and diameters of 7 to $10 \mu\text{m}$ for GC B cells[47], we estimate a nuclear volume of 144 to $419 \mu\text{m}^3$ for the infected cells. Based on these volumes, we predict a mean of 12 to 34 mLANA or kLANA dots, hence viral episomes, per nucleus in latently infected cells within B cell follicles. We also quantified viral genomes in FACS sorted GC B cells from infected mice by qPCR. In YFP⁺ GC B cells the mean number of copies per cell was 80.6 (range 56.5 to 120.1) and 84.9 (range 47 to 115.7) for v-WT.yfp and v-kLANA.yfp, respectively (Fig 5G). The greater number of episomes determined by PCR could relate to an underestimation of nuclear volume when calculating LANA dots per nucleus, or possibly to adjacent genomes being observed as single dots. Together these results indicate that kLANA chimeric virus persists at WT copy number in nuclei of latently infected splenocytes.

Discussion

This work demonstrates that kLANA and mLANA act reciprocally to mediate episome persistence of TR DNA. This functional conservation provided the rationale to assess a chimeric MHV68, with kLANA substituting for mLANA. kLANA rescued mLANA deficiency, with chimeric virus establishing latent infection in vivo. These findings were not necessarily expected. Previous work showed that the rhesus gamma-1 herpesvirus EBNA1 episome maintenance protein acts on the human Epstein-Barr virus (EBV) oriP element in vitro to support episome maintenance[48]. However, the gamma-1 herpesviruses are more closely related compared to the gamma-2 herpesviruses. Gamma-1 herpesviruses infect only humans (EBV) and non human primates[49] and the rhesus gamma-1 herpesvirus is estimated to have diverged from EBV only ~5 million years ago[50]. In contrast, gamma-2 herpesviruses infect humans (KSHV), non human primates, and many non primate species. Correspondingly, MHV68 is estimated to have diverged from KSHV ~60 million years ago[49,50]. Consistent with this degree of evolutionary divergence, mLANA and kLANA differ substantially in sequence (Fig 1A) and also complex differently with DNA[51]; kTR (0.8kb) and mTR (1.2 kb) also differ in size and lack sequence homology, although both are GC rich (84.5% and 77.6% GC for kTR and mTR, respectively)[32]. In agreement with the findings here, functional conservation was observed for kLANA's ability to repress transcription from the mTR, similar to mLANA[52].

The modest attenuation phenotype of v-kLANA in latent infection compared to v-WT could be due to a deficiency in lytic reactivation or to LANA related growth effects. v-kLANA exhibited a 2 log deficiency compared to v-WT in a reactivation based assay (Fig 4A). However, the frequency of v-kLANA latently infected GC B cells was only ~1 log lower (Fig 4B), although it is important to note that the number of GC B cells was modestly decreased in v-kLANA compared to v-WT infected mice (Fig 4C). It remains possible that lytic reactivation may be important to expand the number of infected cells early in latency establishment. However, it is also possible that kLANA fails to fully promote efficient proliferation of infected GC B cells through functions such as mLANA's regulation of protein levels of Myc and NF-kb through ubiquitination[53,54].

Despite a decrease in the number of infected GC B cells, kLANA fully recapitulated mLANA's ability to maintain a WT genome copy number in cells. Episome copy number was similar for v-WT.yfp and v-kLANA.yfp whether determined by the number of mLANA or

kLANA dots per nucleus (each LANA dot corresponds to an episome) (Fig 5F) or by PCR of virus DNA from infected cells (Fig 5G). Although these approaches resulted in modestly different absolute genome copy number estimations, both indicate that kLANA and mLANA infected GC B cells harbor equivalent number of episomes per cell.

The small deficit in lung replication of kLANA chimeric virus suggests that kLANA does not fully replace mLANA in this phase of infection. In previous work, mLANA-null viruses or recombinants harboring C-terminal mLANA mutations that abolish DNA binding, had small lytic growth defects in cultured murine fibroblasts [43,52] and an attenuation in acute lytic lung replication [34,55,56]. Thus, mLANA and in particular the C-terminal DNA binding domain, was deemed required for efficient lytic replication. The lung attenuation phenotype of v- $\Delta_{1007-21}$, which encodes a DNA binding deficient kLANA, is reminiscent of these findings [55].

The finding that kLANA mutations 8A10 or $\Delta_{1007-21}$ abolish MHV68's ability to efficiently establish latency (Fig 4), demonstrates episome persistence is necessary for latency establishment. LANA 8A10 or $\Delta_{1007-21}$ each abolish LANA's ability to replicate DNA and segregate episomes to progeny nuclei by eliminating chromosome association or DNA binding, respectively. These results indicate that the critical function of these kLANA residues is conserved in this chimeric infection model.

This work suggests differences in episome maintenance efficiency between kLANA and mLANA. Although both kLANA and mLANA act on TR DNA to mediate episome persistence, kLANA appeared to act more efficiently on cognate DNA than did mLANA. kLANA maintained episomes in 100% (Table 1) of G418 resistant cell lines after transfection of k8TR DNA, while mLANA maintained episomes in only 25%–58% of puromycin resistant cell lines after transfection of m4TR-P DNA. The use of four mTR copies versus eight kTR copies in these experiments is unlikely to account for the substantially lower mLANA efficiency. In fact, in prior work, kLANA consistently maintained episomes in all G418 resistant cell lines after transfection of plasmids containing two, three, or eight kTR copies ([8,40,57]).

It is possible that mLANA's diminished efficiency relates to inherent differences in the TR elements rather than in differences between mLANA and kLANA. As expected, kLANA mediated episome persistence more efficiently for kTR than for mTR DNA (Table 1). However, mLANA also mediated episome persistence more efficiently for kTR compared to mTR. mLANA mediated persistence of k8TR DNA in 67–93% of cell lines, while persistence of m4TR DNA occurred in only 25–58% of cell lines. Although this difference may be related to the additional 4 TR elements in k8TR versus m4TR, it is possible that KSHV TR elements have evolved to enable a higher level of episome maintenance efficiency.

kLANA and mLANA demonstrate reciprocal binding to each other's recognition sequences, although binding of kLANA to mLBS is substantially weaker than binding to kLBS (S4 Fig). Although kLANA and mLANA DNA binding sites share substantial homology, they are not identical (S4A Fig), and mLBS differs from the high affinity kLBS1 at several nucleotides important for LANA binding [55,58]. Consistent with these findings, the kLANA DBD binds mLBS1-2 with a K_D of 116.0 nM compared to 13.7 nM for kLBS1-2 [51]. kLANA's diminished binding to mLBS may also relate to its inherently different thermodynamic binding mode compared to mLANA.

Despite the less efficient binding of kLANA to mLBS, kLANA enabled episome persistence in spleen follicles with virus persisting at WT levels in infected cells, as evidenced by the number of viral genomes per infected cell. kLANA and mLANA DNA binding domains share significant structural homology and interact to form oligomerized dimers [55,59–61]. It is likely that the presence of multiple TR elements (each of which contains LBS1-2) in MHV68 results in enhanced cooperative binding and/or other oligomerization events that increase binding

efficiency which may allow kLANA to efficiently mediate episome maintenance of mTR DNA and virus persistence. For instance, despite mutations that engendered severe mLANA DNA binding deficiency to mLBS1-2, mLANA efficiently mediated episome persistence in the setting of a full complement of mTRs in MHV68 [62]. Further, the finding of large, recombinant 4TR and 8TR episomes here (Figs 1 and 2; S1 and S2 Figs), and as previously observed [7,63,64] likely reflects the need for ~40 TR elements, similar to that of KSHV, for optimal functional efficiency.

Here, we show that despite more than 60 Ma of evolutionary divergence, mLANA and kLANA exhibit reciprocal episome maintenance function, providing the basis for in vivo analysis of KSHV LANA. This chimeric virus should allow for future investigation of kLANA in a well-established small animal model of MHV68 latent infection. The in vivo model also provides a means to assess kLANA targeting through strategies such as small molecule inhibition. Last, this approach potentially can be applied to other viruses which lack small animal models, but for which model virus systems exist.

Materials and methods

Cell lines

A20 murine B lymphoma cells[65] (ATCC) were cultured with RPMI supplemented with 10% Fetalplex (Gemini) or bovine growth serum (BGS) (Hyclone), beta mercaptoethanol, sodium pyruvate, HEPES, Glutamax (Invitrogen), and 15µg/ml gentamicin. The latently infected cell lines, S11 (MHV68 infected)[66] and BCBL-1 (KSHV infected) (NIH AIDS Reagent Program) were maintained in RPMI with 20% BGS. S11 cells were also supplemented with beta mercaptoethanol. BJAB cells were grown in RPMI medium containing 10% BGS (Hyclone) or Fetalplex (Gemini) and 15µg/ml gentamicin. BJAB cells stably expressing KSHV LANA containing an N-terminal FLAG epitope tag (BJAB-kLANA)[7] were grown in RPMI containing 10% Fetalplex or BGS, and medium was supplemented with hygromycin B (200 units/ml; Calbiochem). 293T (ATCC) cells were grown in DMEM medium containing 10% BGS. NIH-3T3-CRE cells[67] were grown in Dulbecco's modified Eagle's medium (DMEM) supplemented with 10% heat inactivated fetal bovine serum, 2mM glutamine, and 100U/ml penicillin and streptomycin. Baby hamster kidney fibroblasts (BHK-21, clone 13 CCL-10) (ATCC) were cultured in Glasgow's modified Eagle's medium (GMEM) supplemented as for NIH-3T3-CRE cells with the addition of 10% tryptose phosphate buffer. Cells were confirmed to be mycoplasma free.

Plasmids

mLANAF[33] contains mLANA with a 3x C-terminal FLAG tag driven by its native promoter. mLANA with N-terminal Myc and C terminal 3xFLAG epitope tags was generated by digesting pCMV-myc-mLANA-C3F with SacI and XhoI, and the resulting mLANA fragment ligated into pBluescript+II vector digested with SacI and XhoI. m2TR, m4TR and m8TR[33] contain two, four or eight mTR copies of the MHV68 terminal repeat elements. To generate m4TR-P, the neomycin resistance gene was removed from m4TR by digestion with BglII and HpaI and the BglII site blunted. The puromycin resistance gene was removed from pBabe puro[68] by digestion with ClaI and SnaBI, the ClaI site blunted, and the fragment inserted into the HpaI and BglII digested m4TR, generating m4TR-P. To generate pRepCK-P, the mTRs were removed from pm4TR-P by NotI digestion and the NotI site religated. To generate pk8TR-P, p8TR (pk8TR)[40] was digested with MluI and PsiI to release the neomycin resistance gene and then ligated with the MluI/PsiI DNA fragment containing the puromycin resistance gene from pm4TR-P.

Western blot and antibodies

Extracts derived from 0.25×10^6 puromycin resistant cells were loaded per lane for FLAG antibody blots and 0.5×10^6 cells per lane were loaded for the blot probed with anti-mLANA monoclonal antibody 6A3 in [S3 Fig](#). Murine monoclonal antibody 6A3[55], which was raised against mLANA amino acids 140–314, was generated at the Monoclonal Antibody Core Facility, European Molecular Biology Laboratory. Proteins were resolved by 8% SDS-PAGE, transferred to nitrocellulose, and detected with anti-FLAG antibody conjugated to HRP (Sigma) used at a 1:750 dilution, mouse anti-tubulin monoclonal antibody B-5-1-2 (Sigma) used at a 1:1000 dilution, or 6A3 hybridoma supernatant used at a 1:2 dilution. Secondary anti mouse HRP conjugated antibody followed by chemiluminescence was used to detect the anti-tubulin and 6A3 antibodies. Anti-kLANA rat monoclonal antibody (LN53, ABI Sciences) was used at 1:1000, anti-vCyclin (mORF72)[69] (a gift from Samuel Speck) was used at 1:500, rabbit anti-M3 polyclonal[70] was used at 1:3000, mouse anti-eGFP (Clontech) was used at 1:1000 and rabbit anti-actin (Sigma) was used at 1:1000. Horse radish peroxidase (HRP) conjugated secondary antibodies were from GE Healthcare and Jackson ImmunoResearch.

Generation of A20 cells with stable expression of mLANA

Ten million A20 cells in log phase were transfected with 35 μ g of mLANAF or 35 μ g of pRepCK vector in 400 μ l RPMI containing 10% serum, but without antibiotics, by electroporation using the BTX Electroporation System Electrosquare Porator T820 by pulsing the cells at 225 volts for 65 milliseconds once. Three days post transfection, cells were seeded into microtiter plates at 5000, 1000, or 100 cells per well and placed under G418 (400 μ g/ml) (Gemini) selection. G418 resistant clones were expanded and those transfected with mLANAF were screened for mLANAF expression by immunoblot with anti-FLAG antibody.

Episome maintenance assays

G418 resistant A20 cells or G418 resistant A20 cells stably expressing mLANAF were transfected as above with 35 μ g of m4TR-P, pk8TR-P, or pRepCK-P and cultured in RPMI supplemented with 400 μ g/ml G418 (Gemini) for 3 days. Cells were then seeded into 96 well plates at 10, 100, or 1000 cells per well and puromycin 2.5 μ g/ml (Invitrogen) was included in the medium in addition to G418. Cell lines resistant to both puromycin and G418 were expanded.

BJAB-kLANA cells were grown in log phase for three consecutive days and then ten million cells were transfected with 35 μ g of m2TR, m4TR, m8TR, pk8TR, pRepCK, or plasmid DNA rescued from episome containing cells, in 400 μ l of RPMI medium with 10% serum at 200 V and 960 μ F in a 0.4-cm-gap cuvette with a Bio-Rad electroporator. Three days post transfection, cells were seeded in micro titer plates at 1, 10, 100, or 1000 cells per well in medium containing G418 (600 μ g/ml; Gibco or Gemini) and later expanded to 6 well plates.

Gardella gel analysis[71] was performed on A20 or BJAB cell lines. Cells were lysed *in situ* in gel-loading wells embedded with DNase free protease (Sigma #P6911) and sodium dodecyl sulfate, and electrophoresis in Tris-borate-EDTA performed. DNA was then transferred to a nylon membrane and detected by autoradiography using 32 P-labeled probe.

Fluorescence microscopy of suspension cells

G418 resistant BJAB-kLANA cells transfected with m8TR, k8TR or pRepCK, were metaphase arrested by incubation for 16 hours with 1 μ g/mL of colcemid (Calbiochem). 0.2×10^6 cells were resuspended in 1 mL hypotonic buffer (1% NaCitrate, 1mM MgCl_2 , 1mM CaCl_2) for 5 minutes. 300 μ L cells were spread onto a polylysine slide by cytopsin (Thermoshandon), fixed

in 4% formaldehyde, permeabilized with 0.5% triton X-100 and blocked in 20% goat serum. kLANA was detected by incubating with anti-kLANA monoclonal antibody IA-2-12 (gift of Mary Ballestas)[72] diluted 1:1000 in 20% goat serum for two hours, followed by incubation with secondary anti-mouse antibody conjugated to Alexa Fluor 488 (Molecular Probes) diluted 1:1000 in 20% goat serum. DNA was detected using propidium iodide at 1 µg/mL (Invitrogen). Slides were dried in ethanol 70% followed by incubations in 90% and 100% ethanol before coverslips were applied with Aqua-Poly mount (Polysciences). Microscopy was performed with a Zeiss Axioskop, PCM2000 hardware, and C-imaging software (Compix, Inc.).

Recombinant viruses

DNA encoding the kLANA gene and 5' UTR, flanked by MuHV4 genomic sequence, was cloned into pSP72 (Promega). The 5' end of mORF73 and upper flanking region (coordinates 104710–105092, GenBank accession U97553) were PCR amplified from the MuHV-4 genome with primers Imm_TR1 (AAAGAATTCAATCACCTTGGCATCC) and Imm_TR2 (AATGCTGAAGATCTTCCAG). Primer Imm_TR1 introduces an EcoRI site (underlined) four bases downstream of the mORF72 splice donor site (double underlined) and a C104710A mutation (bold) to alter ATG (coordinate 104712) to ATT. Primer Imm_TR2 contains the BglII genomic site (coordinate 105087). The PCR fragment was cloned into the pSP72 using BglII/EcoRI sites to create pSP72_PCR1. The mORF73 ATG (coordinate 104869) and two downstream ATG sequences (coordinates 104779 and 104714) were altered to ATT in pSP72_PCR1 using QuikChange Multi Site-Directed Mutagenesis (Stratagene) and primers Imm_TR5_C104721A (GAATTCAATCACCTTGGAAATCCCGGTGGTGG), Imm_TR6_C104777A (GCGTCTTTTAGGAGGAATGGCTGCTGGTTTG) and Imm_TR7_C104867A (CGGTGGGGATGTGGGAATTATCTGAAAGAG) (mutated nucleotides in bold.) The resulting plasmid was termed pSP72_PCR1_2. The region of KSHV encoding the N-terminal region of kLANA and 5' UTR (coordinates 126473–127886, GenBank accession U75698) was PCR amplified from L54 phage[73] DNA with primers Imm_TR8 (ATCACCCCAGGATCCCTCAGAC), and Imm_TR9 (AAAGAATTCAATTTGGAGGCAGCTGCG). Imm_TR8 contains genomic BamHI site (underlined, coordinate 126473) and Imm_TR9 introduces an EcoRI site (underlined) before the kLANA 5' UTR. The PCR product was ligated into the BamHI/EcoRI sites of pSP72_PCR2 to generate pSP72_PCR1_3. The DNA encoding the remainder of kLANA (corresponding to genomic coordinates 123808–126473) was amplified by PCR from pEGFP kLANA[40] with primers Imm_TR10 (AAAAAGCTTTTATGTCATTTCTGTGG) and Imm_TR11 (CTGAGGGATCCTGGGGTGATG). IMM_TR10 introduces a HindIII site (underlined) downstream of the kLANA stop codon (bold). Imm_TR11 contains a BamHI genomic site (underlined, coordinate 126473). The PCR product was ligated into pSP72_PCR1_3 using HindIII and BamHI sites to create pSP72_PCR1_4. The lower flanking region of mORF73 (coordinates 102728–103934) was obtained by PCR from MuHV-4 DNA with primers Imm_TR3 (AAACTCGAGCAGATGAGATCTGTACTC) and Imm_TR4 (AAAAAGCTTTTCAGACATAAATCACATTC). Imm_TR3 introduces a XhoI site (underlined) 6 nucleotides from the genomic BglII site (coordinate 102728, double underlined) and IMM_TR4 introduces a HindIII site (underlined) after the M11 stop codon (bold). The PCR product was cloned into XhoI/HindIII sites of pSP72_PCR1_4 to generate pSP72_PCR1_5. Alanine substitutions 8LRS10 to 8AAA10 in kLANA were introduced by PCR into pSP72_PCR1_3 using primer kLANA_8AAA10 (CCGGGAATGCGCGCCGAGCGGGACGGAGCACCGG) (mutated nucleotides in bold.) The mutated region was subcloned from pSP72_PCR1_3_8A into BamHI/SacI sites of pSP72_PCR1_5 to create pSP72_PCR1_5_8AAA10. DNA encoding kLANA Δ1007–21 was subcloned from pSG5 kLANA delta 1007–21[41] into

pSP72_kLANA with BamHI and StuI to generate pSP72_PCR1_5_Δ1007–21. Sequence of PCR-derived regions was confirmed by DNA sequencing. The KSHV sequences flanked by MUHV4 genomic sequences from pSP72_PCR1_5, pSP72_8A and pSP72_Δ1007–21 were subcloned into the BamHI-G MuHV-4 genomic fragment cloned in the pST76K-SR shuttle plasmid, using BglII sites. Each recombinant BamHI-shuttle plasmid was transformed into *E. coli* harboring the WT MuHV-4 BAC (pHA3)[74] or yellow fluorescent protein (YFP)-WT MuHV-4 BAC[42]. Following a multi-step selection procedure[74], recombinant BAC genomes were identified by PCR and HindIII, BamHI and EcoRI digestion profiles. Viruses were reconstituted by transfection of BAC DNA into BHK-21 cells using X-tremeGENE HP (Roche Applied Science). The IoxP-flanked BAC cassette was removed by viral passage through NIH-3T3-CRE cells.

Ethics statement

Animal studies were performed in accordance with the Portuguese official Veterinary Directorate (Portaria 1005/92), European Guideline 86/609/EEC, and Federation of European Laboratory Animal Science Associations guidelines on laboratory animal welfare. Animal experiments were approved by the Portuguese official veterinary department for welfare licensing (protocol AEC_2010_017_PS_Rdt_General), and the IMM Animal Ethics Committee.

Viral stocks and in vivo assays

Virus stocks were prepared by infecting BHK-21 cells (0.001 PFU/cell). Viruses were harvested from cleared supernatants by centrifugation at 15000g for 2h at 4°C. Infectious virus titers were determined by plaque assay in BHK-21 cells. For experiments involving mice, sample size was based on our and other previous studies that produce biologically valid data. Specifically, sample size ranged from 3 mice per group to a maximum of 5 depending on the nature of the experiment. No specific randomization or blinding was applied. For in vivo infections, 6 to 8-week old C57BL/6 J female mice (Charles River Laboratories) were inoculated intranasally under isofluorane anaesthesia with 10^4 of PFU in 20 μl PBS. At the indicated times after infection, mice were sacrificed and lungs or spleens harvested. Lungs were homogenized, freeze-thawed and titers determined by plaque assay. Single cell suspensions were prepared from spleens and reactivating virus was quantified by co-culture with BHK-21 cells. Plaque assay was performed in equivalent freeze-thawed samples to determine pre-formed infectious virus. Plates were incubated for 4 days (plaque assay) or 5 day (co-culture assay) then fixed with 4% formaldehyde and stained with 0.1% toluidine blue. Plaques were counted with a plate microscope.

Flow cytometry

Single cell suspensions were prepared from spleens. After lysis of red blood cells in hypotonic NH_4Cl solution, the number of viable cells was determined by trypan blue exclusion. Fc receptors were blocked with anti-CD16/32 (2.4G2) (BD Pharmingen) diluted in FACS buffer (PBS containing 2% fetal bovine serum) for 15 minutes on ice. Cells were incubated for 25 minutes on ice with the following antibodies diluted in FACS buffer: APC-H7-conjugated anti-CD19 (1D3) (BD Pharmingen) used at 1:400, PE-conjugated anti-CD95 (Jo2) (BD Pharmingen) used at 1:800 and eF660-conjugated anti-GL7 (GL7) (eBioSciences Inc) used at 1:200. YFP expression and cell surface markers were detected on a LSR Fortessa (BD BioSciences) using DIVA software and data were analysed with FlowJo 9.3.2 (Tree Star). Cells were gated

on live cells and singlets based on FSC/SSC and FSC-A parameters, respectively. Total number of GC cells was determined based on FACS data and cell count of splenocytes.

Frequencies of viral DNA positive cells

The frequency of viral DNA positive cells was determined in total splenocytes or GC B cells by limiting dilution combined with real time PCR. Splenocytes were pooled from 5 mice. GC B cells (CD19⁺GL7⁺CD95⁺) were purified from pools of 5 spleens using a BD FACSaria Fow Cytometer (BD BioSciences). The purity of sorted cells was $\geq 95\%$. Cells were serially two-fold diluted and 8 replicates of each dilution analysed by real time PCR (Rotor Gene 6000, Corbett Life Science). The primer/probe sets were specific for the M9 MHV68 gene (primers M9-F 5'-GCCACGGTGGCCCTCTA and M9-R 5'-CAGGCCTCCCTCCCTTTG -3, and Taqman probe M9T, 5'-6-FAM-CTTCTGTTGATCTTCC-MGB-3'). Positive and negative reactions were scored using Rotor Gene 6000 software and the frequency of infected cells was determined as described[46].

Viral genome quantification

YFP⁻ and YFP⁺ GC B cells (CD19⁺GL7⁺CD95⁺) were FACS sorted from individual spleens of infected mice using a BD FACSaria Fow Cytometer (BD BioSciences). Viral genomes were detected by real time PCR using M9 primers and Taqman probe described above. Cellular DNA was quantified in parallel by detecting the ribosomal protein L8 (Rpl8) gene (primers mRpl8 F1 5'-CATCCCTTTGGAGGTGGTA and mRpl8 R1 5'-CATCTCTTCGGATGGT GGA and Taqman probe mRpl8T 5'-VIC-ACCACCAGCACATTGGCAAACC-MGB) as previously described. Reactions were performed in a Rotor Gene 6000 (Corbett Life Science) and data were analysed with Rotor Gene 6000 software. PCR products were converted to genome copies by comparison to a standard curve of a plasmid harboring the MHV68 M9 gene or the rpl8 mouse gene (mouse cDNA NM_012053, Origene) serially diluted in the same buffer as the samples. The number of viral genome copies per cell was obtained by dividing the number of M9 copies by one half the number of Rpl8 copies.

Analysis of spleen sections

Spleens were fixed in 10% formalin in PBS for 24 hours at room temperature and paraffin embedded. In situ hybridization to detect MuHV-4-encoded miRNAs was performed in 5μm sections using digoxigenin-labelled riboprobes generated by T7 transcription of pEH1.4, as previously described[30]. For detection of LANA proteins, 4μm sections were cut, de-waxed, acid-treated for antigen recovery and blocked with Protein block (DAKO) for kLANA staining or using the Mouse on Mouse kit (DAKO) for mLANA staining. Sections were incubated for for 1 hour at room temperature with anti-mLANA mAb 6A3 (1:2 dilution of hybridoma supernatant) or rat anti-kLANA antibody (1:1000). For immunohistochemistry primary antibodies were detected with the anti-mouse ENVISION kit (DAKO) or ImmPress HRP anti-Rat IgG Peroxidase Polymer Detection Kit (Vector Laboratories), which use the Peroxidase/DAB detection system. Slides were counterstained with haematoxylin-eosin and images were acquired with a Leica DM2500 microscope coupled to a digital camera. For immunofluorescence, primary antibodies were detected with anti-mouse Alexa 594 or anti-rat Alexa-568 antibodies (Molecular Probes). Sections were mounted in Prolong gold reagent with DAPI (Molecular Probes) to stain DNA. Images were acquired with a Zeiss LSM 710 confocal microscope at 630x magnification and using Zen software. Images were processed with Image J. For quantification of dots, confocal z-stacks of nuclei, identified with DAPI staining, containing mLANA or kLANA dots were acquired from different areas of splenic follicles. The number of

dots in individual nuclei was counted D across the z-stacks. Because most nuclei were not whole in the spleen sections, we determined the number of dots per nuclear volume. First we determined the nuclear volume in each slice, by multiplying the nuclei area, measured using ImageJ, by the thickness of the confocal slice. The final volume for each nucleus was the sum of the slice volumes.

Statistical analysis

Statistical significance was evaluated with unpaired two-tailed non-parametric Mann-Whitney U test or one-way non-parametric ANOVA (Kruskal-Wallis test), as appropriate, using GraphPad Prism software.

Supporting information

S1 Text. TR episomes enlarge through recombination events.

(DOCX)

S2 Text. mLANA acts *in trans* on mTRs to mediate episome persistence.

(DOCX)

S3 Text. Reciprocal binding of kLANA and mLANA to TR DNA recognition sequences.

(DOCX)

S4 Text. Supporting information related materials and methods.

(DOCX)

S1 Fig. TR episomes enlarge through recombination events. (A) Schematic diagram showing digestion sites for m4TR, m8TR or pk8TR plasmids with NotI, or HindIII/XhoI, respectively. Sizes of expected fragments are indicated. TR, one mTR element; tr, one kTR element; us, unique KSHV sequence. (B, C) BJAB cell lines stably expressing kLANA transfected with pk8TR (Fig 1B, lanes 4, 5), pRepCK (Fig 1B, lanes 6 and 7), m8TR (Fig 1C, lanes 19 to 21), or m4TR (Fig 1B, lane 16), were harvested at 76 days of G418 selection. Low molecular weight DNA was isolated, digested with NotI (panel B) or HindIII and XhoI (panel C), and assessed by Southern blot. Exposure times are indicated below each blot. Lane letters correspond to the same letters as in Fig 1. Panel on the left in (B) is a 16 hour exposure and on the right shows lanes 6 to 11 after a 4 day exposure.

(JPG)

S2 Fig. Rescued mTR plasmids from BJAB-kLANA cells have variable mTR copy number and can persist as episomes after transfection. After ~90 days of G418 selection, low molecular weight DNA was purified from a G418 resistant BJAB-kLANA cell line containing k8TR episomes (cell line a, shown in Fig 1C, lane 3, and in Fig 1D, lane 5) or from two G418 resistant BJAB-kLANA cell lines containing m8TR episomes (cell line d, shown in Fig 1C, lane 8 and Fig 1D, lane 10, and cell line f, shown in Fig 1C, lane 10 and Fig 1D, lane 11), transformed by electroporation into bacteria, and bacteria selected for ampicillin resistance. (A) Restriction enzyme digestion with NotI. (B) Restriction enzyme digestion with HindIII and XhoI. (C) Restriction enzyme digestion with HindIII. (D) Gardella gel analysis of Rm8TR-f.i in BJAB-kLANA cells after 58 days of G418 selection. Blot was probed with ³²P-m8TR DNA. O, gel origin. Vertical line at right indicates mTR episomes. For plasmid DNA, the fastest migrating signal is circular, covalently closed DNA. Lane 13 was positive for episomal DNA on longer exposure. Smeared signal in lanes 12–23 in lower half of gel is due to DNA degradation.

(JPG)

S3 Fig. mLANA mediates episome persistence in trans. (A) Immunoblots of mLANA detected by 6A3 monoclonal or FLAG antibody. A20 cells are G418 resistant. mLANAF-m4TR lanes are from cells with episomes at 47 days of G418 selection. Lane 9 has A20 cells transfected with mLANAF-m4TR at 3 days post transfection. mLANAF migrated slightly slower than S11 mLANA due to the 3xFLAG. 0.5×10^6 cells (top panel) or 0.25×10^6 cells (FLAG blot) were loaded per lane. (B, C) Gardella gel analyses of A20 cells or A20-mLANA cell lines transfected with m4TR-P. $2-3 \times 10^6$ cells were loaded per lane. O, gel origin; E, S11 episomes; L, S11 linear genomes due to lytic replication; vertical lines indicate m4TR episomes; asterisk indicates ccc plasmid DNA. (D) Immunoblot of mLANA puromycin resistant cell lines from panel C. (E) Immunoblot of mLANA puromycin resistant cell lines from panel D. 0.25×10^6 cells were loaded per lane. Bottom panels show tubulin.

(JPG)

S4 Fig. Reciprocal binding of kLANA and mLANA to TR DNA. (A) Alignment of kLBS 1–2 with mLBS 1–2. Identical nucleotides are shown in blue. (B) EMSA with in vitro translated mLANA or kLANA or (C) EMSA with purified mLANA or kLANA DBD. (B) Long exposure of lanes 11–14 is shown at right. Star (lane 18) or asterisks (lane 14) indicate supershifted complexes. (C) solid circle indicates shifted complexes in lanes 13, 14. P, free ^{32}P probe.

(TIF)

S5 Fig. Lytic growth of MHV68 chimeric viruses. Expression of viral proteins after infection of BHK-21 cells for 6 hours with 3 PFU/cell of v-WT or v-kLANA virus. (A) Confocal images after immunofluorescence staining of mLANA or kLANA. DNA was stained with DAPI. Magnification 630x. (B) Immunoblot for kLANA, mLANA, vCyclin, or M3. (C) BHK-21 cells were infected with 0.01 PFU/cell of v-WT or v-kLANA virus and titers determined. There was no significant statistical difference between infection groups ($p > 0.05$ using one-way non-parametric ANOVA Kruskal-Wallis.) (D) Lung virus titers after infection with 10^4 PFU of the indicated viruses. Each circle represents an individual mouse, bars indicate the mean. Titers differed significantly between v-WT and v- $\Delta 1007-21.yfp$ at day 7 ($*p < 0.05$, using one-way non-parametric ANOVA Kruskal-Wallis followed by Dunn's multiple comparison test). There were no other statistically significant differences.

(TIF)

S6 Fig. v-kLANA latent infection after intranasal or intraperitoneal inoculation. C57 Bl/6 mice were infected with v-WT or v-kLANA virus and spleens were harvested at day 11, 14 (panels A, B) or 21 (C, D) after infection. (A, C) Reactivation virus titers (closed circles) and titers of pre-formed infectious virus (open circles). Circles represent titers of individual mice. Bars indicate mean and dashed line shows the limit of detection of the assay. (B, D) Frequency of infected splenocytes determined in parallel in pools of spleens from each infection group. Bars represent the frequency of viral DNA-positive cells and error bars indicate 95% confidence intervals.

(TIF)

S1 Table. Puromycin or G418 resistant cell outgrowth.

(DOCX)

S2 Table. Oligonucleotides used for EMSAs.

(DOCX)

S3 Table. Detection of mTR episomes in BJAB-kLANA cells after transfection of plasmids containing greater than eight copies of mTR.

(DOCX)

Acknowledgments

Horng-Shen Chen cloned m4TR-P and Kambez Benam cloned pCMV-myc-mLANA-C3F. Mary Ballestas provided anti-LANA antibody. We thank the Histology and Comparative Pathology and Bioimaging and Flow Cytometry units, Instituto de Medicina Molecular Lisboa. We thank Tânia Carvalho for thoughtful discussions.

Author Contributions

Conceptualization: Aline C. Habison, Marta Pires de Miranda, Chantal Beauchemin, Min Tan, Sofia A. Cerqueira, Bruno Correia, Rajesh Ponnusamy, Edward J. Usherwood, Colin E. McVey, J. Pedro Simas, Kenneth M. Kaye.

Formal analysis: Aline C. Habison, Marta Pires de Miranda, Chantal Beauchemin, Min Tan, Sofia A. Cerqueira, Bruno Correia, Rajesh Ponnusamy, Colin E. McVey, J. Pedro Simas, Kenneth M. Kaye.

Funding acquisition: Colin E. McVey, J. Pedro Simas, Kenneth M. Kaye.

Investigation: Aline C. Habison, Marta Pires de Miranda, Chantal Beauchemin, Min Tan, Sofia A. Cerqueira, Bruno Correia, Rajesh Ponnusamy, Edward J. Usherwood, Colin E. McVey, J. Pedro Simas, Kenneth M. Kaye.

Project administration: Edward J. Usherwood, J. Pedro Simas, Kenneth M. Kaye.

Supervision: Colin E. McVey, J. Pedro Simas, Kenneth M. Kaye.

Writing – original draft: Aline C. Habison, Marta Pires de Miranda, Chantal Beauchemin, Min Tan, Colin E. McVey, J. Pedro Simas, Kenneth M. Kaye.

Writing – review & editing: Marta Pires de Miranda, J. Pedro Simas, Kenneth M. Kaye.

References

1. Damania BA, Cesarman E (2013) Kaposi's sarcoma-associated herpesvirus. In: Knipe DM, Howley PM, editors. *Fields Virology*. Philadelphia: Lippincott Williams & Wilkins. pp. 2081–2128.
2. Chang Y, Cesarman E, Pessin MS, Lee F, Culpepper J, et al. (1994) Identification of Herpesvirus-like DNA Sequences in AIDS-Associated Kaposi's Sarcoma. *Science* 266: 1865–1869. PMID: [7997879](#)
3. Cesarman E, Chang Y, Moore PS, Said JW, Knowles DM (1995) Kaposi's Sarcoma-Associated Herpesvirus-Like DNA Sequences in AIDS-Related Body-Cavity-Based Lymphomas. *NEJM* 332: 1186–1191. <https://doi.org/10.1056/NEJM199505043321802> PMID: [7700311](#)
4. Moore PS, Chang Y (1995) Detection of herpesvirus-like DNA sequences in Kaposi's sarcoma in patients with and without HIV infection [see comments]. *N Engl J Med* 332: 1181–1185. <https://doi.org/10.1056/NEJM199505043321801> PMID: [7700310](#)
5. Soulier J, Grollet L, Oksenhendler E, Cacoub P, Cazals-Hatem D, et al. (1995) Kaposi's Sarcoma-Associated Herpesvirus-Like DNA Sequences in Multicentric Castlemann's Disease. *Blood* 86: 1276–1280. PMID: [7632932](#)
6. Decker LL, Shankar P, Khan G, Freeman RB, Dezube BJ, et al. (1996) The Kaposi sarcoma-associated herpesvirus (KSHV) is present as an intact latent genome in KS tissue but replicates in the peripheral blood mononuclear cells of KS patients. *J Exp Med* 184: 283–288. PMID: [8691144](#)
7. Ballestas ME, Chatiss PA, Kaye KM (1999) Efficient persistence of extrachromosomal KSHV DNA mediated by latency-associated nuclear antigen. *Science* 284: 641–644. PMID: [10213686](#)
8. Ballestas ME, Kaye KM (2001) Kaposi's sarcoma-associated herpesvirus latency-associated nuclear antigen 1 mediates episome persistence through cis-acting terminal repeat (TR) sequence and specifically binds TR DNA. *J Virol* 75: 3250–3258. <https://doi.org/10.1128/JVI.75.7.3250-3258.2001> PMID: [11238851](#)
9. Ye FC, Zhou FC, Yoo SM, Xie JP, Browning PJ, et al. (2004) Disruption of Kaposi's sarcoma-associated herpesvirus latent nuclear antigen leads to abortive episome persistence. *J Virol* 78: 11121–11129. <https://doi.org/10.1128/JVI.78.20.11121-11129.2004> PMID: [15452232](#)

10. Barbera AJ, Chodaparambil JV, Kelley-Clarke B, Joukov V, Walter JC, et al. (2006) The nucleosomal surface as a docking station for Kaposi's sarcoma herpesvirus LANA. *Science* 311: 856–861. <https://doi.org/10.1126/science.1120541> PMID: 16469929
11. Garber AC, Shu MA, Hu J, Renne R (2001) DNA binding and modulation of gene expression by the latency-associated nuclear antigen of Kaposi's sarcoma-associated herpesvirus. *J Virol* 75: 7882–7892. <https://doi.org/10.1128/JVI.75.17.7882-7892.2001> PMID: 11483733
12. Garber AC, Hu J, Renne R (2002) Latency-associated nuclear antigen (LANA) cooperatively binds to two sites within the terminal repeat, and both sites contribute to the ability of LANA to suppress transcription and to facilitate DNA replication. *J Biol Chem* 277: 27401–27411. <https://doi.org/10.1074/jbc.M203489200> PMID: 12015325
13. Cotter MA 2nd, Subramanian C, Robertson ES (2001) The Kaposi's sarcoma-associated herpesvirus latency-associated nuclear antigen binds to specific sequences at the left end of the viral genome through its carboxy-terminus. *Virology* 291: 241–259. <https://doi.org/10.1006/viro.2001.1202> PMID: 11878894
14. Cotter MA 2nd, Robertson ES (1999) The latency-associated nuclear antigen tethers the Kaposi's sarcoma-associated herpesvirus genome to host chromosomes in body cavity-based lymphoma cells. *Virology* 264: 254–264. <https://doi.org/10.1006/viro.1999.9999> PMID: 10562490
15. Di Bartolo DL, Cannon M, Liu YF, Renne R, Chadburn A, et al. (2008) KSHV LANA inhibits TGF-beta signaling through epigenetic silencing of the TGF-beta type II receptor. *Blood* 111: 4731–4740. <https://doi.org/10.1182/blood-2007-09-110544> PMID: 18199825
16. Lu F, Day L, Gao SJ, Lieberman PM (2006) Acetylation of the latency-associated nuclear antigen regulates repression of Kaposi's sarcoma-associated herpesvirus lytic transcription. *J Virol* 80: 5273–5282. <https://doi.org/10.1128/JVI.02541-05> PMID: 16699007
17. Ottinger M, Christalla T, Nathan K, Brinkmann MM, Viejo-Borbolla A, et al. (2006) Kaposi's sarcoma-associated herpesvirus LANA-1 interacts with the short variant of BRD4 and releases cells from a BRD4- and BRD2/RING3-induced G1 cell cycle arrest. *J Virol* 80: 10772–10786. <https://doi.org/10.1128/JVI.00804-06> PMID: 16928766
18. Shamay M, Krithivas A, Zhang J, Hayward SD (2006) Recruitment of the de novo DNA methyltransferase Dnmt3a by Kaposi's sarcoma-associated herpesvirus LANA. *Proc Natl Acad Sci U S A* 103: 14554–14559. <https://doi.org/10.1073/pnas.0604469103> PMID: 16983096
19. Verma SC, Borah S, Robertson ES (2004) Latency-associated nuclear antigen of Kaposi's sarcoma-associated herpesvirus up-regulates transcription of human telomerase reverse transcriptase promoter through interaction with transcription factor Sp1. *J Virol* 78: 10348–10359. <https://doi.org/10.1128/JVI.78.19.10348-10359.2004> PMID: 15367601
20. Kim KY, Huerta SB, Izumiya C, Wang DH, Martinez A, et al. (2013) Kaposi's Sarcoma-Associated Herpesvirus (KSHV) Latency-Associated Nuclear Antigen Regulates the KSHV Epigenome by Association with the Histone Demethylase KDM3A. *J Virol* 87: 6782–6793. <https://doi.org/10.1128/JVI.00011-13> PMID: 23576503
21. Hu J, Garber AC, Renne R (2002) The latency-associated nuclear antigen of Kaposi's sarcoma-associated herpesvirus supports latent DNA replication in dividing cells. *J Virol* 76: 11677–11687. <https://doi.org/10.1128/JVI.76.22.11677-11687.2002> PMID: 12388727
22. Grundhoff A, Ganem D (2003) The Latency-Associated Nuclear Antigen of Kaposi's Sarcoma-Associated Herpesvirus Permits Replication of Terminal Repeat-Containing Plasmids. *J Virol* 77: 2779–2783. <https://doi.org/10.1128/JVI.77.4.2779-2783.2003> PMID: 12552022
23. Fejer G, Medveczky MM, Horvath E, Lane B, Chang Y, et al. (2003) The latency-associated nuclear antigen of Kaposi's sarcoma-associated herpesvirus interacts preferentially with the terminal repeats of the genome in vivo and this complex is sufficient for episomal DNA replication. *J Gen Virol* 84: 1451–1462. <https://doi.org/10.1099/vir.0.18940-0> PMID: 12771414
24. Uppal T, Banerjee S, Sun Z, Verma SC, Robertson ES (2014) KSHV LANA—the master regulator of KSHV latency. *Viruses* 6: 4961–4998. <https://doi.org/10.3390/v6124961> PMID: 25514370
25. Fakhari FD, Jeong JH, Kanan Y, Dittmer DP (2006) The latency-associated nuclear antigen of Kaposi sarcoma-associated herpesvirus induces B cell hyperplasia and lymphoma. *J Clin Invest* 116: 735–742. <https://doi.org/10.1172/JCI26190> PMID: 16498502
26. Dittmer D, Stoddart C, Renne R, Linquist-Stepps V, Moreno ME, et al. (1999) Experimental transmission of Kaposi's sarcoma-associated herpesvirus (KSHV/HHV-8) to SCID-hu Thy/Liv mice [In Process Citation]. *J Exp Med* 190: 1857–1868. PMID: 10601360
27. Parsons CH, Adang LA, Overdevest J, O'Connor CM, Taylor JR Jr., et al. (2006) KSHV targets multiple leukocyte lineages during long-term productive infection in NOD/SCID mice. *J Clin Invest* 116: 1963–1973. <https://doi.org/10.1172/JCI27249> PMID: 16794734

28. Wang LX, Kang G, Kumar P, Lu W, Li Y, et al. (2014) Humanized-BLT mouse model of Kaposi's sarcoma-associated herpesvirus infection. *Proc Natl Acad Sci U S A* 111: 3146–3151. <https://doi.org/10.1073/pnas.1318175111> PMID: 24516154
29. Flano E, Woodland DL, Blackman MA (2002) A mouse model for infectious mononucleosis. *Immunol Res* 25: 201–217. <https://doi.org/10.1385/IR.25:3:201> PMID: 12018460
30. Simas JP, Efsthathiou S (1998) Murine gammaherpesvirus 68: a model for the study of gammaherpesvirus pathogenesis. *Trends Microbiol* 6: 276–282. PMID: 9717216
31. Speck SH, Ganem D (2010) Viral latency and its regulation: lessons from the gamma-herpesviruses. *Cell Host Microbe* 8: 100–115. <https://doi.org/10.1016/j.chom.2010.06.014> PMID: 20638646
32. Virgin HWt, Latreille P, Wamsley P, Hallsworth K, Weck KE, et al. (1997) Complete sequence and genomic analysis of murine gammaherpesvirus 68. *J Virol* 71: 5894–5904. PMID: 9223479
33. Habison AC, Beauchemin C, Simas JP, Usherwood EJ, Kaye KM (2012) Murine Gammaherpesvirus 68 LANA Acts on Terminal Repeat DNA To Mediate Episome Persistence. *J Virol* 86: 11863–11876. <https://doi.org/10.1128/JVI.01656-12> PMID: 22915819
34. Moorman NJ, Willer DO, Speck SH (2003) The gammaherpesvirus 68 latency-associated nuclear antigen homolog is critical for the establishment of splenic latency. *J Virol* 77: 10295–10303. <https://doi.org/10.1128/JVI.77.19.10295-10303.2003> PMID: 12970414
35. Fowler P, Marques S, Simas JP, Efsthathiou S (2003) ORF73 of murine herpesvirus-68 is critical for the establishment and maintenance of latency. *J Gen Virol* 84: 3405–3416. <https://doi.org/10.1099/vir.0.19594-0> PMID: 14645921
36. Paden CR, Forrest JC, Moorman NJ, Speck SH (2010) Murine gammaherpesvirus 68 LANA is essential for virus reactivation from splenocytes but not long-term carriage of viral genome. *J Virol* 84: 7214–7224. <https://doi.org/10.1128/JVI.00133-10> PMID: 20444892
37. Dittmer D, Lagunoff M, Renne R, Staskus K, Haase A, et al. (1998) A cluster of latently expressed genes in Kaposi's sarcoma-associated herpesvirus. *J Virol* 72: 8309–8315. PMID: 9733875
38. Allen RD 3rd, Dickerson S, Speck SH (2006) Identification of spliced gammaherpesvirus 68 LANA and v-cyclin transcripts and analysis of their expression in vivo during latent infection. *J Virol* 80: 2055–2062. <https://doi.org/10.1128/JVI.80.4.2055-2062.2006> PMID: 16439562
39. Coleman HM, Efsthathiou S, Stevenson PG (2005) Transcription of the murine gammaherpesvirus 68 ORF73 from promoters in the viral terminal repeats. *J Gen Virol* 86: 561–574. <https://doi.org/10.1099/vir.0.80565-0> PMID: 15722515
40. Barbera AJ, Ballestas ME, Kaye KM (2004) The Kaposi's sarcoma-associated herpesvirus latency-associated nuclear antigen 1 N terminus is essential for chromosome association, DNA replication, and episome persistence. *J Virol* 78: 294–301. <https://doi.org/10.1128/JVI.78.1.294-301.2004> PMID: 14671111
41. Komatsu T, Ballestas ME, Barbera AJ, Kelley-Clarke B, Kaye KM (2004) KSHV LANA1 binds DNA as an oligomer and residues N-terminal to the oligomerization domain are essential for DNA binding, replication, and episome persistence. *Virology* 319: 225–236. <https://doi.org/10.1016/j.virol.2003.11.002> PMID: 14980483
42. Collins CM, Boss JM, Speck SH (2009) Identification of infected B-cell populations by using a recombinant murine gammaherpesvirus 68 expressing a fluorescent protein. *J Virol* 83: 6484–6493. <https://doi.org/10.1128/JVI.00297-09> PMID: 19386718
43. Forrest JC, Paden CR, Allen RD 3rd, Collins J, Speck SH (2007) ORF73-null murine gammaherpesvirus 68 reveals roles for mLANA and p53 in virus replication. *J Virol* 81: 11957–11971. <https://doi.org/10.1128/JVI.00111-07> PMID: 17699571
44. Toptan T, Fonseca L, Kwun HJ, Chang Y, Moore PS (2013) Complex alternative cytoplasmic protein isoforms of the Kaposi's sarcoma-associated herpesvirus latency-associated nuclear antigen 1 generated through noncanonical translation initiation. *J Virol* 87: 2744–2755. <https://doi.org/10.1128/JVI.03061-12> PMID: 23255808
45. Canham M, Talbot SJ (2004) A naturally occurring C-terminal truncated isoform of the latent nuclear antigen of Kaposi's sarcoma-associated herpesvirus does not associate with viral episomal DNA. *J Gen Virol* 85: 1363–1369. <https://doi.org/10.1099/vir.0.79802-0> PMID: 15166417
46. Decalf J, Godinho-Silva C, Fontinha D, Marques S, Simas JP (2014) Establishment of murine gammaherpesvirus latency in B cells is not a stochastic event. *PLoS Pathog* 10: e1004269. <https://doi.org/10.1371/journal.ppat.1004269> PMID: 25079788
47. Hawkins JB, Jones MT, Plassmann PE, Thorley-Lawson DA (2011) Chemotaxis in densely populated tissue determines germinal center anatomy and cell motility: a new paradigm for the development of complex tissues. *PLoS One* 6: e27650. <https://doi.org/10.1371/journal.pone.0027650> PMID: 22145018

48. Blake NW, Moghaddam A, Rao P, Kaur A, Glickman R, et al. (1999) Inhibition of antigen presentation by the glycine/alanine repeat domain is not conserved in simian homologues of Epstein-Barr virus nuclear antigen 1. *J Virol* 73: 7381–7389. PMID: [10438828](#)
49. Wang F, Rivallier P, Rao P, Cho Y (2001) Simian homologues of Epstein-Barr virus. *Philos Trans R Soc Lond B Biol Sci* 356: 489–497. <https://doi.org/10.1098/rstb.2000.0776> PMID: [11313007](#)
50. McGeoch DJ, Gatherer D, Dolan A (2005) On phylogenetic relationships among major lineages of the Gammaherpesvirinae. *J Gen Virol* 86: 307–316. <https://doi.org/10.1099/vir.0.80588-0> PMID: [15659749](#)
51. Ponnusamy R, Petoukhov MV, Correia B, Custodio TF, Juillard F, et al. (2015) KSHV but not MHV-68 LANA induces a strong bend upon binding to terminal repeat viral DNA. *Nucleic Acids Res* 43: 10039–10054. <https://doi.org/10.1093/nar/gkv987> PMID: [26424851](#)
52. Paden CR, Forrest JC, Tibbetts SA, Speck SH (2012) Unbiased Mutagenesis of MHV68 LANA Reveals a DNA-Binding Domain Required for LANA Function In Vitro and In Vivo. *PLoS Pathog* 8: e1002906. <https://doi.org/10.1371/journal.ppat.1002906> PMID: [22969427](#)
53. Rodrigues L, Filipe J, Seldon MP, Fonseca L, Anrather J, et al. (2009) Termination of NF-kappaB activity through a gammaherpesvirus protein that assembles an EC5S ubiquitin-ligase. *EMBO J* 28: 1283–1295. <https://doi.org/10.1038/emboj.2009.74> PMID: [19322197](#)
54. Rodrigues L, Popov N, Kaye KM, Simas JP (2013) Stabilization of Myc through heterotypic poly-ubiquitination by mLANA is critical for gamma-herpesvirus lymphoproliferation. *PLoS Pathog* 9: e1003554. <https://doi.org/10.1371/journal.ppat.1003554> PMID: [23950719](#)
55. Correia B, Cerqueira SA, Beauchemin C, Pires de Miranda M, Li S, et al. (2013) Crystal Structure of the Gamma-2 Herpesvirus LANA DNA Binding Domain Identifies Charged Surface Residues Which Impact Viral Latency. *PLoS Pathog* 9: e1003673. <https://doi.org/10.1371/journal.ppat.1003673> PMID: [24146618](#)
56. Song MJ, Hwang S, Wong WH, Wu TT, Lee S, et al. (2005) Identification of viral genes essential for replication of murine gamma-herpesvirus 68 using signature-tagged mutagenesis. *Proc Natl Acad Sci U S A* 102: 3805–3810. <https://doi.org/10.1073/pnas.0404521102> PMID: [15738413](#)
57. Kelley-Clarke B, De Leon-Vazquez E, Slain K, Barbera AJ, Kaye KM (2009) Role of Kaposi's sarcoma-associated herpesvirus C-terminal LANA chromosome binding in episome persistence. *J Virol* 83: 4326–4337. <https://doi.org/10.1128/JVI.02395-08> PMID: [19225000](#)
58. Srinivasan V, Komatsu T, Ballester ME, Kaye KM (2004) Definition of sequence requirements for latency-associated nuclear antigen 1 binding to Kaposi's sarcoma-associated herpesvirus DNA. *J Virol* 78: 14033–14038. <https://doi.org/10.1128/JVI.78.24.14033-14038.2004> PMID: [15564510](#)
59. Hellert J, Weidner-Glunde M, Krausz J, Lunsdorf H, Ritter C, et al. (2015) The 3D structure of Kaposi sarcoma herpesvirus LANA C-terminal domain bound to DNA. *Proc Natl Acad Sci U S A*.
60. Domsic JF, Chen HS, Lu F, Marmorstein R, Lieberman PM (2013) Molecular Basis for Oligomeric-DNA Binding and Episome Maintenance by KSHV LANA. *PLoS Pathog* 9: e1003672. <https://doi.org/10.1371/journal.ppat.1003672> PMID: [24146617](#)
61. Hellert J, Weidner-Glunde M, Krausz J, Richter U, Adler H, et al. (2013) A Structural Basis for BRD2/4-Mediated Host Chromatin Interaction and Oligomer Assembly of Kaposi Sarcoma-Associated Herpesvirus and Murine Gammaherpesvirus LANA Proteins. *PLoS Pathog* 9: e1003640. <https://doi.org/10.1371/journal.ppat.1003640> PMID: [24146614](#)
62. Cerqueira SA, Tan M, Li S, Juillard F, McVey CE, et al. (2016) Latency-Associated Nuclear Antigen E3 Ubiquitin Ligase Activity Impacts Gammaherpesvirus-Driven Germinal Center B Cell Proliferation. *J Virol* 90: 7667–7683. <https://doi.org/10.1128/JVI.00813-16> PMID: [27307564](#)
63. De Leon Vazquez E, Kaye KM (2011) The internal Kaposi's sarcoma-associated herpesvirus LANA regions exert a critical role on episome persistence. *J Virol* 85: 7622–7633. <https://doi.org/10.1128/JVI.00304-11> PMID: [21593163](#)
64. De Leon Vazquez E, Juillard F, Rosner B, Kaye KM (2014) A short sequence immediately upstream of the internal repeat elements is critical for KSHV LANA mediated DNA replication and impacts episome persistence. *Virology* 448: 344–355. <https://doi.org/10.1016/j.virol.2013.10.026> PMID: [24314665](#)
65. Kim KJ, Kanellopoulos-Langevin C, Merwin RM, Sachs DH, Asofsky R (1979) Establishment and characterization of BALB/c lymphoma lines with B cell properties. *J Immunol* 122: 549–554. PMID: [310843](#)
66. Usherwood EJ, Stewart JP, Nash AA (1996) Characterization of tumor cell lines derived from murine gammaherpesvirus-68-infected mice. *J Virol* 70: 6516–6518. PMID: [8709292](#)
67. Stevenson PG, May JS, Smith XG, Marques S, Adler H, et al. (2002) K3-mediated evasion of CD8(+) T cells aids amplification of a latent gamma-herpesvirus. *Nat Immunol* 3: 733–740. <https://doi.org/10.1038/ni818> PMID: [12101398](#)

68. Morgenstern JP, Land H (1990) Advanced mammalian gene transfer: high titre retroviral vectors with multiple drug selection markers and a complementary helper-free packaging cell line. *Nucleic Acids Res* 18: 3587–3596. PMID: [2194165](#)
69. van Dyk LF, Hess JL, Katz JD, Jacoby M, Speck SH, et al. (1999) The murine gammaherpesvirus 68 v-cyclin gene is an oncogene that promotes cell cycle progression in primary lymphocytes. *J Virol* 73: 5110–5122. PMID: [10233974](#)
70. Jensen KK, Chen SC, Hipkin RW, Wiekowski MT, Schwarz MA, et al. (2003) Disruption of CCL21-induced chemotaxis in vitro and in vivo by M3, a chemokine-binding protein encoded by murine gamma-herpesvirus 68. *J Virol* 77: 624–630. <https://doi.org/10.1128/JVI.77.1.624-630.2003> PMID: [12477865](#)
71. Gardella T, Medveczky P, Sairenji T, mulder C (1984) Detection of circular and linear herpesvirus DNA molecules in mammalian cells by gel electrophoresis. *Journal of Virology* 50: 248–254. PMID: [6321792](#)
72. Sun Q, Tsurimoto T, Juillard F, Li L, Li S, et al. (2014) Kaposi's sarcoma-associated herpesvirus LANA recruits the DNA polymerase clamp loader to mediate efficient replication and virus persistence. *Proc Natl Acad Sci U S A* 111: 11816–11821. <https://doi.org/10.1073/pnas.1404219111> PMID: [25071216](#)
73. Cesarman E, Nador RG, Bai F, Bohenzky RA, Russo JJ, et al. (1996) Kaposi's sarcoma-associated herpesvirus contains G protein-coupled receptor and cyclin D homologs which are expressed in Kaposi's sarcoma and malignant lymphoma. *J Virol* 70: 8218–8223. PMID: [8892957](#)
74. Adler H, Messerle M, Wagner M, Koszinowski UH (2000) Cloning and mutagenesis of the murine gammaherpesvirus 68 genome as an infectious bacterial artificial chromosome. *J Virol* 74: 6964–6974. PMID: [10888635](#)

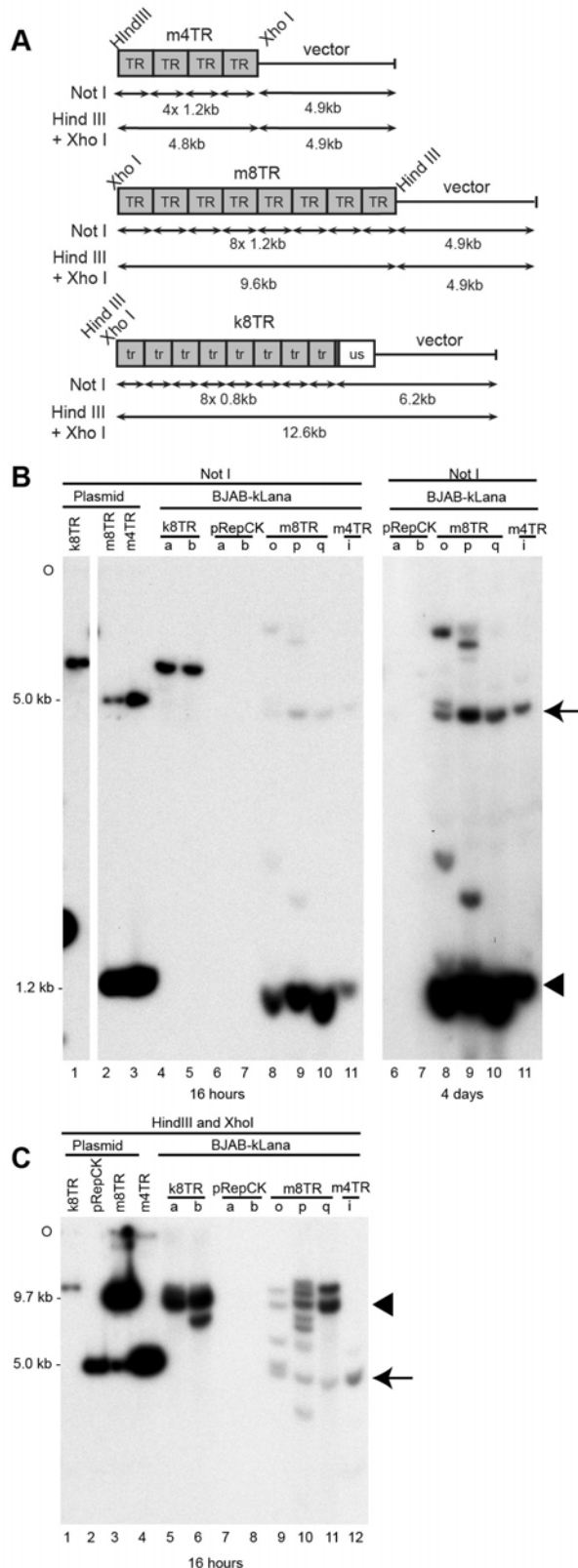
Supporting Information

TR episomes enlarge through recombination events

Following growth under G418 selection, k8TR and mTR episomes migrated more slowly than input plasmid ccc DNA on Gardella gels, consistent with substantial enlargement through recombination events. After 27 days of G418 selection, most k8TR episomal DNA migrated similarly to ccc pk8TR plasmid DNA (Fig. 1B, compare predominant bands in lanes 3 and 4 with fastest migrating, ccc k8TR DNA band in lane 1). However, after 87 days of G418 selection, the episomal DNA migrated much more slowly than ccc pk8TR DNA (Fig. 1D, compare lanes 5, 6 with lane 1). Similarly, both m4TR and m8TR episomal DNA migrated much more slowly than ccc plasmid DNA (Fig. 1B-D, compare episomal DNA bands with fastest migrating, ccc m4TR (Fig. 1B, lane 3; Fig. 1D, lane 4) or m8TR (Fig. 1C, lane 2; Fig. 1D, lane 3) bands. We previously observed selection for larger episomes through recombination events as cells are carried in culture over time[1-5].

To investigate potential recombination events, low molecular weight DNA was isolated, digested with NotI (S1B Fig.) or HindIII and XhoI (S1C Fig.), and assessed by Southern blot. NotI digestion of k8TR episomal DNA (S1B Fig.) resulted in expected ~6.2 kb vector size bands (S1B Fig., lanes 4, 5)(see S1A Fig. for expected sizes.) NotI digestion of mTR episomes resulted in the expected ~4.9 kb vector (arrow) and ~1.2 kb mTR (arrowhead) bands. The mTR band is hyperintense due to multiple mTR copies. Additional, bands migrating above or below vector band for cell lines o and p (S1B Fig., lanes 8, 9) represent likely aberrant recombination events.

HindIII/XhoI digestion linearizes k8TR plasmid to a ~12.6 kb band (S1C Fig., lane 1) and digestion of Hirt DNA from k8TR cell lines (S1C Fig., lanes 5, 6) had major bands of ~12.6 kb (although cell line b also had an additional, minor band.) Since HindIII/XhoI linearizes k8TR plasmid, this result suggests the large episomes are comprised of tandem head to tail k8TR multimers. HindIII/XhoI digestion of m4TR plasmid DNA produced a single band since the plasmid vector (~4.9kb) and insert of four mTR elements (~4.8 kb) co-migrate (S1C Fig., lane 4) and digestion of Hirt DNA from m4TR cell line i (S1C Fig., lane 12) also produced a ~4.9 kb band. HindIII/XhoI digestion of m8TR plasmid DNA produced a band at ~9.6 kb (from eight 1.2 kb mTR elements) and the 4.9kb plasmid vector backbone (S1C, lane 3).



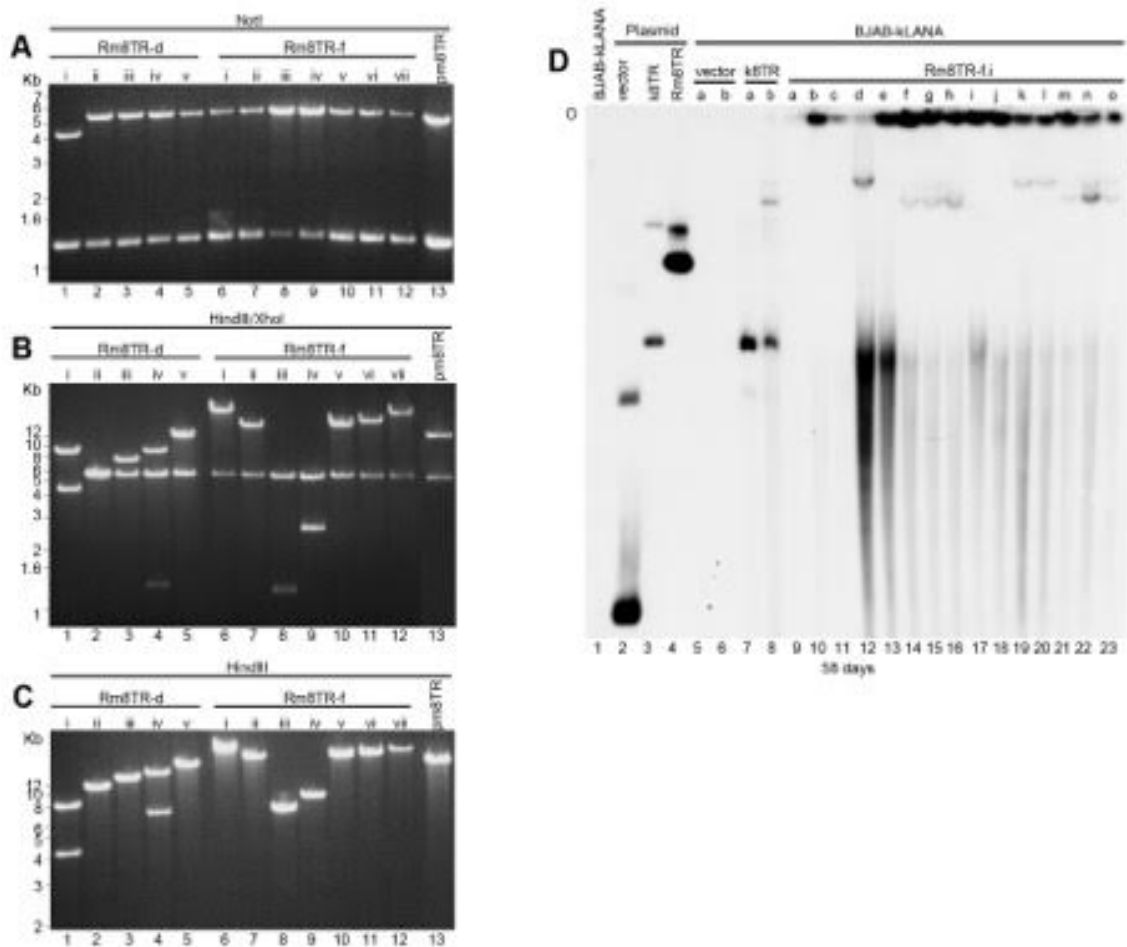
S1 Fig. TR episomes enlarge through recombination events.

(A) Schematic diagram showing digestion sites for m4TR, m8TR or pk8TR plasmids with NotI, or HindIII/XhoI, respectively. Sizes of expected fragments are indicated. TR, one mTR element; tr, one kTR element; us, unique KSHV sequence. (B, C) BJAB cell lines stably expressing kLANA transfected with pk8TR (Fig 1B, lanes 4, 5), pRepCK (Fig 1B, lanes 6 and 7), m8TR (Fig 1C, lanes 19 to 21), or m4TR (Fig 1B, lane 16), were harvested at 76 days of G418 selection. Low molecular

weight DNA was isolated, digested with NotI (panel B) or HindIII and XhoI (panel C), and assessed by Southern blot. Exposure times are indicated below each blot. Lane letters correspond to the same letters as in Fig 1. Panel on the left in (B) is a 16 hour exposure and on the right shows lanes 6 to 11 after a 4 day exposure.

Digestion of Hirt DNA from m8TR cell lines had the expected ~9.6 kb mTR (arrowhead) and ~4.9 kb vector (arrow) bands (S1C Fig., lanes 9-12). m8TR cell line q (S1C Fig., lane 11) had one additional band of ~10.8kb, consistent with 9 mTR copies, and lines o and p (S1C Fig., lanes 9, 10) had additional bands that could result from expansion or contraction of mTR copy number and/or vector rearrangements. Overall, these results suggest the large, recombinant episomes are comprised of input plasmids arranged in tandem head to tail multimers, and that additional recombination events, likely including expansion and contraction of tandem mTRs also occur.

To further investigate recombinant events in mTR episomes persisting in BJAB-kLANA cells, episomal DNA clones were isolated in bacteria (S2A-C Fig.) After ~90 days of G418 selection, low molecular weight DNA was purified from a G418 resistant BJAB-kLANA cell line containing k8TR episomes (cell line a, shown in Fig. 1C, lane 3, and in Fig. 1D, lane 5) or from two G418 resistant BJAB-kLANA cell lines containing m8TR episomes (cell line d, shown in Fig. 1C, lane 8 and Fig. 1D, lane 10, and cell line f, shown in Fig. 1C, lane 10 and Fig. 1D, lane 11), transformed by electroporation into bacteria, and bacteria selected for ampicillin resistance. We only expected to rescue smaller episomes, since large episomes comprised of tandem multimers of ~14.5 kb input plasmid are unlikely to efficiently transform or persist in bacteria. Transformation of DNA from cells containing k8TR episomes yielded over 800 cfu, compared with six cfu for cell line “d” and eight cfu for cell line “f”. Rescue of only 6 and 8 m8TR clones compared with over 800 k8TR clones was likely due to fewer m8TR episomes, especially those of smaller size comigrating with ccc plasmid DNA, present in these cells, and consistent with the fainter signal in the Gardella gel analysis for m8TR DNA cell lines “d” and “f” compared with that of the k8TR cell line “a” (Fig. 1C, D).



S2 Fig. Rescued mTR plasmids from BJAB-kLANA cells have variable mTR copy number and can persist as episomes after transfection.

After ~90 days of G418 selection, low molecular weight DNA was purified from a G418 resistant BJAB-kLANA cell line containing k8TR episomes (cell line a, shown in Fig 1C, lane 3, and in Fig 1D, lane 5) or from two G418 resistant BJAB-kLANA cell lines containing m8TR episomes (cell line d, shown in Fig 1C, lane 8 and Fig 1D, lane 10, and cell line f, shown in Fig 1C, lane 10 and Fig 1D, lane 11), transformed by electroporation into bacteria, and bacteria selected for ampicillin resistance. (A) Restriction enzyme digestion with NotI. (B) Restriction enzyme digestion with HindIII and XhoI. (C) Restriction enzyme digestion with HindIII. (D) Gardella gel analysis of Rm8TR-f.i in BJAB-kLANA cells after 58 days of G418 selection. Blot was probed with ^{32}P -m8TR DNA. O, gel origin. Vertical line at right indicates mTR episomes. For plasmid DNA, the fastest migrating signal is circular, covalently closed DNA. Lane 13 was positive for episomal DNA on longer exposure. Smeared signal in lanes 12–23 in lower half of gel is due to DNA degradation.

Rescued m8TR (designated Rm8TR) plasmids were assessed by restriction enzyme analyses. Digestion with NotI, which releases mTR elements from the vector (S1A Fig.), resolved all but one plasmid (S2A, lane 1) into expected size vector (~4.9kb) and mTR (~1.2 kb) bands. Digestion with HindIII and XhoI, which releases the mTRs en bloc from the vector (S1A Fig.), revealed several clones with larger mTR cassettes (S2B, lanes 6, 7, 10-12) than the input m8TR plasmid (lane 13). The plasmid in S2B, lane 2 has four mTR

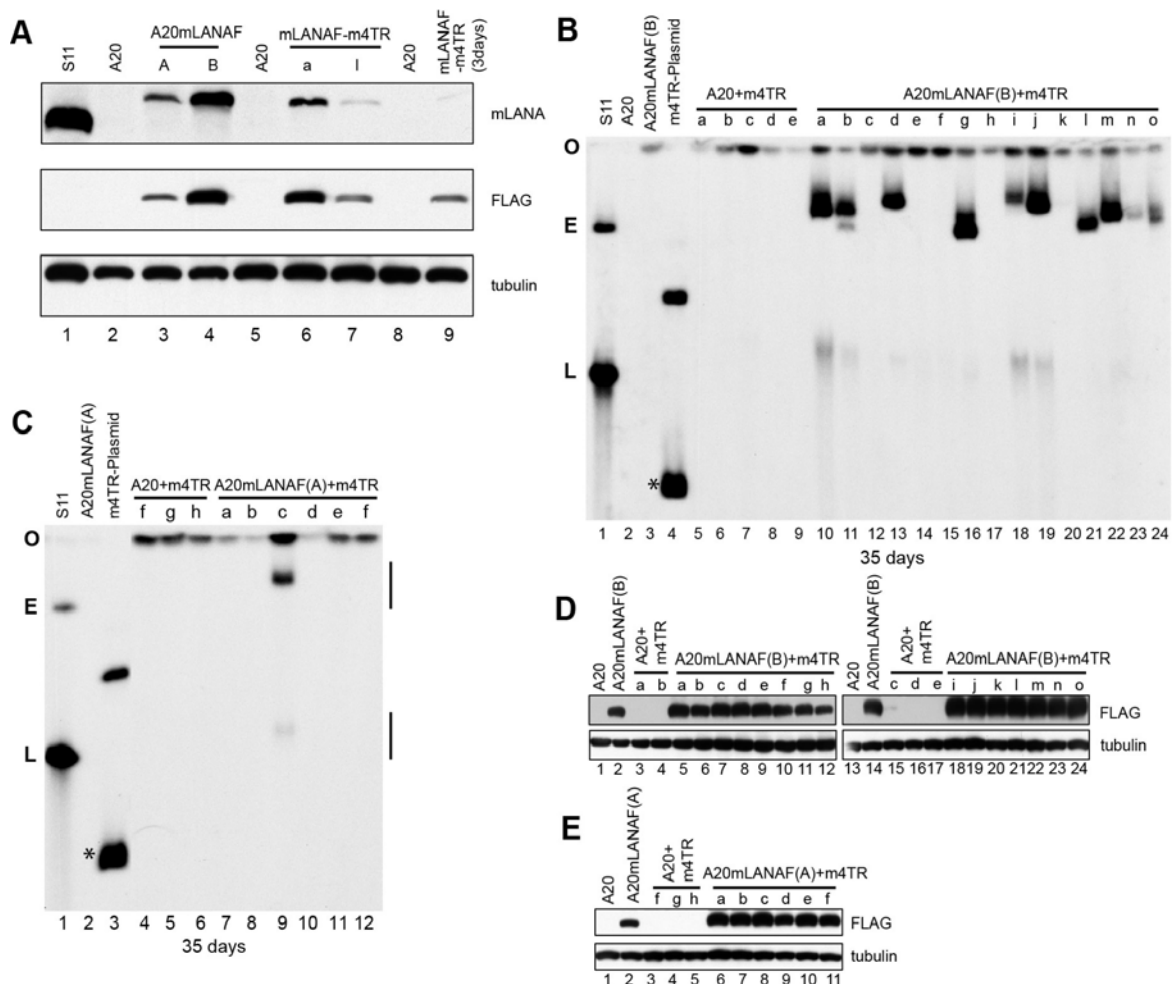
copies resulting in co-migration of the mTR band with vector. The ~1.2kb size of the mTR band in S2B Fig., lane 8 was consistent with one mTR copy and the ~2.4kb band in lane 9 was consistent with two mTR copies. For one clone, HindIII/XhoI digestion resulted in an additional ~1.2kb mTR band of one mTR (S2B, Fig., lane 4), consistent with an erroneous recombination event. Digestion with HindIII, which linearizes the m8TR plasmid (S1A Fig.) showed plasmids contained a single band of expected size (when accounting for the increased or decreased number of mTR elements) except for two (S2C, lanes 1 and 4), each of which contained two bands, consistent with erroneous recombination events. Therefore, all but one of the rescued m8TR episomes contained recombination events within the mTR elements resulting in expansion or contraction of the number of mTRs.

To assess whether rescued m8TR plasmids containing more than eight m8TR copies were enhanced for episome persistence efficiency in BJAB-kLANA cells, k8TR, pRepCK vector, or rescued plasmid DNA derived from Rm8TR-f.i (S2 Fig, lane 6 in panels A, B, and C) or three other clones (S3 Table) was transfected into BJAB-kLANA cells, and cells were seeded into microtiter plates and placed under G418 selection. Gardella gel analysis was performed after 58 days of G418 selection. Only one rescued mTR clone resulted in a higher percentage of episome containing cell lines (S2D Fig., S3 Table) compared to that of the parental m8TR DNA (38%) (Table 1) indicating that the increased numbers of mTR elements in these plasmids did not consistently enhance episome maintenance efficiency.

mLANA acts *in trans* on mTRs to mediate episome persistence.

mLANA acts on mTRs to mediate episome persistence when both are *in cis* [5], and we assessed here if mLANA can also act *in trans* to mediate persistence. For these experiments, we used two independently derived G418 resistant cell lines, A20-mLANAF(A) or A20-mLANAF(B), each of which stably express mLANAF. A20-mLANAF(B) (S3A Fig.) expressed mLANA at a slightly reduced level compared to S11, an MHV68 latently infected, murine B tumor cell line, while mLANA expression was lower in A20-mLANAF(A) (described in [5]) (S3A Fig.). However, mLANA levels in A20-mLANAF(A) and (B) were similar to or higher than that of mLANA in two cell lines stably maintaining episomes containing mLANA and four mTRs *in cis* (mLANAF—m4TR) (described in [5]) (S3A Fig.). Therefore, A20-mLANAF(A) and (B) express mLANA at physiologic levels. A20-mLANAF(A) and (B) grew more slowly than parental A20 cells, consistent with a mild mLANA inhibitory effect on cell growth as previously observed [5];

growth rates inversely correlated with mLANA expression levels with A20-mLANAF(B), doubling at about half the rate of A20 cells.



S3 Fig. mLANA mediates episome persistence in *trans*.

(A) Immunoblots of mLANA detected by 6A3 monoclonal or FLAG antibody. A20 cells are G418 resistant. mLANAF-m4TR lanes are from cells with episomes at 47 days of G418 selection. Lane 9 has A20 cells transfected with mLANAF-m4TR at 3 days post transfection. mLANAF migrated slightly slower than S11 mLANA due to the 3xFLAG. 0.5x10⁶ cells (top panel) or 0.25x10⁶ cells (FLAG blot) were loaded per lane. (B, C) Gardella gel analyses of A20 cells or A20-mLANAF cell lines transfected with m4TR-P. 2-3x10⁶ cells were loaded per lane. O, gel origin; E, S11 episomes; L, S11 linear genomes due to lytic replication; vertical lines indicate m4TR episomes; asterisk indicates ccc plasmid DNA. (D) Immunoblot of mLANA puromycin resistant cell lines from panel C. (E) Immunoblot of mLANA puromycin resistant cell lines from panel D. 0.25x10⁶ cells were loaded per lane. Bottom panels show tubulin.

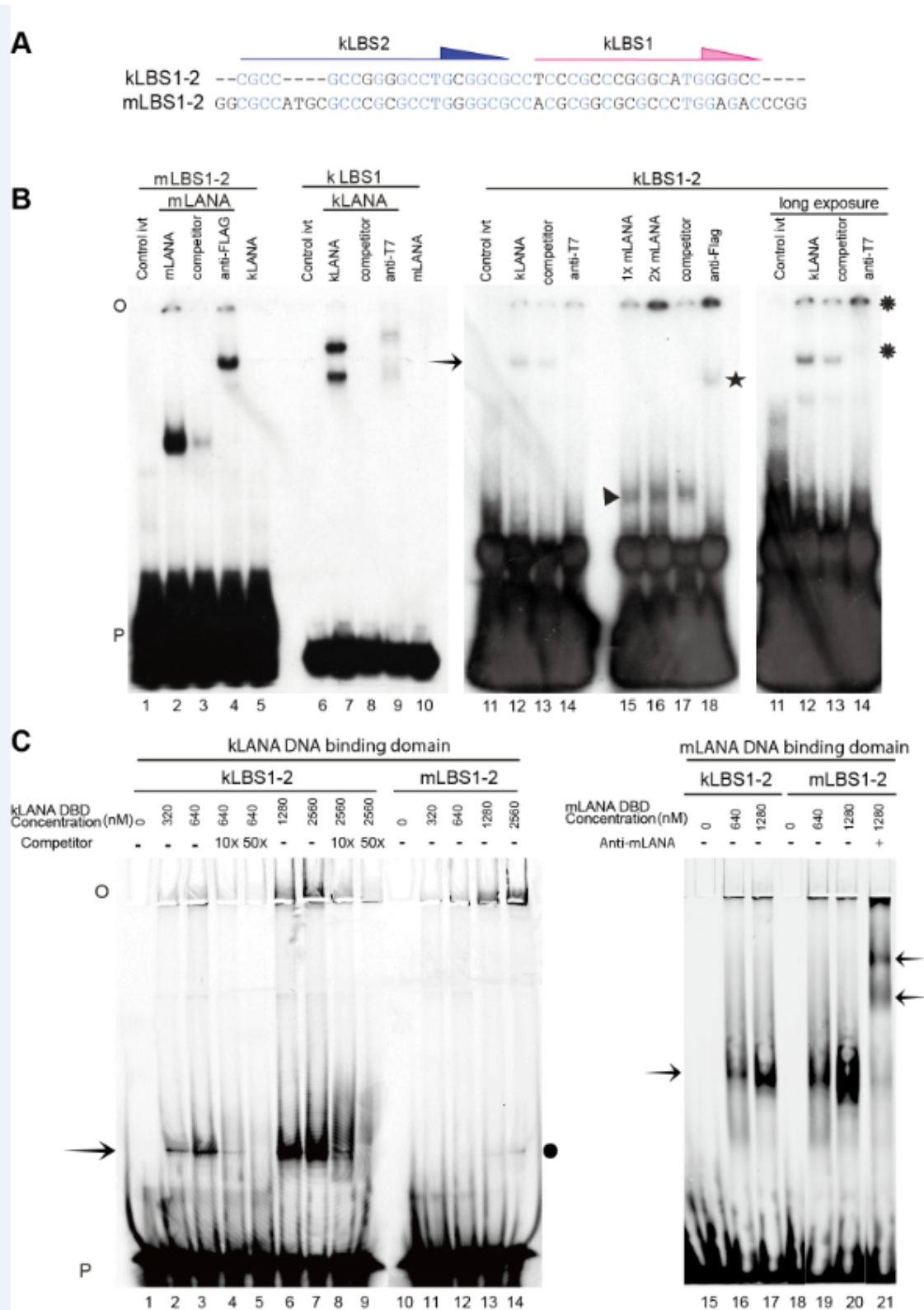
DNA containing four mTR copies (m4TR-P) or vector (pRepCK-P) was transfected into A20-mLANAF(A) or A20-mLANAF(B) cells. Puromycin resistant outgrowth (conferred by the plasmid vector) was low after transfection of pRepCK-P and higher after transfection

of m4TR-P regardless of the presence of mLANA (S1 Table). This result could be due to absence of mLANA episome persistence or episome persistence efficiency similar to that of integration. In the absence of LANA episome maintenance, integration is required for m4TR persistence. m4TR DNA integrated in A20 cells at higher rates than pRepCK-P vector, similar to previous observations (S1 Table) [5].

After expansion of cells, Gardella gel analyses[6] were performed to assess for the presence of episomes. As expected, no episomes were present in the absence of mLANA (S3B Fig.). In contrast, m4TR-P episomes were present in 10 of 15 lanes for A20-mLANAF (B) (S3B Fig.). Most episomal DNA migrated much more slowly than the circular, covalently closed (ccc) plasmid (S3B Fig., asterisk), migrating similarly to ~200kb MHV68 episomes (E) in the S11 cells. In five experiments with A20-mLANAF(B) cells, 48 of 83 (58%) of puromycin resistant cell lines had episomes (Table 1). Episomal DNA was also present in one of six puromycin resistant A20-mLANAF(A) cell lines (S3C Fig.). In two experiments with A20-mLANAF(A) cells, 5 of 20 (25%) cell lines had episomes. The lower percentage of puromycin resistant cell lines with m4TR-P episomes may be due to the lower mLANA expression level in the A20-mLANAF(A) cells compared with that of A20-mLANAF(B) (S3A Fig.). In contrast, episomes were never seen in 34 puromycin resistant cell lines after transfection of m4TR-P into A20 cells. Immunoblot analysis demonstrated that puromycin resistant A20-mLANAF(A) or (B) cells continued to express mLANAF, even in cell lines that lacked episomes (S3D, S3E Fig.). Consequently, the absence of episomes in some puromycin resistant cell lines was not due to lack of mLANA expression. Therefore, mLANA acts in trans on mTR DNA to mediate episome persistence.

Reciprocal binding of kLANA and mLANA to TR DNA recognition sequences

Since kLANA acts on mTR DNA and mLANA acts on kTR DNA to mediate episome persistence, and since TR DNA binding is essential for LANA mediated episome persistence [7], we assessed if kLANA or mLANA can bind to the other's TR DNA recognition sequence. As expected, incubation of in vitro translated mLANA with mLBS1-2 probe resulted in a shifted complex which was competed with excess cold mLBS1-2 competitor oligonucleotide and supershifted with anti-FLAG antibody (which detects the FLAG epitope tagged mLANA) (S4B Fig.). In contrast, incubation of in vitro translated kLANA with mLBS1-2 did not result in a detectable complex (S4B Fig., lane 5), consistent with reduced or absent binding of kLANA to mLBS1-2.

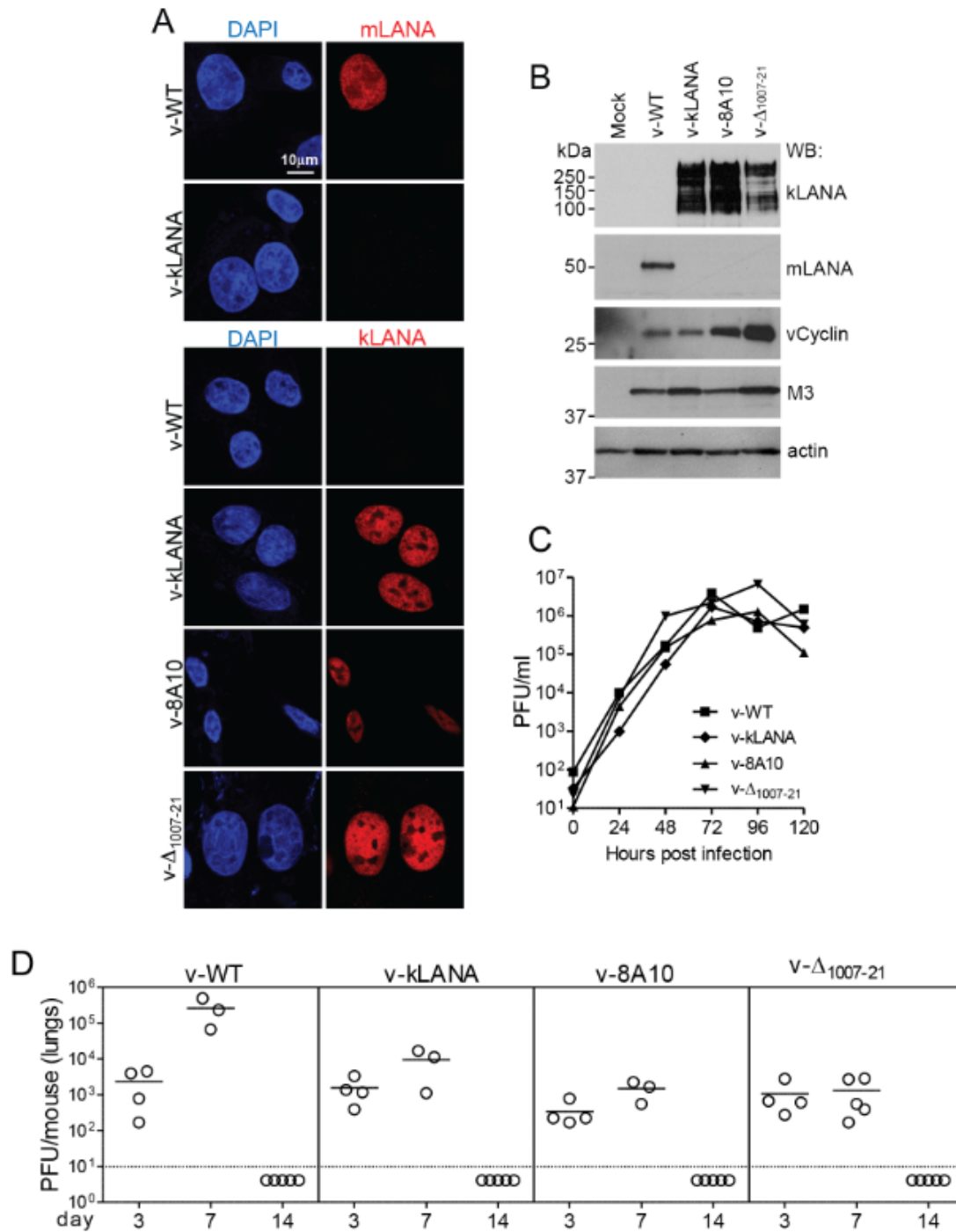


S4 Fig. Reciprocal binding of kLANA and mLANA to TR DNA.

(A) Alignment of kLBS 1–2 with mLBS 1–2. Identical nucleotides are shown in blue. (B) EMSA with in vitro translated mLANA or kLANA or (C) EMSA with purified mLANA or kLANA DBD. (B) Long exposure of lanes 11–14 is shown at right. Star (lane 18) or asterisks (lane 14) indicate supershifted complexes. (C) solid circle indicates shifted complexes in lanes 13, 14. P, free 32 P probe.

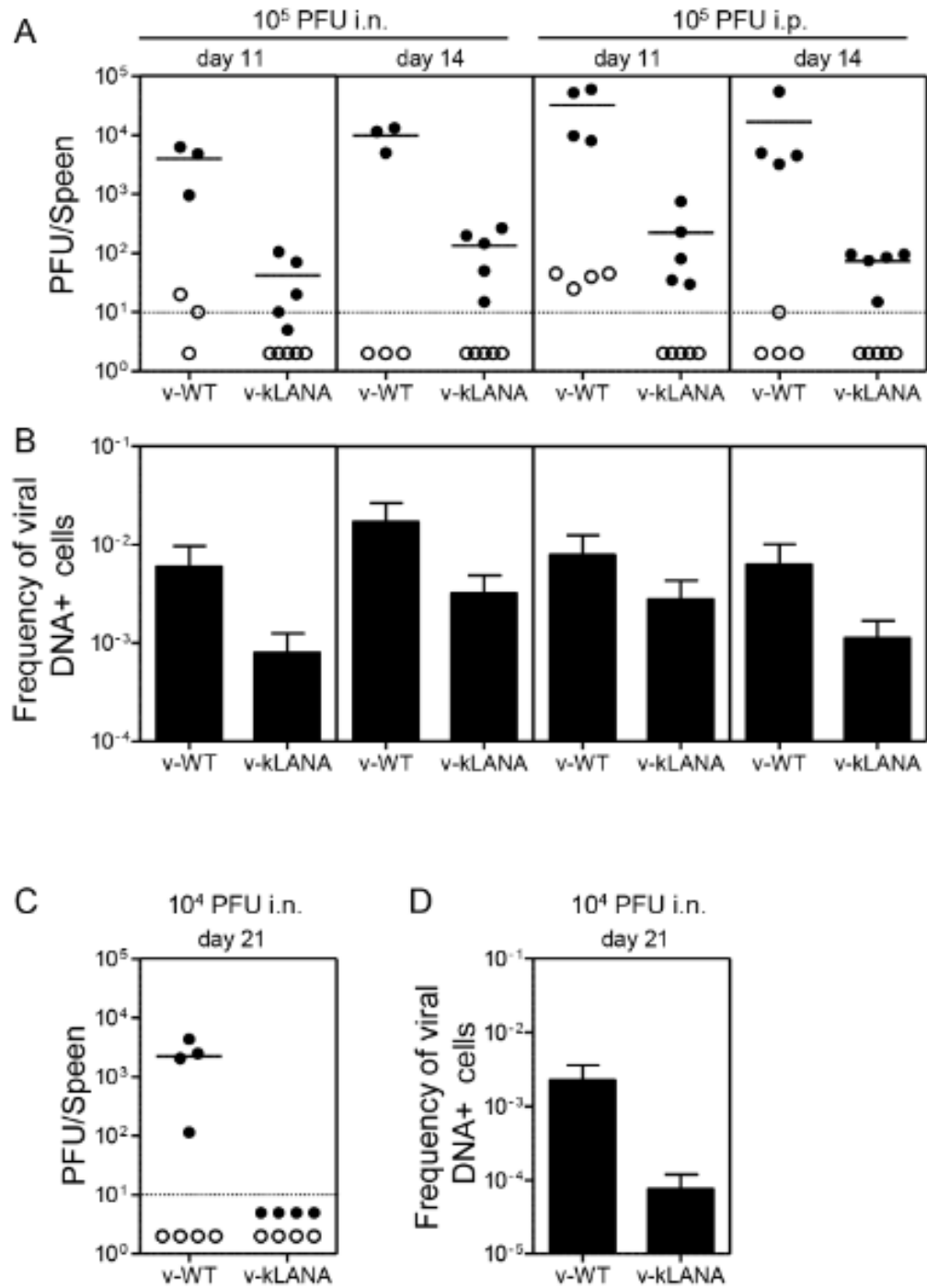
Since in vitro translation experiments use relatively small amounts of LANA, we further assessed binding with larger amounts of purified LANA DBD. kLANA at concentrations of at least 1280 nM resulted in detectable complexes with mLBS1-2 (S4C Fig., lanes 13, 14, solid circle), although these produced substantially weaker signal compared to complexes formed with kLANA and kLBS1-2 (S4C Fig.). Therefore, kLANA binds mLBS1-2, but with substantially less efficiency than to kLBS1-2.

We also assessed binding of mLANA to kLBS. As expected, incubation of in vitro translated kLANA with kLBS1 probe resulted in two shifted complexes (as previously observed [1,8]), which were efficiently competed with excess, unlabelled kLBS1 competitor and supershifted after incubation with anti-T7 antibody (which detects the T7 epitope tagged kLANA) (S4B Fig.). In contrast, incubation of in vitro translated mLANA did not result in a shifted complex with LBS1 (S4B Fig., lane 10). Since LANA cooperatively binds LBS1-2[9,10], we also assessed mLANA binding to kLBS1-2. Incubation of mLANA with kLBS1-2 resulted in easily detectable complex migrating faster than kLANA complexed with kLBS1-2 (S4B Fig., arrowhead) due to the mLANA's smaller size. Purified mLANA DBD also resulted in easily detectable complexes with kLBS1-2 (S4C Fig.). Therefore, kLANA and mLANA bind reciprocally to each other's TR DNA recognition sequences, although binding of kLANA to mLBS is a relatively weak interaction.



S5 Fig. Lytic growth of MHV68 chimeric viruses.

Expression of viral proteins after infection of BHK-21 cells for 6 hours with 3 PFU/cell of v-WT or v-kLANA virus. (A) Confocal images after immunofluorescence staining of mLANA or kLANA. DNA was stained with DAPI. Magnification 630x. (B) Immunoblot for kLANA, mLANA, vCyclin, or M3. (C) BHK-21 cells were infected with 0.01 PFU/cell of v-WT or v-kLANA virus and titers determined. There was no significant statistical difference between infection groups ($p > 0.05$ using one-way non-parametric ANOVA Kruskal-Wallis.) (D) Lung virus titers after infection with 10^4 PFU of the indicated viruses. Each circle represents an individual mouse, bars indicate the mean. Titers differed significantly between v-WT and v- Δ 1007-21.yfp at day 7 ($*p < 0.05$, using one-way non-parametric ANOVA Kruskal-Wallis followed by Dunn's multiple comparison test). There were no other statistically significant differences.



S6 Fig. v-kLANA latent infection after intranasal or intraperitoneal inoculation.

C57 Bl/6 mice were infected with v-WT or v-kLANA virus and spleens were harvested at day 11, 14 (panels A, B) or 21 (C, D) after infection. (A, C) Reactivation virus titers (closed circles) and titers of pre-formed infectious virus (open circles). Circles represent titers of individual mice. Bars indicate mean and dashed line shows the limit of detection of the assay. (B, D) Frequency of infected splenocytes determined in parallel in pools of spleens from each infection group. Bars represent the frequency of viral DNA-positive cells and error bars indicate 95% confidence intervals.

S1 Table. Puromycin or G418 resistant cell outgrowth

Cell line	Transfected DNA ¹	Outgrowth ² 1000 cells/well	Outgrowth 100 cells/well	Outgrowth 10 cells/well
BJAB-kLANA ³	pk8TR	96 (0)	96 (0.4)	55 (24)
BJAB-kLANA ³	m2TR	96 (0.5)	41 (9)	3 (2)
BJAB-kLANA ³	m4TR	96 (0.4)	85 (3)	13 (3)
BJAB-kLANA ³	m8TR	96 (0)	94 (3)	23 (6)
BJAB-kLANA ³	pRepCK	55 (18)	10 (3)	1 (0.5)
BJAB ⁴	pk8TR	62 (57,67)	13 (8, 17)	2 (1, 3)
BJAB ⁴	pRepCK	50 (47, 52)	6 (2, 9)	1 (0, 1)
BJAB ⁴	m2TR	77 (71, 82)	14 (11, 16)	2 (0, 3)
BJAB ⁴	m4TR	84 (92, 76)	23 (26, 20)	3 (2, 3)
BJAB ⁴	m8TR	95 (95, 95)	40 (38, 41)	10 (8, 12)
A20-mLANAF(A)	m4TR-P	82	17	12
A20-mLANAF(B) ⁵	m4TR-P	95 (1)	23 (5)	3 (2)
A20-mLANAF(A)	pRepCK-P	1	0	0
A20-mLANAF(B) ⁵	pRepCK-P	9 (5)	1 (0.5)	0 (0)
A20 ⁵	m4TR-P	71 (9)	18 (6)	3 (0.5)
A20-mLANAF(B) ⁴	pk8TR-P	96 (96, 96)	35 (23, 46)	3 (3, 3)
A20 ⁵	pk8TR-P	43 (19)	7 (3)	1 (0.5)
A20 ⁵	pRepCK-P	13 (8)	2 (1)	0 (0)

¹Plasmids with “P” suffix encode puromycin resistance; others encode G418 resistance.

²Number of wells of puromycin or G418 resistant outgrowth per 96 well microtiter plate at the indicated seeding density. ³Average of at least three experiments with standard deviation shown in italics. ⁴Average of two experiments with individual values in parenthesis. ⁵Average of three experiments with standard deviation shown in italics.

S2 Table. Oligonucleotides used for EMSAs¹

LBS probe	dsDNA sequence
kLBS1	5' - GGAT <u>TCCC</u> CGCCCGGGCATGGGGCCG 3' - <u>AGGG</u> CGGGCCCGTACCCCGGCTAGG - 5'
kLBS1-2	5' - GATC <u>CGCC</u> CGCCCGGGGCTGCGGCGCC <u>TCCC</u> CGCCCGGGCATGGGGCCG-3' 3' - <u>GCGG</u> CGGGCCCGGACGCGCGG <u>AGGG</u> CGGGCCCGTACCCCGGCTAG-5'
mLBS1-2	5' - GATC <u>GGCG</u> CCATGCGCCCGCGCCTGGGGCGCCACGCGGCGCGCCCTGGAGACCCGGG-3' 3' - <u>CCGCG</u> GTACGCGGGCGCGGACCCCGCGGTGCGCCGCGCGGGACCTCTGGGCCCTAG-5'
Flc-kLBS1-2	[Flc] 5' - TTTGAC <u>CGCC</u> CGCCCGGGGCTGCGGCGCC <u>TCCC</u> CGCCCGGGCATGGGGCCG-3' 3' - CT <u>GCGG</u> CGGGCCCGGACGCGCGG <u>AGGG</u> CGGGCCCGTACCCCGGCG-5'
Flc-mLBS1-2	[Flc] 5' - TTT <u>TCCC</u> CGCGCCTGGGGCGCCACGCGGCGCGCCCTGGAGACCCGGG-3' 3' - <u>GGGCG</u> CGGACCCCGCGGTGCGCCGCGCGGGACCTCTGGGCC-5'
Unlabeled, competitor kLBS1-2	5' - GAC <u>CGCC</u> CGCCCGGGGCTGCGGCGCC <u>TCCC</u> CGCCCGGGCATGGGGCCG-3' 3' - CT <u>GCGG</u> CGGGCCCGGACGCGCGG <u>AGGG</u> CGGGCCCGTACCCCGGCG

¹kLBS1[1] is in bold and underlined, kLBS2 site is bold and italicized, mLBS1-2 is underlined[2,3].

1. Garber AC, Hu J, Renne R (2002) Latency-associated nuclear antigen (LANA) cooperatively binds to two sites within the terminal repeat, and both sites contribute to the ability of LANA to suppress transcription and to facilitate DNA replication. J Biol Chem **277**: 27401-27411.
2. Paden CR, Forrest JC, Tibbetts SA, Speck SH (2012) Unbiased Mutagenesis of MHV68 LANA Reveals a DNA-Binding Domain Required for LANA Function In Vitro and In Vivo. PLoS Pathog **8**: e1002906.
3. Correia B, Cerqueira SA, Beauchemin C, Pires de Miranda M, Li S, et al. (2013) Crystal Structure of the Gamma-2 Herpesvirus LANA DNA Binding Domain Identifies Charged Surface Residues Which Impact Viral Latency. PLoS Pathog **9**: e1003673.

S3 Table. Detection of mTR episomes in BJAB-kLANA cells after transfection of plasmids containing greater than eight copies of mTR.

Transfected DNA	Number of cell lines assessed	Cell lines with episomal DNA	Percent with episomal DNA
pRepCK	3	0	0 (%)
pk8TR	2	2	100 (%)
Rm8TR-f.i	15	10	67 (%)
Rm8TR-f.v	15	5	33 (%)
Rm8TR-f.vi	15	5	33 (%)
Rm8TR-f.vii	15	1	7 (%)

Materials and Methods for Supplementary Information

Hirt DNA extraction, digestion and Southern blot. Ten million G418 resistant BJAB-kLANA cells transfected with m4TR, m8TR, k8TR, or vector control (pRepCK) were harvested after 76 days of selection for low molecular weight DNA isolation by the Hirt method[11]. Cells were lysed in 2 ml lysis buffer (0.6%SDS, 10mM EDTA, 10mM Tris-HCl pH 7.5, 50ug/ml RnaseA) and incubated at 37°C for 2 hours. NaCl was then added to a final concentration of 1M and incubated overnight at 4°C. After centrifugation at 11,000 x g at 4°C for 30 minutes to precipitate chromosomal DNA, low molecular weight DNA was extracted with phenol:chloroform (1:1), then twice with chloroform:isoamyl alcohol (24:1) and ethanol precipitated. The DNA pellet was washed with 70% ethanol, air dried and resuspended in TE buffer (10mM Tris pH8, 0.1mM EDTA). 30µg of Hirt DNA was digested overnight with either NotI or HindIII and XhoI, resolved in a 0.8% agarose gel and transferred to a nylon membrane for detection by Southern blotting with ³²P radiolabeled probe.

Plasmid rescue of episomal DNA into bacteria. Low molecular weight DNA was isolated from ten million G418 resistant BJAB-kLANA cells initially transfected with pk8TR, m4TR, m8TR or pRepCK, using Qiagen's R.E.A.L. Prep 96 Plasmid Kit according to the manufacturer's instructions, with the exception that 2x volumes of R1, R2 and R3 were used and DNA pellets were resuspended in ddH₂O. Ten µL of DH10B competent cells (New England Biolabs) were transformed by electroporation of 5µl of purified DNA using settings of 2.0 kV, 200 Ω, and 25 µF with a BTX *E. coli* TransPorator, plated onto LB-Ampicillin, and incubated at 30°C. For larger scale plasmid preparations, plasmids were transformed by heat shock into STBL2 competent cells (MaxiPrep Invitrogen) and DNA used for Southern blot analysis or transfection into BJAB-kLANA cells to assess episome maintenance.

EMSA For electrophoretic mobility shift assays (EMSA), T7-kLANA or Myc-mLANA-C3F were in vitro translated using TNT Quick-coupled reticulocyte lysate systems (Promega). Ten µL (or 20 µL) of in vitro-translated proteins were incubated in DNA binding buffer [20 mM Tris (pH 7.5), 10% glycerol, 50 mM KCl, 0.1 mM dithiothreitol, 10 mM MgCl₂, 1 mM EDTA, 20 µg/ml of poly(dI-dC)] with 50,000 counts per minute of ³²P-labeled TR probe for 30 min on ice. Probes were prepared by annealing kLBS (kLANA binding site) or mLBS encoding oligonucleotides (shown in S2 Table), and filling in the ends. For supershift

assays, after the 30-min incubation, samples were incubated for 15 min at room temperature with 1 µg of anti-T7 tag antibody (Novagen) for kLANA or 1 µg of anti-Flag (Sigma) for mLANA. Fifty fold excess, unlabeled oligonucleotide was included for competition assays. Bound complexes were resolved on a 4% nondenaturing polyacrylamide gel. Signal was detected by autoradiography.

For EMSAs performed with purified protein, mLANA (mLANA₁₂₄₋₃₁₄) or kLANA (kLANA₁₀₀₈₋₁₁₅₀) proteins were expressed and purified as previously described[9,12]. DNA probes corresponding to regions containing kLBS1-2 or mLBS1-2 were generated using fluorescein-labeled DNA oligonucleotides (Sigma-Aldrich), Flc-5'-TTT-mLBS1-2, Flc-5'-TTT-kLBS1-2, or unlabeled competitor oligonucleotide, kLBS1-2 (S2 Table). To generate probes, synthetic oligonucleotides were mixed together in equimolar amounts in buffer containing 10 mM Tris-HCl pH 8, 50mM NaCl, 5mM MgCl₂ 1mM EDTA and annealed by heating the mixed oligonucleotides to 95°C for 10 minutes and gradually cooled in a stepwise manner to 4°C over a period of 2 h using a MyCycler™ thermal cycler (BioRAD). The annealed oligonucleotides were stored at -20°C prior to use.

Prior to incubation with oligonucleotides, proteins were buffer exchanged into buffer containing 20mM Tris-HCl pH7.5, 300mM KCl, 10mM MgCl₂ and 10% glycerol. Binding reactions were performed overnight by incubating LANA protein with 1 µM of each DNA oligonucleotide, supplemented with 1mM EDTA, 0.01 mg/ml poly dI-dC, 0.1 mM DTT and 0.1% Tween 20, in a final volume of 30 µL. For supershift assays, five fold excess of purified α-mLANA 6A3 antibody was included in the incubation with the mLANA protein. For competition experiments, ten or fifty fold excess unlabeled oligonucleotide of kLBS1-2 was included in the incubation. Reactions were loaded on a native 4% TBE-acrylamide gel and run at 200V for 3h in 1X TBE buffer. Complexes were visualized after exposure to a Fujifilm-FLA5100 scanner with an LPB filter at 473 nm wavelength.

Supporting Information References

1. **Ballestas ME, Kaye KM** (2001) Kaposi's sarcoma-associated herpesvirus latency-associated nuclear antigen 1 mediates episome persistence through cis-acting terminal repeat (TR) sequence and specifically binds TR DNA. *J Virol* **75**: 3250-3258.
2. **De Leon Vazquez E, Kaye KM** (2011) The internal Kaposi's sarcoma-associated herpesvirus LANA regions exert a critical role on episome persistence. *J Virol* **85**: 7622-7633.
3. **De Leon Vazquez E, Carey VJ, Kaye KM** (2013) Identification of Kshv Lana Regions Important for Episome Segregation, Replication and Persistence. *J Virol* **87**: 12270-12283.
4. **De Leon Vazquez E, Juillard F, Rosner B, Kaye KM** (2014) A short sequence immediately upstream of the internal repeat elements is critical for KSHV LANA mediated DNA replication and impacts episome persistence. *Virology* **448**: 344-355.
5. **Habison AC, Beauchemin C, Simas JP, Usherwood EJ, Kaye KM** (2012) Murine Gammaherpesvirus 68 LANA Acts on Terminal Repeat DNA To Mediate Episome Persistence. *J Virol* **86**: 11863-11876.
6. **Gardella T, Medveczky P, Sairenji T, mulder C** (1984) Detection of circular and linear herpesvirus DNA molecules in mammalian cells by gel electrophoresis. *Journal of Virology* **50**: 248-254.
7. **Komatsu T, Ballestas ME, Barbera AJ, Kelley-Clarke B, Kaye KM** (2004) KSHV LANA1 binds DNA as an oligomer and residues N-terminal to the oligomerization domain are essential for DNA binding, replication, and episome persistence. *Virology* **319**: 225-236.
8. **Srinivasan V, Komatsu T, Ballestas ME, Kaye KM** (2004) Definition of sequence requirements for latency-associated nuclear antigen 1 binding to Kaposi's sarcoma-associated herpesvirus DNA. *J Virol* **78**: 14033-14038.
9. **Correia B, Cerqueira SA, Beauchemin C, Pires de Miranda M, Li S, et al.** (2013) Crystal Structure of the Gamma-2 Herpesvirus LANA DNA Binding Domain Identifies Charged Surface Residues Which Impact Viral Latency. *PLoS Pathog* **9**: e1003673.
10. **Garber AC, Hu J, Renne R** (2002) Latency-associated nuclear antigen (LANA) cooperatively binds to two sites within the terminal repeat, and both sites contribute to the ability of LANA to suppress transcription and to facilitate DNA replication. *J Biol Chem* **277**: 27401-27411.
11. **Hirt B** (1967) Selective extraction of polyoma DNA from infected mouse cell cultures. *J Mol Biol* **26**: 365-369.
12. **Ponnusamy R, Petoukhov MV, Correia B, Custodio TF, Juillard F, et al.** (2015) KSHV but not MHV-68 LANA induces a strong bend upon binding to terminal repeat viral DNA. *Nucleic Acids Res* **43**: 10039-10054.
13. **Paden CR, Forrest JC, Tibbetts SA, Speck SH** (2012) Unbiased Mutagenesis of MHV68 LANA Reveals a DNA-Binding Domain Required for LANA Function In Vitro and In Vivo. *PLoS Pathog* **8**: e1002906.

5 Acknowledgements

I would like to thank Prof. Dr. Kenneth Kaye for giving me the opportunity to conduct my research in his lab and to gain new experiences at the Brigham and Women's Hospital, a teaching affiliate of Harvard Medical School, Boston, USA.

I would also like to thank Prof. Dr. Hermann Katinger and Prof. Dr. Reingard Grabherr for their supervision from the University of Natural Resources and Life Sciences, Vienna, Austria.

Further, I would like to thank Prof. Dr. Pedro Simas and his lab, especially Dr. Marta Pires de Miranda, from the University of Lisbon, Portugal, for believing in the idea that KSHV LANA can functionally substitute for MHV68 LANA, the generation of kLANA-MHV68 chimeric viruses and testing them in a mouse model.

I also thank my lab colleagues for long discussions and support in the lab, especially my friend Dr. Chantal Beauchemin, who also did some of the fluorescence microscopy and performed the EMSAs.

And, of course, I want to thank my family and closest friend for letting me go, the millions of phone calls, the visits to the US and their endless support in challenging times.

6 Curriculum Vitae

Dipl.-Biol. Aline-Christine Habison

Address: Lochnerallee 37
41063 Mönchengladbach
E-Mail: a.c.habison@gmail.com
Phone: +49 15170076014
Place of birth: Vienna, Austria
Date of birth: December 31, 1979



Education

- 2009 – 2017 **Doctoral studies**
University of Applied Life Sciences and Natural Resources,
Institute of Biotechnology, Vienna
- Murine Gammaherpesvirus 68 LANA mediates Episome Persistence through a cross-species conserved Mechanism that provides a Basis for an in-vivo Model of KSHV
- 2004 – 2005 **Diploma Thesis**
Fraunhofer USA, Center for Molecular Biotechnology,
Newark (DE, USA)
- Presentation of RSV-F B-cell epitopes on the surface of Alfalfa Mosaic Virus particles as potential vaccine candidates.
- 2000 – 2005 **Diploma Studies**
Rheinisch Westfälische Technische Hochschule (RWTH),
Aachen
- Focus on Immunology and Molecular Biotechnology
 - passed with distinction
- 1998 – 2000 **Diploma Studies**
University of Vienna
- 1996 – 1997 **High School**
North Boone High School, Illinois (USA)
- 1989 – 1998 **High School (Gymnasium)**
Theresianische Akademie Vienna
- Matura (grade: 1,2)

Practical Experience

06/2017 – 12/2017	Consultant Medizinisches Versorgungszentrum Dr. Stein und Kollegen, Mönchengladbach (Deutschland) <ul style="list-style-type: none">• Improvement of automated medical data entry
06/2016 – 05/2017	Scientific Trainee Molecular Diagnostics / TA Hematology Dachverband der Laborgemeinschaften, Mönchengladbach
06/2015 – 05/2016	Data Entry / TA Internship Molecular Diagnostics ILMED Labor-und Medizintechnik, Mönchengladbach
11/2006 – 10/2011	Research Fellow Brigham and Women's Hospital, Harvard Medical School, Boston (MA, USA)
10/2004 – 09/2005	Trainee Fraunhofer USA, Center for Molecular Biotechnology, Newark (DE, USA)
03/2004 – 06/2004	Practical Teaching Assistant RWTH Aachen, Institute for Molecular Biotechnology
02/2004	Internship Baxter AG, Research and Development, Vienna (Austria)
08/2003	Practical Teaching Assistant RWTH Aachen, Institute for Microbiology

Publication and Presentation

Aline C. Habison, Marta Pires de Miranda, Chantal Beauchemin, Min Tan, Sofia A Cerqueira, Bruno Correia, Rajesh Ponnusamy, Edward J. Usherwood, Colin E McVey, J Pedro Simas, and Kenneth M. Kaye. **2017**. Cross-species conservation of episome maintenance provides a basis for in vivo investigation of Kaposi's sarcoma herpesvirus LANA. **PLOS Pathogens** 13(9):e1006555.

Aline C. Habison, Chantal Beauchemin, J. Pedro Simas, Edward J. Usherwood and Kenneth M. Kaye. **2012**. Murine Gammaherpesvirus 68 LANA Acts on Terminal Repeat DNA to Mediate Episome Persistence. **Journal of Virology** 86(21): 11863-76.

Aline C. Habison, Chantal Beauchemin and Kenneth M. Kaye. **2011**. Role of MHV68 ORF73 in episome maintenance, is MHV68 ORF73 the KSHV LANA? Presentation and poster at 14th International Workshop on Kaposi's Sarcoma Associated Herpesvirus and Related Agents, Helsinki (Finland).